MSc. Thesis

Driver behaviour near the vehicle handling limits in vehicles with an extended linear handling region

TU Delft

R.M.A.Bekkers

Driver behaviour near the vehicle handling limits in vehicles with an extended linear handling region

by

R.M.A. Bekkers

to obtain the degree of Master of Science
at the Delft University of Technology,
to be defended publicly on Monday August 6, 2018 at 1:00 PM.

Student number:	4150953	
Project duration:	November 1, 2017 – August 6, 2018	
Thesis committee:	Prof. dr. ir. D. A. Abbink,	TU Delft, supervisor
	Dr. ir. B. Shyrokau,	TU Delft, supervisor
	Ir. S. B. Kolekar,	TU Delft, supervisor
	Ir. T. Melman,	TU Delft, supervisor
	Dr. ir. D. M. Pool,	TU Delft, external member
	Dr. ir. A. Vrijdag	TU Delft, external member

An electronic version of this thesis is available at `http://repository.tudelft.nl/`.

TU Delft

Preface

This thesis is submitted for the Master of Science degree in Mechanical Engineering at Delft University of Technology. In this study lateral assistance systems which assist the driver to improve the lateral driving performance are considered. During my literature study, I found many communication methods of these systems to inform the driver to keep him/her in the control loop. However, for systems such as Active Rear Steering (ARS)/ Torque Vectoring (TV), which aim to extend the linear handling region, no such communication methods have been found. When using ARS/TV near the vehicle handling limit (VHL), the change in vehicle dynamics will be very abrupt compared to a conventional vehicle. This might cause problems in the driver his/her control performance. During this study, I took the first step in identifying these problems by performing a human factors driving simulator experiment. Please refer to chapter 1 for the paper of this study.

R.M.A. Bekkers
Delft, July 2018

Acknowledgements

First of all I would like to thank Prof.dr.ir. David A. Abbink, Dr.ir. Barys Shyrokau, Ir. Sarvesh B. Kolekar and Ir. Timo Melman for their supervision, guidance and support during this thesis project. We had many efficient and effective discussions enabling myself to assure the best possible outcome.

I am grateful to Nissan Motor Corporation in Atsugi, Japan, who helped me to understand vehicle chassis control during an internship of six months.

Finally, I would like to thank my parents, grandparents, Tijs, Stijn and Nadège for their continuous support and encouragements. Without you I could not have done this. Thank you!

R.M.A. Bekkers
Delft, July 2018

Contents

1

Paper

Bekkers, R.M.A. (2018). *Driver behaviour near the vehicle handling limits in vehicles with an extended linear handling region*

Driver behaviour near the vehicle handling limits in vehicles with an extended linear handling region

R.M.A. Bekkers[a]

[a]*Delft University of Technology, Department of BioMechanical Engineering, Faculty of 3ME, Mekelweg 2, 2628 CD Delft, The Netherlands.*

Abstract

Lateral acceleration is a key aspect of the vehicle response perceived by the driver. Assistance systems such as Active Rear Steering (ARS) or Torque Vectoring (TV) are developed to modify the lateral acceleration response such that the vehicle has an improved stability and an extended linear handling region. With this extended linear handling region the vehicle abruptly reaches tyre friction limitations (representing an entry into the vehicle handling limits (VHL)), this can potentially lead to dangerous situations. This thesis aims to quantify driver behaviour when being forced to drive near the VHL, in terms of how often the VHL is entered and what happens after entry. To assess this, a human factors experiment ($N = 18$) in a fixed base driving simulator was performed. In this experiment three different vehicle configurations were compared: (1) a conventional vehicle (*Passive*) (2) a vehicle with an extended linear handling region (*Active*) (3) a vehicle with an extended linear handling region and increased yaw response (*Active Sport*). In these configurations, the drivers need to drive with a fixed velocity on an oval track with Electronic Stability Control (ESC) switched off. It was expected that a conventional vehicle enters the VHL more often compared to the vehicles with an extended linear handling region. However, when entering the VHL, the vehicle with an extended linear handling region was expected to be more difficult to control due to the abrupt change in vehicle dynamics and corresponding steering feel. The results indicate that the *Passive* vehicle entered the VHL more frequently compared to the *Active* and *Active Sport* configurations. However, when the *Active Sport* configuration entered the VHL, significantly more road departures and an increased steering reversal rate compared to the *Passive* configuration resulted. Therefore, it can be concluded drivers enter the VHL less frequently in a vehicle with an extended linear handling region (caused by systems such as ARS or TV). However when the VHL is entered it is more difficult and dangerous for a driver to control compared to a conventional vehicle.

Keywords: Active Rear Steering, Torque Vectoring, Vehicle dynamics, Lateral acceleration, Human factors driving simulator experiment, Extended linear handling region, Abrupt change in dynamics

1. Introduction

Accident statistics show that the human driver is not always able to perform the lateral driving task (such as lane keeping) without errors (Cicchino, 2018). Therefore, over the last decade, lateral assistance systems (e.g. lane departure warning (Bartels et al., 2016a)) that assist the driver to enhance safety, are developed for passenger vehicles. These lateral assistance systems can be divided into three different categories based on the lateral acceleration of a vehicle (Figure 1).

The solid line in Figure 1 represents the lateral acceleration response of a conventional understeering vehicle at a constant vehicle speed to a steering wheel angle. The lateral acceleration of a vehicle increases with the steering angle up to a so called "Vehicle Handling Limit" (VHL), where the acceleration cannot be increased further due to tyre limitations and the vehicle starts skidding (Rajamani, 2011). The resulting three different categories for the lateral assistance systems based on the lateral acceleration response of the vehicle are:

(I) *Linear region systems* are supporting the driver in the perception of the environment. An example is a Lane Departure Warning (LDW) system that warns the driver when he/she is leaving the lane unintentionally (Kozak et al., 2006). Another example is Lane Keeping Assist (LKA) that guides the driver to keep the vehicle inside the lane boundaries (Mulder et al., 2008).

(II) *Non-linear region systems* such as Active Rear Steering (ARS) (Reimann et al., 2016), Active Suspension (AS), Torque Vectoring (TV) (Ivanov et al., 2012) and Active Front Steering (AFS) (He et al., 2006) aim to extend the linear vehicle handling region, reduce the understeer gradient and increase the maximum lateral acceleration of a vehicle, illustrated by the dashed line in Figure 1.

Email address: R.M.A.Bekkers@student.tudelft.nl (R.M.A. Bekkers)

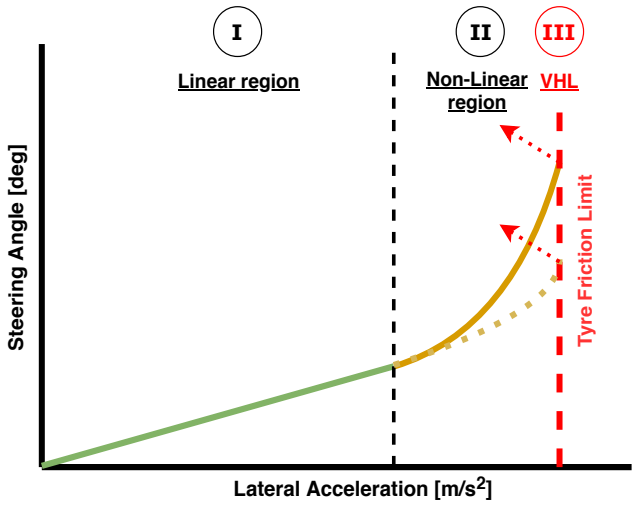

Figure 1: Schematic Vehicle Handling Characteristic. The vehicle handling characteristic is divided in three handling regions: (I) linear handling region (II) non-linear handling region, where systems such as Active Rear Steering or Torque Vectoring can be used to extend the linear handling region (dashed line) (III) vehicle handling limits which is entered after reaching the tyre friction limits where the vehicle behaviour is difficult to predict, increasing the steering angle further will decrease the lateral acceleration of the vehicle.

(III) *Vehicle Handling Limit systems* assist the driver in preventing dangerous situations, takes the driver out of the loop and brings back the vehicle to the safe linear region just before reaching the tyre friction limits, e.g. Electronic Stability Control (ESC) (van Zanten and Kost, 2014).

For the systems in region II, which aim to extend the linear handling region, the vehicle abruptly reaches tyre friction limitations (representing an entry into the vehicle handling limits (VHL)) (Ivanov et al., 2012), (He, 2005). The study of He et al. (2006) illustrates, by using computer simulations for vehicles without ESC and with an extended linear handling region, that once the VHL is entered the dynamics change abruptly (these vehicles will behave in a more unstable manner) compared to a conventional vehicle. This abrupt change of vehicle dynamics and corresponding steering feel has the potential to lead to dangerous situations, however "the driver in the loop" response is unknown.

The goal of this thesis is to evaluate the driver behaviour when driving near the VHL, in terms of how often the VHL is entered and what happens after entry, in a vehicle with an extended linear handling region (caused by systems such as ARS or TV). It is expected when driving in a vehicle with an extended linear handling region, the vehicle will enter the VHL less frequently compared to a conventional vehicle. The main reason for this is that the vehicle response is more stable due to the extended linear handling region (He et al., 2006). However, once these vehicles start skidding (entry into the VHL), there is an increased chance that the driver will lose control of the vehicle and run off the road due to the abrupt change in dynamics. Therefore, the following hypotheses are investigated in this paper:

1. *When driving a vehicle with an extended linear handling region, the vehicle will enter the VHL less frequently compared to a conventional vehicle*
2. *When vehicles with an extended linear handling region enter the VHL, it will be more difficult for the driver to control the vehicle in a safe manner compared to a conventional vehicle*

In order to test these hypotheses four steps are taken. First, the development and validation of a vehicle model (section 2.1). Second, the design of different vehicle configurations (section 2.2). Third, the design of the steering feel corresponding to the developed vehicle configurations (section 2.3). The fourth step involves a human factor driving simulator experiment, described in section 2.4. ESC is not included in this experiment since it will prevent entry into the VHL and therefore it is possible to test if drivers are able to correct/prevent entry into the VHL and utilize the full potential of systems like ARS or TV. Finally, the results (section 3), discussion (section 4) and conclusion (section 5) are presented.

2. Method

The method used to identify the driver behaviour in vehicles with an extended linear handling region when driving near the VHL, consists of the following four steps:

1. *Development and validation of a vehicle model.* A vehicle model, representing a Renault Megane, is developed and subsequently validated using IPG CarMaker software. This model has realistic dynamics when driving close to the VHL.
2. *Design of different vehicle configurations.* In this step the three vehicle configurations used in the experiment are developed (i.e. *Passive*, *Active* and *Active Sport*).
3. *Design of the steering feel.* The self-aligning moment (which is a main contributor to the steering feel) is valuable feedback for the driver when driving close to the VHL (Rajamani, 2011), (Milliken et al., 2003). This is experimentally proved by a study of Katzourakis et al. (2014a), where the effect of the self-aligning moment is exaggerated such that the drivers are able to perceive it better. Therefore, it is required to have a valid steering feel corresponding to the different vehicle configurations designed in step 2.

4. *Human factors driving simulator experiment.* In this experiment the main focus is to drive close to an entry of the VHL, which is not a situation that occurs on a regular basis. Therefore, the drivers are forced to drive close to this VHL. This is achieved by letting the drivers drive a vehicle with a fixed velocity on a three lane oval track. The combination of the fixed velocity and the radii of the turns forces the driver to drive close to the VHL when keeping the vehicle on the road.

2.1. Vehicle Dynamics Model

The vehicle dynamics are modelled using a two track vehicle model with an adapted version of the Pacejka '94 tyre model to include the non-linear dynamics. The lateral vehicle dynamics with the corresponding Pacejka '94 tyre model are given in section 2.1.1. Subsequently, the vehicle yaw-dynamics which affect the lateral dynamics are described in section 2.1.2. An important aspect of the yaw dynamics is the self-aligning moment of the tyres. Therefore, in section 2.1.3 the calculation of the self-aligning moment is described. This self aligning moment and the amount of force a tyre can produce on the road surface depend on the vertical load on the tyre, see section 2.1.4. Finally, the lateral dynamics of the vehicle are validated using two types of manoeuvres in section 2.1.5. In the validation process only the lateral vehicle dynamics are considered since the longitudinal vehicle velocity will be held constant throughout the experiment.

2.1.1. Lateral vehicle dynamics

The lateral equations of motion, using the second law of Newton, can be described by equation 1:

$$M_v(\dot{v_y} + v_x \cdot r) = Fy_{fl} + Fy_{fr} + Fy_{rl} + Fy_{rr} \quad (1)$$

In this equation, M_v represents the vehicle mass, v_y the lateral vehicle velocity, v_x the longitudinal vehicle velocity and r is the yaw-rate of the vehicle. Moreover, Fy_{ij} represents the lateral tyre force of each individual wheel (i = front or rear, j = left or right) which is determined using an adapted version of the Pajecka '94 tyre model described by equations 2 to 7:

$$Fy = coFy \cdot Fy0 \quad (2)$$

$$coFy = cos(A) \text{ where } -0.5\pi \leq A \leq 0.5\pi \quad (3)$$

$$A = \frac{am0 \cdot (1.4 - 0.5\mu)}{0.9} \cdot tan^{-1}\Big(\big(am2 \cdot cos(tan^{-1}(am_3 - \alpha_{ij}))\big) \cdot \kappa_{ij}\Big) \quad (4)$$

$$Fy0 = B \cdot sin(\boldsymbol{a_0} \cdot tan^{-1}(C \cdot \alpha)) \quad (5)$$

$$B = \mu Fz \cdot (\boldsymbol{a_1} F_z + \boldsymbol{a_2}) \quad (6)$$

$$C = \begin{cases} \frac{\boldsymbol{a_3} \cdot sin(2 \cdot tan^{-1}(Fz/\boldsymbol{a_4}))}{\boldsymbol{a_0} \cdot B} \text{ if } \boldsymbol{a_0} \cdot B \neq 0 \\ 0 \text{ if } \boldsymbol{a_0} \cdot B = 0 \end{cases} \quad (7)$$

In these equations, F_z represents the tyre vertical load, α the tyre side slip and κ the longitudinal tyre slip. The tyre dynamics are modelled in CarMaker using Delft-tyre 6.1 with a Magic Formula steady-state slip model describing non-linear slip forces and moments. This model represents realistic tyre forces and has been extensively validated (TNO Automotive, 2008). However, Delft-tyre 6.1 is a protected tyre model which cannot be used in the simulator used in this experiment. Therefore, the tyre parameters $\boldsymbol{a_0}$ to $\boldsymbol{a_4}$ of the Pacejka'94 tyre model are identified to represent the characteristic of the Delft-tyre 6.1 model at different vertical tyre loads ($1000N$, $4000N$ and $8000N$). For this identification, the longitudinal tyre slip is assumed to be small ($abs(\kappa) < 0.02$) since the longitudinal speed is constant during the experiment. To check if the Pacejka '94 model with identified parameters closely represents the Delft-tyre 6.1 model, these models are compared using the *Variance Accounted For (VAF)* metric (equation 8).

$$VAF(\%) = \left(1 - \frac{\sum_i (y_i - \hat{y}_i)^2}{\sum_i (y_i)^2}\right) \cdot 100 \quad (8)$$

In the equations described above, y is the benchmark data (Delft-tyre 6.1) and $\hat{y}$ is the data from the model with identified parameters (Pacejka '94). The VAF values of the lateral tyre force for the three different vertical tyre loads are given in Table 1. All VAF values are above 95% which indicates that for different tyre loads the modified Pacejka '94 tyre model closely represents Delft-tyre 6.1.

Table 1: VAF values for the identified Pacejka '94 tyre model

VAF (%)	$1000N$	$4000N$	$8000N$
F_y Validation	99.41	99.94	95.32
M_z Validation	83.70	86.26	97.47

2.1.2. Vehicle yaw dynamics

Forces that have an effect on the yaw dynamics are the longitudinal and lateral tyre forces and the tyres self aligning moments (M_z). With inclusion of the self-aligning moment, the equations of motion for the yaw dynamics are represented by equation 9:

$$\begin{aligned} I_{zz}\dot{r} = {} & (Fy_{fl} + Fy_{fr}) \cdot l_f - (Fy_{rl} + Fy_{rr}) \cdot l_r \\ & + (-Fx_{fl} + Fx_{fr}) \cdot \frac{1}{2} t_f + (-Fx_{rl} + Fx_{rr}) \cdot \frac{1}{2} t_r \\ & - (M_{z,fl} + M_{z,fr} + M_{z,rl} + M_{z,rr}) \end{aligned} \quad (9)$$

In this equation t_f represents the front axle track, t_r the rear axle track, r the yaw rate and I_{zz} the moment of inertia around the vertical axis. Moreover, l_f represents the distance of the centre of gravity (COG) towards the front axle and l_r the distance from the COG to the rear axle. The self-aligning moments are calculated using the empirical equations corresponding to the Pacejka '94 tyre model, which is further explained in section 2.1.3.

2.1.3. Self-aligning moment

With Pacejka '94, the self aligning moment is calculated using the empirical equation obtained from the manual of ADAMS (MSC Software, 2010). See Appendix A for the empirical equations of the self aligning moment.

The parameters of this empirical equation are identified for a range of vertical tyre loads ($1000N$, $4000N$ and $8000N$) using the self-aligning moment calculated by Delft-tyre 6.1 (used in CarMaker) as a benchmark. For the identification the longitudinal slip is assumed to be small ($abs(\kappa) < 0.02$).

The VAF values of the self-aligning moment for the different vertical tyre loads are given in Table 1. These VAF values range between 83% (at $1000N$) and 97% ($8000N$). The maximum self-aligning moment at a vertical load of $1000N$ is approximately $3Nm$, while for the vertical load of $8000N$ this is approximately $150Nm$. Therefore, the lower VAF value on the vertical tyre load of $1000N$ has a lower impact on the total self-aligning moment.

2.1.4. Vertical tyre load dynamics

The amount of force a tyre can produce on the road surface depends on the vertical load. This vertical load consists of a static part (load balance based on the dimensions of the vehicle and the position of the COG in the vehicle) and a dynamic part, which is affected by lateral and longitudinal acceleration and roll dynamics of the vehicle. Hence, the vertical tyre load is determined using equations 10 to 13.

$$Fz_{f,l} = \frac{1}{2}M_v\left(\frac{l_r}{l}g - \frac{h_{COG}}{l}a_x\right) - M_v\frac{l_r}{l}\frac{h_{roll,f}}{t}a_y \quad (10)$$

$$Fz_{f,r} = \frac{1}{2}M_v\left(\frac{l_r}{l}g - \frac{h_{COG}}{l}a_x\right) + M_v\frac{l_r}{l}\frac{h_{roll,f}}{t}a_y \quad (11)$$

$$Fz_{r,l} = \frac{1}{2}M_v\left(\frac{l_f}{l}g + \frac{h_{COG}}{l}a_x\right) - M_v\frac{l_f}{l}\frac{h_{roll,r}}{t}a_y \quad (12)$$

$$Fz_{r,r} = \frac{1}{2}M_v\left(\frac{l_f}{l}g + \frac{h_{COG}}{l}a_x\right) + M_v\frac{l_f}{l}\frac{h_{roll,r}}{t}a_y \quad (13)$$

In the above equations a_x represents the longitudinal acceleration, g the gravitational acceleration (set equal to $9.81m/s^2$) and l the wheelbase of the vehicle. The roll dynamics are included by identifying the h_{roll} term, such that the vertical load transfer of the tyres is in accordance with CarMaker. In this study h_{roll} term is identified using the validation manoeuvres described in section 2.1.5. Increasing h_{roll} will increase the effect of roll dynamics on vertical tyre load transfer.

2.1.5. Vehicle Model Validation

To validate the developed vehicle model the lateral dynamics represented by the lateral acceleration (a_y), - velocity (v_y) and yaw-rate (r) are compared with the CarMaker model for two different types of manoeuvres:

- *Sinusoidal* steering torque input with an amplitude of $2Nm$ and a frequency of $0.2Hz$. The vehicle is accelerating from 0 to $100km/h$ with an average acceleration of $2.23m/s^2$.
- *Skid-pad* test on a track with a radius of $100m$. On this track the vehicle accelerates with an average acceleration of $0.25m/s^2$ from $30km/h$ until it the moment the vehicle departs from the road. The IPG-Driver model (an adaptive driver model with artificial intelligence) is used to control the steering and gas pedal input of the vehicle.

In Table 2, the VAF values of the most important variables that describe the lateral vehicle motion (i.e. yaw rate and lateral acceleration) are given for both validation manoeuvres. The VAF values are all above 98%, hence the vehicle model is validated and suitable for the experiment. In Figure 2, one can see that the lateral dynamics of the vehicle model represents the CarMaker vehicle behaviour accurately. Please refer to Appendix A for additional validation plots.

Table 2: VAF in skid-pad and sinusoidal vehicle manoeuvres

VAF (%)	*Sinusoid*	*Skid-pad*
yaw rate	99.99	99.91
lateral velocity	98.22	99.66
lateral acceleration	99.97	99.92

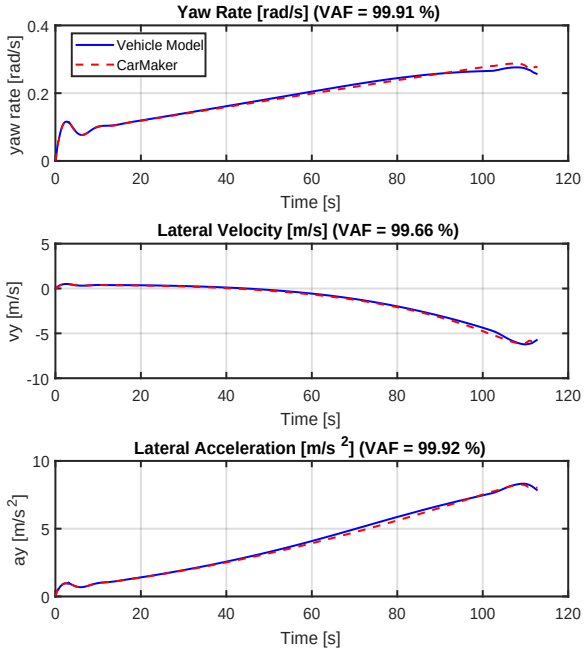

Figure 2: Validation of the vehicle model for a skid-pad test

2.2. Vehicle Configurations

The second main step is the development of vehicle configurations with an extended linear region and corresponding abrupt change of dynamics when entering the VHL. This is achieved by the modification of the tyre parameters ($\boldsymbol{a_0}$ to $\boldsymbol{a_4}$) of the Pacejka '94 tyre model.

During the experiment, a conventional vehicle as a benchmark will be compared with two configurations of a vehicle with an extended linear handling region. One configuration to mainly test the effect of the abrupt change in steering feel, another to test the effect of the abrupt change in dynamics combined with the steering feel.

- Conventional vehicle, as a benchmark, with a smooth transfer towards the VHL and higher stability in the VHL (*Passive*)
- Vehicle with extended linear handling region and corresponding abrupt transfer into the VHL (*Active*). The vehicle has a similar type of stability as the conventional vehicle in the VHL. The main difference is the abrupt change in steering feel.
- Vehicle with increased yaw response, resulting in a more sportive vehicle handling in the linear region, and extended linear handling region (*Active Sport*). When entering the VHL there will be an abrupt change in vehicle dynamics together with the steering feel.

The three characteristics are shown in Figure 3, which all have the same cornering potential illustrated by the tyre friction limit line. For creation of these characteristics the vehicle is driving at $100km/h$ and the steering wheel is turned from 0 to 360 degrees with a steering velocity of $3deg/s$.

2.3. Steering Feel

The third step is the design of the steering feel corresponding to the vehicle handling characteristics developed in the previous step. The steering feel can be modelled by the simplified steering dynamics given in equation 14.

$$I_{sw,col}\ddot{\delta}_{sw} + C_{sw}\dot{\delta}_{sw} = T_{sw} - \frac{M_z + Fy_f \cdot (r_{wheel} \cdot tan(\nu))}{u_{w-r} \cdot u_{r-sw}} + T_{assist} \tag{14}$$

$Fy_f \cdot (r_{wheel} \cdot tan(\nu))$ represents the effect of mechanical trail times the lateral tyre force, this adds an additional torque on the steering rack. The mechanical trail is due to the caster angle ν. T_{assist} represents a possible additional assistance torque. $I_{sw,col}$ is the inertia of the steering wheel and column combined and C_{sw} the damping coefficient. The steering torque (T_{sw}) is validated using CarMaker. The steering dynamics used in the simulation of the CarMaker vehicle is modelled as a Pfeffer steering model (for the parameters of this model please refer to Appendix A). The sinusoidal steering manoeuvre of section 2.1.5 is used to identify the parameters of the simplified steering dynamics, represented by equation 14, such that it results in the same Steering Wheel Angle (SWA) for a given torque input as the Pfeffer steering model. With the above described method, a valid steering feel can be created for a conventional vehicle ($VAF = 99.96\%$, see Appendix A).

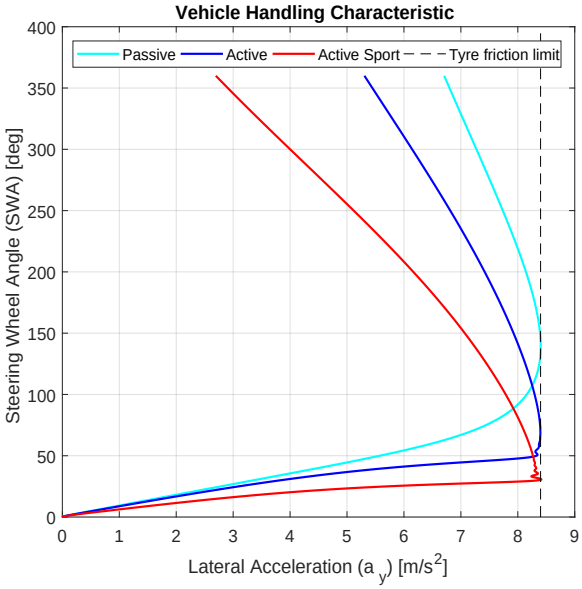

Figure 3: Vehicle handling characteristic at a vehicle velocity of $100km/h$ and a steering velocity of $3deg/s$ for the three vehicle configurations: conventional benchmark vehicle (*Passive*), vehicle with extended linear region (*Active*) and vehicle with increased yaw gain and extended linear region (*Active Sport*)

2.3.1. Steering Feel Conventional Vehicle (Passive)

In Figure 4, the driver steering torque versus lateral acceleration of the vehicle is shown. The self-aligning moment reaches it peak value at a lower side slip angle than the point where the peak lateral tyre force occurs, since the pneumatic trail reduces as the slip angle increases. So, the self-aligning moment starts to decrease before entering the VHL (Dixon, 1996). Consequently, the applied driver torque will gradually go towards zero when approaching the VHL.

2.3.2. Steering Feel of vehicles with extended linear region

The vehicle configurations with an abrupt entry into the VHL are created by modifying the tyre characteristics. Therefore, the side slip angles for the tyres will not be in correspondence with the self-aligning moment equations. As a consequence, the steering feel is manually created by a fixed rotational stiffness versus SWA relation, such that the steering feel is in accordance with the vehicle handling characteristics displayed in Figure 3.

For a vehicle equipped with ARS/TV, the slip of the front wheels can be compensated by steering with the rear wheels or using torque vectoring (Ivanov et al., 2012).

Thus, the self-aligning moment will stay high for larger lateral accelerations. When the assistance systems cannot compensate the slip of the front wheels anymore (the vehicle enters the VHL), the front wheels suddenly start slipping significantly, leading to an abrupt drop of the self-aligning moment.

In this study, the VHL entry point is determined by the inflection point of the vehicle handling characteristic, instead of the body slip angle of the vehicle i.e. (He et al., 2006). The reason for this is that body slip angle is not a valid measure of entry into the VHL since the vehicle dynamics are slightly modified to ensure the vehicle velocity is constant in this study (by removing the effect of lateral vehicle speed and yaw-rate on the longitudinal speed). Please refer to Appendix B for a further explanation.

The inflection point of the vehicle handling characteristic depends on the vehicle velocity, which is constant in this study, and the average steering velocity when entering the turn. Steering is assumed to be initiated when the driver steers the steering wheel with a velocity higher than $3deg/s$ (Theeuwes et al., 2002). However, this steering velocity alone is not necessary the moment the driver starts entering the turn. Other reasons could be that the driver is positioning the vehicle for the entry of the turn. Therefore, the additional requirement is that the applied SWA by the driver should be at least $3deg$ in the direction of the turn. Average steering velocity is taken from this point onward until the steering velocity $< 3deg/s$. Three participants drove the vehicle configurations to determine the average steering velocities when entering the turn. The resulting inflection points are at a SWA of $45deg$ for the *Active Sport* condition and $75deg$ for the *Active* condition. For a further explanation of the calculation of the inflection points, please refer to Appendix B. For the manual created steering stiffness vs SWA relations, please refer to Appendix C.

2.4. Human Factors Experiment

Forth step is the human factors experiment used to test the driver behaviour when driving near the VHL, in vehicles with an extended linear handling region. This section starts with a description of the driving simulator used in the experiment. Followed by the experimental protocol and corresponding task description for the participants (sections 2.4.2 and 2.4.3). Finally, the metrics used in conjunction with this experiment to identify the driver behaviour are presented in section 2.4.5.

2.4.1. Apparatus

The experiment was conducted in a fixed-base simulator at the Control and Simulation Department in the faculty Aerospace Engineering of Delft University of Technology. Within this simulator the scenery is visualized using three projectors with a horizontal field-of-view of 180 degrees. The vehicle model calculations and data logging where running at 100 Hz, while the visuals were refreshed at 50 Hz. Car vibrations when the vehicle was outside of the road were implemented using a high frequency ($500Hz$) torque vibration on the steering wheel.

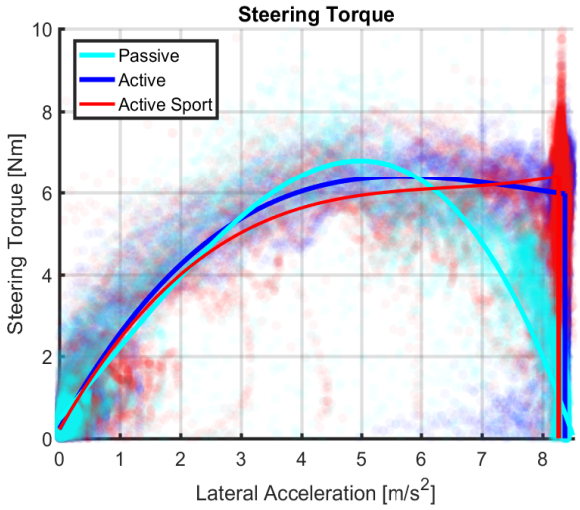

Figure 4: Steering torque versus lateral acceleration of the vehicle configurations: Conventional Vehicle (*Passive*), vehicle with extended linear region (*Active*) and vehicle with increased yaw gain and extended linear region (*Active Sport*). Solid lines represent the average lateral acceleration vs steering toque and transparent dots are the measurement points This data is collected at a vehicle speed of $100km/h$.

2.4.2. Experimental Protocol

The experiment has a within subject design in which the drivers will be subject to the three different vehicle configurations. A within subject design has one major drawback: a learning- and carry over effect influences the results. These effects are reduced by training beforehand and counterbalancing between the three different configurations using a Latin square method (Greenwald, 1976).

During the experiment a participant was required to drive the three different vehicle configurations: *Passive*, *Active* and *Active Sport*. For each configurations the driver completes four different phases, hence one participant had to complete a total of 12 phases:

- *Familiarization phase and catch trial 1* - To let the participants familiarize with the simulator and vehicle dynamics in the linear region. The participant will drive with a vehicle speed of $100km/h$ on a track for six minutes. In this track the turns have a large radius such that the driver will not enter the VHL. At the end of the track there will be a sharper turn (radius of $93m$; see Appendix D for more information) where the driver needs to drive close to the VHL to take the turn (catch trial 1). To ensure the levels of acceleration are close to the VHL, the radius is determined by using equation 15.

$$a_y = \frac{V_x^2}{Radius} \tag{15}$$

- *Training phase* - To train the participants in near VHL situations. In this phase the driver will have to drive the vehicle counter clockwise on an oval track with two turns that have a radius of 94.75m and a road width of nine meters. Therefore, when passing the turn on the inside of the road next to the road boundary, a lateral acceleration of 8.46m/s^2 is required. The outside of the turn requires a lateral acceleration of 7.85m/s^2. If the driver stays more on the outside of the road, the level of acceleration is lower and it will be easier to go through the corner. To motivate the participants to drive near the VHL a point scoring system is applied in which the score is higher when driving closer to the inner road boundary. On the dashboard two scores are presented to the participant, one is the score gained in the latest turn and the other one is the cumulative score. To prevent the drivers from taking excessive risks, the cumulative score will go to zero when crossing the road boundary on the in or outside of the turn. Moreover, on the straights the driver is unable to increase/decrease the score, except for the last 30 meters before entry in the turn to motivate the drivers are on the track before the start of the turn. Participants complete this phase once they are able to complete four consecutive turns with a minimum of 50 points without having a road departure. The design of the track with corresponding dimensions is shown in Figure 5. To give the driver a perception of the vehicle speed, cones are placed along the road on both sides every 10 meters. Moreover, the road is subdivided into three lanes, which can be used as a reference by the driver when going through the turn.

- *Main phase* - This is the core of the experiment. The participant will drive 10 laps (20 turns) on the same oval track as in the training phase (Figure 5). The goal for the participants during this main phase will be to score the highest possible cumulative score.

- *Post experiment run and catch trial 2* - This phase of the experiment is used to test if the driver who has learned the vehicle dynamics during the previous phases, is able to control the vehicle in unexpected near VHL situations. The participant needs to drive the vehicle for two minutes on an winding road. The same catch trial turn is used as in the familiarization phase. However, the complete track with corresponding dimensions is different and given in Appendix D.

2.4.3. Task Description

All participants received an informed consent form in advance of the experiment by email, see Appendix E. The participants were instructed that they needed to drive three different vehicle configurations in the above described four phases. After completing each configuration, the drivers had a break of at least two minutes before starting with a different configuration. Moreover, the drivers were instructed that the goal of the experiment is to score the highest possible cumulative score in the main phase, such that they had to make a trade-off between safely going through the corner with a low score or taking more risk and scoring a higher number of points. Furthermore, the drivers were informed that steering towards the maximum SWA in the simulator of 360 degrees is not the optimal strategy for going through the turn. Before the start of the experiment, the participants were also required to fill in a short additional questionnaire. Please refer to Appendix E for this questionnaire. By using this additional questionnaire, participant characteristics such as driving experience and previous participation in skid training, were collected.

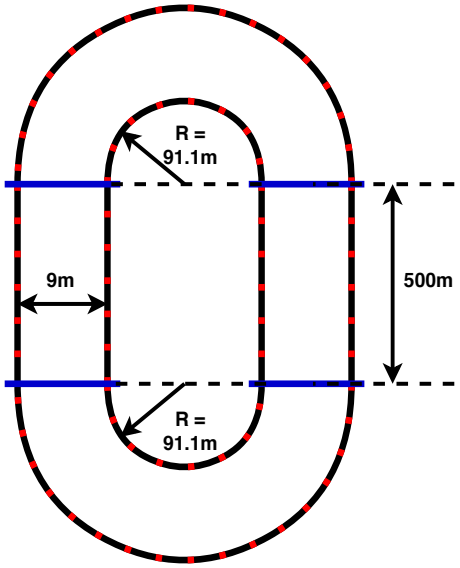

Figure 5: Oval track used during the training- and main phase of the experiment. The length of the straights is 500 meters and the radii of the turns are 91.1m on the inside. For the centre of the road the radius is 94.7m. The angular span of the turns is 180 degrees. On the side of the road cones are placed every 10 meters to give the driver a speed perception. Furthermore, the road is subdivided into three lanes of equal width. The driver can use these lanes as a reference when going through the turn.

2.4.4. Participants

Eighteen participants (17 males) between 18 and 36 years old (M = 23,3 SD = 4.04) volunteered for the driving simulator experiment. All participants had their driving licence for at least one year (M = 5.2 years, SD = 3.83) and were driving minimally twice a month (M = 8.5 times per month, SD = 8.16).

2.4.5. Metrics

For the analysis, the data measured on the straights of the oval track (except for the last 70 meters before the turn starts which were used for determining the curve entry) are disregarded because the main goal of the experiment was

to investigate the driver behaviour near the VHL, which is only reached in the turns. The metrics used for this experiment can be categorized in the following two categories:

- Safety
- Effort/Workload

Safety

To measure the safety level with each vehicle configuration, the following metrics are applied:

- *Percentage of turns where the vehicle enters the VHL.* This metric is calculated by the ratio between the turns where the VHL is entered within the road boundary and the total number of turns. VHL entry is defined as the point where the drivers steer more than the SWA corresponding to the inflection point on the vehicle handling characteristic, which is previously explained in section 2.3.2.
- *Percentage of turns where the vehicle departs from the road after entering the VHL.* This metric is calculated by the ratio between the turns where the vehicle departs from the road due to entry in the VHL and the number of turns where the driver enters the VHL inside the road boundary. Turns with a road departure before entry in the VHL are neglected since these are due to misinterpretation of the vehicle dynamics in the linear region and not due to VHL entry.

Effort/Workload

During this study two commonly used metrics are used to define the driver workload (Melman et al., 2017).

- *Mean Steering Reversal Rate (SRR).* SRR rate is defined as the number of times the driver reverses the steering wheel with an angle > 2 degrees (McLean and Hoffmann, 1975). The SRR is calculated using the local minima and maxima of the SWA. A reversal is counted if the difference between two neighbouring peaks is $> 2deg$. SRR can be used to assess the high frequent control activity and the task demand (Macdonald and Hoffmann, 1980). However, as mentioned in (Macdonald and Hoffmann, 1980) and (Mulder et al., 2008) the relation between an increasing SRR and the task difficulty, depends on the driver's capacity and task difficulty. The driving task during the experiment is difficult, however the oval turns are repetitive so the drivers are expected to have learned the task. Moreover, all participants in the study are frequent drivers. Consequently, the SRR is expected to increase with task difficulty.
- *Mean absolute driver torque.* The driver's physical effort can be measured using the torque applied by the driver on the steering wheel (Melman et al., 2017). The absolute value is taken such that steering to the left or right does not influence the result.

2.5. Statistical Analysis

Statistical tests were applied on the safety and effort metrics obtained in the main phase. For each metric a matrix was created with 18 rows (corresponding to 18 participants) and 3 columns (three vehicle configurations). Subsequently, this matrix was rank-transformed in accordance with Conover and Iman (1981) to create a matrix consisting of the numbers 1 to 54. A one way Repeated Measures (RM) ANOVA with the three vehicle configurations as within subject factor, has been used to test if differences between these were significant. Followed by a post-hoc Bonferroni correction for the three pairwise comparisons between the configurations. The significance level is set as $\alpha = 0.05$.

3. Results

3.1. VHL entry points

As described in section 2.3.2, the SWA's corresponding to an entry in the VHL (inflection points) are determined using the average steering velocity, see Appendix B for a further explanation. When the average steering velocities of all the participants per configuration are used, the VHL entry points of Table 3 result. These VHL entry points are used in the analysis of the safety related metrics.

Table 3: VHL entry points

Passive	*Active*	*Active Sport*
$140.91deg$	$75.03deg$	$45.61deg$

3.2. Safety

Figure 7 shows there is a significant difference in entry of the VHL between the three vehicle configurations. The pairwise post-hoc test (Table 5) indicates that the *Passive* configuration significantly enters the VHL more frequently compared to the configurations with an extended linear handling region.

In Figure 8, the result of the percentage of turns with a road departure after entering the VHL is given. The one way RM ANOVA test shows that the participants have a significantly different percentage of road departures after entering the VHL during a turn $F(2, 34) = 7.91, p = 1.52 \cdot 10^{-3}$) (Table 5). The *Active Sport* configuration departs from the road with significant higher percentage compared to the *Passive* vehicle when the vehicle has entered the VHL during the turn. No significant differences were observed between the *Passive* - *Active* configurations and the *Active* - *Active sport* configurations.

3.3. Workload/Effort

Table 5 shows that the mean SRR was significantly higher for the *Active Sport* configuration compared to the *Passive* configuration. The mean absolute steering torque the driver applies on the steering wheel during a turn is

significantly higher in the *Active* ($M = 5.17Nm$) and *Active Sport* ($M = 5.35Nm$) configurations compared to the *Passive* one ($M = 2.06Nm$). Hence, more physical effort is required by the drivers when driving the vehicle equipped with ARS/TV near the limit of vehicle handling.

3.4. Strategy

In Figure 6, one can see the average trajectories taken by the drivers during the main phase. On average, all the drivers will approach the turn from the outside of the curve and subsequently steer towards the inside, which is also known as corner cutting behaviour (Macadam, 2003). In the average trajectory, the lateral distance to the inner road boundary is approximately equal in the three configurations, see Figure 6. This is supported by the average lateral distance and average number of points per turn scored during the experiment when the vehicle did not depart from the road (Table 5), where no significant differences between the configurations are found. In Figure 9, the trajectories in the three configurations of a single participant can be seen, in these trajectories a red line represents a vehicle in the VHL. For the trajectories of all the participants please refer to Appendix G.17.

3.5. Learning effect

In Table 4, the number of participants which have a road departure, in the training and post experiment phases, are given for each vehicle configuration. The results show a reduction in road departures. However, the high number of road departures in catch trial 2 during the post experiment run, indicates that the task stays difficult for the participants, even after extensive training. The participants do not improve in *Active Sport* configuration. For the trajectories taken by the participants during catch trial 1 and 2 please refer to Appendix G.18.5.

Table 4: Road departures in catch trials one and four

Road Departure	Catch trial 1	Catch trial 2
Passive	17	14
Active	17	8
Active Sport	13	13

3.6. Effect of participant characteristics on the result

In Appendix F, one can find the Spearman correlations between participant characteristics and the metrics. The correlation coefficients between the metrics on one hand and the participant characteristics, on the other, ranges between approximately -0.3 and 0.3. This suggests that the performance on these metrics are not correlated with the personal characteristics of the participants.

4. Discussion

4.1. Main Result

The goal of this thesis is to quantify driver behaviour when driving close to the VHL, in terms of how often the VHL is entered, and what happens after entry, in a vehicle with an extended linear handling region (caused by systems such as ARS/TV). In order to investigate this, four steps were completed. First, a valid vehicle model was developed and validated (section 2.1). Second, the three different vehicle configurations were developed (section 2.2). Third, the designed steering feel corresponding to the configurations (section 2.3). Fourth, a human factors experiment to investigate the driver behaviour in terms of safety and effort.

In terms of safety, the *Active Sport* configuration has a higher percentage of road departures after the vehicle enters the VHL while being on the road ($M = 49\%$), compared to the *Passive* configuration ($M = 19\%$) (see Figure 8). This result can also be observed in the trajectories taken by one single participant (Figure 9). The *Active Sport* configuration departs from the road more often after the VHL is entered (trajectory is red), compared to the other configurations. Furthermore, the mean SRR in the VHL indicates that the *Active Sport* configuration requires more steering effort (see Table 5) and has a higher task difficulty. This observation is supported by the cumulative score obtained by the participants during the experiment, see Table 5. In the *Active* ($M = 567$) or *Passive* ($M = 828$) configuration the cumulative score is significantly better compared to the *Active Sport* ($M = 253$) configuration. For other task difficulty measures e.g. number of turns in training, the means for *Active Sport* conditions show the worst performance (higher number of turns and road departures). However, these findings are not significant. All these metrics are consistent in showing that *it is more dangerous to drive the Active Sport configuration (with a more abrupt change in dynamics in the VHL) compared to the conventional vehicle (Passive) in the VHL.* Comparison between the *Active* and *Passive* configuration do not show statistical significant differences for these metrics. This might be the consequence of the design choices that there is a less abrupt change in dynamics for the *Active* compared to the *Active Sport* configuration when the VHL is entered.

Drivers have a significant higher percentage of entry into the VHL while being inside the road boundaries with the *Passive* configuration compared ($M = 65\%$) to the *Active* ($M = 37\%$) and *Active Sport* ($M = 28\%$) configurations (Table 5). This result can also be observed in the average SWA (see bottom of Figure 6). The average SWA of the *Passive* configuration is above the initialization of the VHL, hence in this configuration the vehicle is more in the VHL. The trajectories taken by one participant also show a higher percentage of VHL entry with the *Passive*

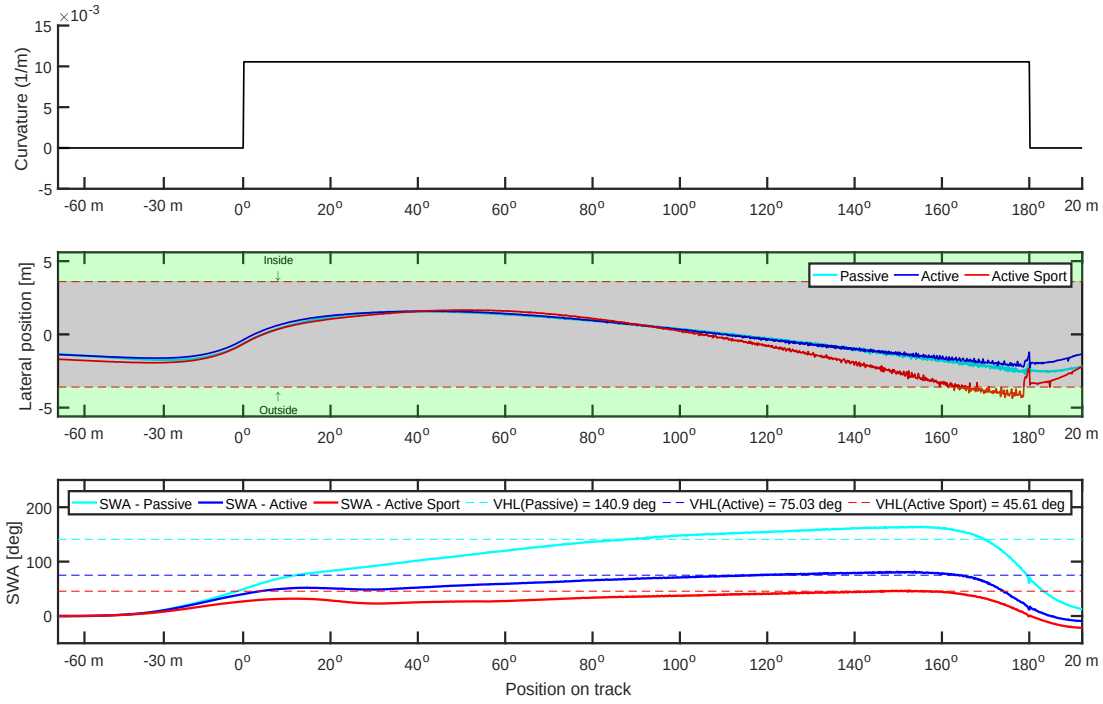

Figure 6: Top: curvature ($1/R_{curve}$) of the road. Middle: average trajectory across all the participants per vehicle configuration. The dashed lines indicate the road boundary and the solid lines represent the trajectory of the COG of the vehicle. Bottom: average SWA input across all the participants. If the SWA of a vehicle configuration is above the corresponding dashed line, the vehicle is in the VHL. The position on track is defined by meters and degrees. $-60m$ implies that the vehicle is at the point 60 meters before the turn starts and for example $20deg$ implies the vehicle position is at an angular span of 20 degrees in the turn.

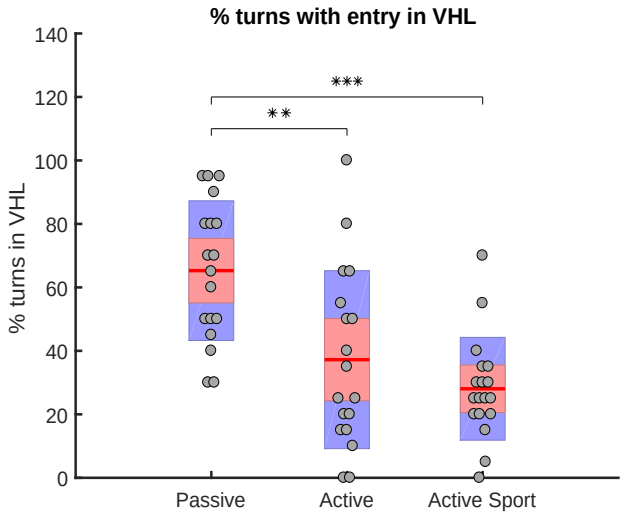

Figure 7: Percentage of turns where the vehicle enters the VHL within the road boundaries. The grey points represent the raw data, the 95% confidence interval on the mean is given in red and the standard deviation in blue. * mean $p \leq 0.05$, ** mean $p \leq 0.01$ and *** $p \leq 0.001$. So, in the *Passive* vehicle configuration there is a significant higher percentage of turns with a VHL entry compared to the vehicles with an extended linear region.

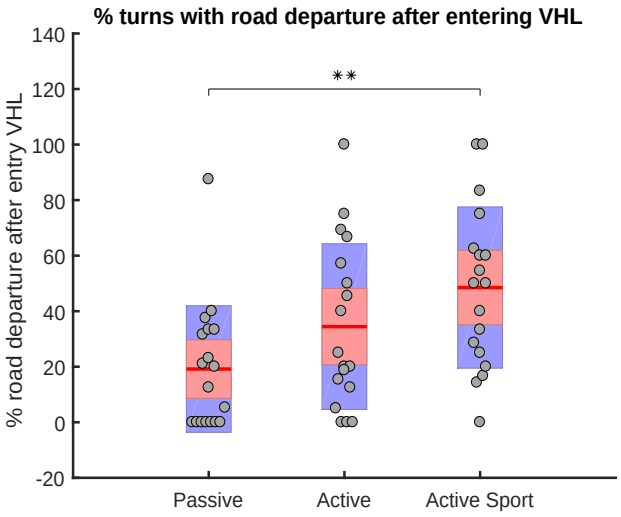

Figure 8: Percentage of turns where the vehicle departs from the road after entering the VHL. The grey points represent the raw data, the 95% confidence interval on the mean is given in red and the standard deviation in blue. * mean $p \leq 0.05$, ** mean $p \leq 0.01$ and *** $p \leq 0.001$. So, there are more road departures after entering the VHL with the *Active Sport* configuration compared to the *Passive* one.

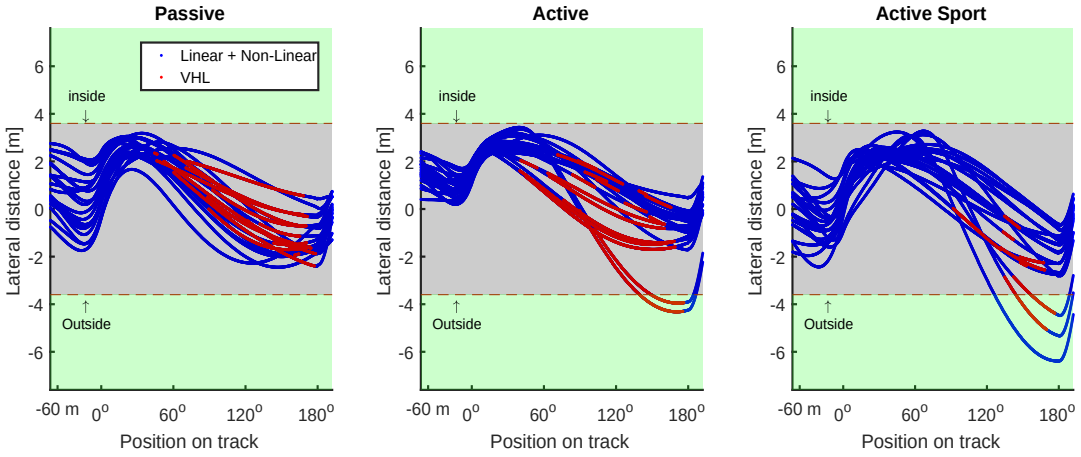

Figure 9: Trajectories of a single participant in the three vehicle configurations during the main phase of the experiment. When the trajectory is blue, the vehicle is in the linear or non-linear region. A red line represents part of the trajectory where the vehicle is in the VHL. The position on track is defined by meters and degrees. $-60m$ implies that the vehicle is at the point 60 meters before the turn starts and for example $20deg$ implies the vehicle position is at an angular span of 20 degrees in the turn.

configuration (Figure 9). So, *the vehicles with an extended linear handling region will enter the VHL less frequently compared to a conventional vehicle.* The fact that drivers are more in the VHL region with the *Passive* configuration is the consequence of a combination of several factors.

Firstly, the vehicle behaviour is more stable before entering the VHL, due to the extended linear handling region (He et al., 2006).

Secondly, the abrupt change in stiffness on the steering wheel, could inform the driver when entering the VHL. The required torque to turn the steering wheel, when entering the VHL, abruptly decreases when the vehicle uses ARS/TV, this can be observed in Figure 4. For the *Passive* configuration the change in stiffness is more gradual, that makes the entrance point in the VHL less distinct. As a consequence, it will be more difficult for the driver to determine when the VHL is entered. Similar results are found in the study of Katzourakis et al. (2014a) and Van Doornik (2014). In these studies haptic support exaggerated the drop of the self-aligning moment near the VHL, which resulted in an improved control performance and less tyre slip.

Thirdly, as already shown above it is more difficult and dangerous for a driver to control a vehicle with an abrupt entry into the VHL. Therefore, the drivers will presumably be more cautious to prevent entry into the VHL.

Finally, with the *Passive* configuration, larger changes in the steering wheel are required to change the lateral acceleration/yaw rate of the vehicle compared to the the *Active Sport* configuration. Moreover, when the *Passive* configuration enters the VHL, the vehicle is still able to go through the turn (see the average trajectory plot in the middle of Figure 6). So, for the *Active Sport* configuration, there are less excessive steering inputs.

4.2. Road departures (RD)

To make a fair comparison between the configurations it was required they have approximately the same cornering abilities. Therefore, the lateral acceleration at the tyre friction limit is equal for the three vehicle configurations (Figure 3). Consequently, the fact that no differences in percentages of turns with a road departure and an outside road departure over the three vehicle configurations are found (Table 5) is a consequence of the design choice.

4.3. Driver response to unexpected encounters near the VHL

The results regarding the catch trials (Table 4) indicate that even after extensive training it is difficult for the drivers to safely go through the turn (road departures in catch trial 2) in unexpected encounters near the VHL. The number of road departures is decreased in catch trial 2, except for the *Active Sport* configuration where the the number of road departures stays equal. This result can be combined with the relatively higher task difficulty of the *Active Sport* configuration indicated by the increased number of road departures in the VHL and the higher mean SRR in the VHL (Table 5). Similar results regarding driver control performance in unexpected encounters near the VHL are found in Katzourakis et al. (2014b), in which the steering stiffness drop based on self-aligning moment did not lead to an improved control performance when driving on a track with different turns. In contrast, when the vehicle drove on a skid-pad (similar to the oval track), which enabled the driver to continuously interact with the haptic feedback, less tyre slip and improved vehicle control were observed (Katzourakis et al., 2014a). This proves that driving near the VHL is an extremely difficult task, even after excessive training, indicating the need for safety systems such as ESC.

Table 5: Results of the main phase of the experiment with means (M), standard deviations (SD) and the result of the repeated measures ANOVA (F,p) and corresponding pairwise comparisons per metric. X is $p \leq 0.05$, XX is $p \leq 0.01$ and XXX is $p \leq 0.001$.

	Passive (1)	**Active (2)**	**Active Sport (3)**		Pairwise Comparison		
	M (SD)	M (SD)	M (SD)	**p-value** $F(2,34)$	1-2	1-3	2-3
Safety							
Turns with entry in VHL (%)	65.28 (21.99)	37.22 (28.04)	28.06 (16.19)	$p = 3.29 \cdot 10^{-6}$ $F = 18.73$	XX	XXX	
Turns with road departure after entering VHL (%)	19,17 (22.78)	34,45 (29.83)	48.51 (29.03)	$p = 1.52 \cdot 10^{-3}$ $F = 7.91$		XX	
Effort/Workload							
Mean SRR (reversals/sec)	0,57 (0,30)	0,65 (0,43)	0,70 (0,33)	$p = 8.36 \cdot 10^{-3}$ $F = 5,52$		X	
Mean absolute driver torque (Nm)	2,06 (0,67)	5,17 (0,53)	5,35 (0,30)	$p = 1,91 \cdot 10^{-11}$ $F = 55,60$	XXX	XXX	
Other Results							
Turns with outside road departure (%)	17.78 (20,31)	14.44 (11,49)	21.40 (13,91)	$p = 0,21$ $F = 1,62$			
Turns with inside road departure (%)	1.67 (3.43)	4.44 (6.62)	5.28 (7.57)	$p = 0.13$ $F = 2.21$			
Turns with road departure (%)	19,44 (21,69)	18,89 (14.61)	26,47 (14,75)	$p = 4.98 \cdot 10^{-2}$ $F = 3,28$			
Turns in training phase (-)	11,33 (6,90)	10,06 (7,06)	15,39 (13,47)	$p = 0,27$ $F = 1,37$			
Cumulative Score (-)	828.03 (781.39)	567.54 (543.24)	253.14 (338.10)	$p = 2.00 \cdot 10^{-2}$ $F = 4.40$		X	X
Total obtained points (-)	1465.30 (415.92)	1460.10 (323.55)	1358.00 (323.36)	$p = 0.18$ $F = 1.80$			
Mean score per turn with no road departure (-)	91.20 (14.87)	90.57 (15.35)	91.98 (12.40)	$p = 0.95$ $F = 5.02 \cdot 10^{-2}$			
Mean of maximum score per turn (-)	125.76 (26.14)	121.94 (26.40)	127.76 (26.39)	$p = 0.91$ $F = 9.99 \cdot 10^{-2}$			
Mean lateral distance per turn with no road departure (m)	2.85 (0.44)	2.82 (0.45)	2.84 (0.33)	$p = 0.96$ $F = 4.10 \cdot 10^{-2}$			
Mean SRR in VHL (reversals/sec)	0.93 (0.40)	1.19 (0.58)	1.59 (0.73)	$p = 2.68 \cdot 10^{-5}$ $F = 15.26$		XXX	X

4.4. ARS limitation and ESC exclusion

When ARS is applied in a vehicle, at high vehicle speeds the rear wheels will steer in the same direction as the front wheels to improve stability (Furukawa et al., 1989), (Reimann et al., 2016). This method is applied because driving with high speeds and steering the rear wheels in opposite direction could lead to vehicle instability (He, 2005). Therefore, in the study of He et al. (2006), the AFS or ARS system improves the vehicle steerability, by reducing the understeer gradient of the vehicle up to mid-range levels of acceleration (0.6g). Everything above this level of acceleration could lead to vehicle instability. ESC will act at high levels of acceleration and the ARS system control authority will be switched off to guarantee the vehicle stability.

This thesis assumes that ARS can steer the rear wheels in opposite direction throughout the whole lateral acceleration range at high vehicle speeds. This will extend the linear region and reduce the tyre slip of the front wheels. Furthermore, systems like TV are functioning at higher levels of acceleration, thereby extending the linear region (see Figure 1). In commercial vehicles, ESC is used to prevent entry into the VHL, by taking the driver out of the loop and brings back the vehicle to a safe linear state. ESC is not included in this experiment to identify whether drivers are able to correct/prevent entry into the VHL. Moreover, this enables us to test if the drivers are able to utilize the full potential of systems like ARS or TV without the intervention of ESC. The results of this study can be used for the development of a haptic steering support which informs the driver of the upcoming VHL while using systems such as ARS/TV. Besides for commercial vehicles, the result of this study can be used for racing cars which do not use ESC and apply TV (e.g. DUT racing team).

4.5. Limitations of this research

The experiment took place in a fixed base driving simulator. Driving in a fixed base simulator does not provide the vestibular feedback a driver normally perceives when driving in a real vehicle. Drivers use this feedback to improve control of the vehicle (Alm, 1996). It is therefore expected the control errors increase due to the absence of this vestibular feedback in the fixed base simulator (Greenberg et al., 2003). However, the goal was to observe the differences between the three vehicle configurations. Even though the control errors increase for the three configurations, the differences between these are assumed to stay valid. Moreover, as mentioned, the simulator does not fully represent the vehicle response of a real vehicle, yet it was ideal for this experiment, since driving a vehicle near the VHL without ESC can lead to dangerous situations (van Zanten and Kost, 2014).

Besides the missing vestibular feedback, the simulator missed auditory sound feedback when the tyres are screeching which is a cue for vehicle slip used by a driver. This implies that the driver did not hear when the tyres started screeching which could have had an effect on the obtained result. For future studies this effect should be included.

Drivers where only able to change the lateral acceleration of the vehicle via steering wheel adaptations, while normally drivers combine change in vehicle velocity and SWA to keep the levels of acceleration under a safe threshold (Reymond et al., 2001). The benefit of the fixed velocity is that the interaction with the steering wheel is emphasised, which provides a valuable type of feedback near the entry of the VHL, via the self-aligning moment (Rajamani, 2011). An additional effect of the fixed velocity is that the drivers are forced to drive near the VHL.

The fixed velocity of the vehicle was achieved by removing the effect of the lateral vehicle velocity and yaw-rate on the longitudinal acceleration. The drawback of this is that the body slip angle cannot be used as an entry point of the VHL (see Appendix B). Moreover, in a real vehicle, the velocity will reduce when applying excessive steering inputs. This speed reduction could have been compensated by adding an additional throttle input instead of modification of the vehicle dynamics. This additional throttle input can be achieved by adding cruise control to the vehicle which tries to maintain a constant velocity. With cruise control there will be a delay in the response due to engine dynamics, which can cause that the vehicle speed is not the same for all the participants. Therefore, it was decided to remove the effect of the lateral vehicle velocity and yaw-rate on the longitudinal acceleration. For future studies it is advised to use a cruise control system to maintain a constant vehicle velocity such that the dynamics of the vehicle do not have to be modified.

In this experiment, the goal in general was to identify the response for all drivers, regardless of their driving experience, when driving near the VHL in vehicles with an extended linear handling region. When driving near the VHL, indicated by the drop of self-aligning moment, a race driver will cautiously increase the SWA, since it can result in extreme understeer of the vehicle (Katzourakis et al., 2014a), (Farrelly et al., 2007). Non race drivers will have more difficulty in using this type of feedback. Especially since the drop of self-aligning moment is concealed under non-linear steering dynamic components such as power steering (Pfeffer et al., 2008) and suspension compliance (Dixon, 1996). However, as mentioned in Katzourakis et al. (2014a), even if the self-aligning moment would be more notable, it is still difficult to notice by less experienced drivers since they miss an internal model for these type of situations due to the fact that driving near the VHL is not a regular driving task. In the experiment for this thesis, the participants had their licence for at least one year (M = 5.2 years, SD = 3.83) and drove a vehicle minimally twice a month (M = 8.5 times per month, SD = 8.16), but were no race drivers, thus unfamiliar to near VHL situations. Combining this with fact that the obtained results during the post experiment run indicates that driving near the VHL is extremely difficult even after extensive training (see section 4.3) will increase the variability between the participants and configurations. To prevent very high levels of variability and make the comparison of the configurations possible, the drivers were trained and tested extensively on an oval track with repetitive turns. In normal driving however, the drivers are not driving close to the VHL on a regular basis and when driving close to the VHL it is often unexpected (e.g. suddenly driving on low road-friction surface). So for future studies, the unexpected near VHL situations should be further investigated.

The results of the experiment are related to VHL entry, which are determined by the inflection points on the vehicle handling characteristic (see Figure 3 and section 2.3). The SWA's corresponding to these inflection points depend on the vehicle velocity (which is constant) and average steering velocity. The average steering velocity is determined by taking the mean of the average steering velocity of all the participants from the point steering is initiated (steering velocity $> 3deg/s$ (Theeuwes et al., 2002) and SWA $> 3deg$) until the steering velocity $< 3deg/s$. In Appendix B the handling characteristics measured during the experiment indicate that the resulting inflection points (Table 3) are a good method for representing VHL entry, since the lateral acceleration after this point reduces with increasing SWA. Moreover, if the inflection point is selected such that it corresponds to drop of steering stiffness ($Active = 75deg$, $Active\ Sport = 45deg$), the same statistical significant differences for the safety related metrics resulted, see Appendix G.15. The same holds for the VHL entry points which are participant specific, see Appendix G.16.

The participants were free to choose their own strategy

for going through the turn. However, they were motivated to stay closer to the inner road boundary using a scoring system (see section 2.4.2). Without this score, the participants might have decided to stay further from the inner road boundary for reducing the lateral acceleration of the vehicle. The obtained score will drop to zero when going outside of the road during the turn. Therefore, during the experiment the participants have to make a trade-off between a higher score and a safer turn. This is illustrated by the average trajectories of the participants during the experiment (see Figure 6). The participants decided to start the turn on the outside, even though the score would be lower. In a future study it might be interesting to investigate what the effect of the scoring systems is on the obtained trajectories and results.

The extended linear handling region is created by modification of lateral tyre force parameters ($\boldsymbol{a_0}$ to $\boldsymbol{a_4}$) of the Pacejka '94 tyre model. The obtained results can be used to get an indication of the driver behaviour near the VHL in vehicles with a extended linear handling region (caused by systems such as ARS or TV). Moreover, steering model complexity will significantly affect the steering feel as shown by the study of Shyrokau et al. (2016). So, to find the exact driver behaviour in vehicles with ARS or TV near the VHL, it is recommended to include extensive models of ARS or TV with their corresponding controller together with an accurate steering dynamics model such as the Pfeffer steering model used in CarMaker.

4.6. Recommendations for further research

This thesis illustrates that drivers experience problems when controlling a vehicle with abrupt changes in vehicle dynamics. These abrupt changes can be the consequence of entry into VHL with systems such as ARS or TV. However, other abrupt changes in vehicle dynamics due to systems such as Multi-Sense by Renault or drive select by Audi, could potentially lead to similar problems.

For future research, one should more extensively consider the unexpected near VHL situations, in situations such as a changing road-friction surfaces.

Moreover, the fact that vehicles with extended linear handling region entering the VHL are more dangerous and difficult to drive by the participants, indicates the need to assist the driver. This could be achieved by adding an additional safety system such as ESC, which is activated when the body slip angle of the vehicle starts to become unstable (He et al., 2006). However, the speed reduction combined with these type of systems is not always perceived as pleasant and the driver is taken out of the loop. To keep the driver in the loop, lateral assistance systems should inform the driver of their action by a certain communication method. This will enhance driver safety, -pleasure and acceptance (Katzourakis et al., 2014a). This thesis illustrates that the abrupt drop in steering stiffness potentially informed the drivers when entering the VHL, since with the *Active* and *Active Sport* configurations there is a lower percentage of turns with an entry in the VHL (Figure 7). Therefore, communicating this drop of steering stiffness in a timely manner towards the driver might assist him/her in preventing entry into the VHL. The effectiveness of such a type of feedback should be investigated in a future study.

Additionally, one could consider using a different type of simulator. In this thesis a fixed base simulator is used, which is sufficient in showing the difference between the vehicle configurations. However, when testing communication methods, inclusion of the motion and auditory tyre screeching clue might influence the result (Alm, 1996), especially near the VHL.

5. Conclusions

The purpose of this thesis was to quantify driver behaviour when being forced to drive near the VHL, in terms of how often the VHL is entered, and what happens after entry, in a vehicle with an extended linear handling region (caused by systems such as ARS/TV).

- As hypothesized, the percentage of turns where the drivers enter the VHL is significantly lower with the *Active* ($M = 37\%$) and *Active Sport* ($M = 28\%$) configurations in comparison to the *Passive* ($M = 65\%$) one. This is potentially the consequence of the more stable vehicle response before entry in the VHL, combined with the abrupt change in stiffness of the steering wheel. For the *Passive* configuration the drop in stiffness is more gradual. Providing the abrupt steering stiffness drop in a timely manner could potentially assist the driver when approaching the VHL.

- It is more difficult and dangerous for a driver to control a vehicle with an extended linear handling region (caused by systems such as ARS/TV) and an abrupt change in dynamics in the VHL, compared to a conventional vehicle. This is shown by the higher number of road departures after entering the VHL with the *Active Sport* ($M = 49\%$) configuration, compared to the *Passive* ($M = 19\%$) one. Moreover, the mean SRR in the VHL (*Active Sport*: $M = 1.59 rev/s$ & *Passive*: $M = 0.93 rev/s$) illustrates that the *Active Sport* configuration has a higher task demand. This result indicates that the driver needs to be assisted when driving close to the VHL in vehicles with an extended linear handling region.

6. References

Alm, H., 1996. Driving simulators as research tools: a validation study based on the vti driving simulator.

Bartels, A., Rohlfs, M., Hamel, S., Saust, F., Klauske, L. K., 2016a. Lateral guidance assistance. In: Handbook of driver assistance systems. Springer, pp. 1207–1233.

Cicchino, J. B., 2018. Effects of lane departure warning on police-reported crash rates. Journal of Safety Research 66, 61–70.

Cohen, J., 1988. Statistical power analysis for the behavioural sciences hillsdale. NJ: Lawrence Earlbaum Associates 2.

Conover, W. J., Iman, R. L., 1981. Rank transformations as a bridge between parametric and nonparametric statistics. The American Statistician 35 (3), 124–129.

Dixon, J. C., 1996. Tires, suspension and handling. Warrendale, PA: Society of Automotive Engineers, 1996. 636.

Farrelly, J. O. P., Stevens, S. D., Barton, A. D., Jun. 26 2007. Haptic controller for road vehicles. US Patent 7,234,564.

Furukawa, Y., Yuhara, N., Sano, S., Takeda, H., Matsushita, Y., 1989. A review of four-wheel steering studies from the viewpoint of vehicle dynamics and control. Vehicle system dynamics 18 (1-3), 151–186.

Greenberg, J., Tijerina, L., Curry, R., Artz, B., Cathey, L., Kochhar, D., Kozak, K., Blommer, M., Grant, P., 2003. Driver distraction: Evaluation with event detection paradigm. Transportation Research Record: Journal of the Transportation Research Board (1843), 1–9.

Greenwald, A. G., 1976. Within-subjects designs: To use or not to use? Psychological Bulletin 83 (2), 314.

He, J., 2005. Integrated vehicle dynamics control using active steering, driveline and braking. Ph.D. thesis, University of Leeds.

He, J., Crolla, D. A., Levesley, M., Manning, W., 2006. Coordination of active steering, driveline, and braking for integrated vehicle dynamics control. Proceedings of the Institution of Mechanical Engineers, Part D: Journal of Automobile Engineering 220 (10), 1401–1420.

Ivanov, V., Augsburg, K., Savitski, D., 2012. Torque vectoring for improving the mobility of all-terrain electric vehicles. In: Proc. 12th European Regional Conf. Int. Soc. for Terrain-Vehicle Systems.

Katzourakis, D. I., Velenis, E., Holweg, E., Happee, R., 2014a. Haptic steering support for driving near the vehicle's handling limits; skid-pad case. International Journal of Automotive Technology 15 (1), 151–163.

Katzourakis, D. I., Velenis, E., Holweg, E., Happee, R., 2014b. Haptic steering support for driving near the vehicle's handling limits: Test-track case. IEEE Transactions on Intelligent Transportation Systems 15 (4), 1781–1789.

Kozak, K., Pohl, J., Birk, W., Greenberg, J., Artz, B., Blommer, M., Cathey, L., Curry, R., 2006. Evaluation of lane departure warnings for drowsy drivers. In: Proceedings of the human factors and ergonomics society annual meeting. Vol. 50. Sage Publications Sage CA: Los Angeles, CA, pp. 2400–2404.

Lu, J., Filev, D., Prakah-Asante, K., Tseng, F., Kolmanovsky, I. V., 2009. From vehicle stability control to intelligent personal minder: real-time vehicle handling limit warning and driver style characterization. In: Computational Intelligence in Vehicles and Vehicular Systems, 2009. CIVVS'09. IEEE Workshop on. IEEE, pp. 43–50.

Macadam, C. C., 2003. Understanding and modeling the human driver. Vehicle System Dynamics 40 (1-3), 101–134.

Macdonald, W. A., Hoffmann, E. R., 1980. Review of relationships between steering wheel reversal rate and driving task demand. Human Factors 22 (6), 733–739.

McLean, J. R., Hoffmann, E. R., 1975. Steering reversals as a measure of driver performance and steering task difficulty. Human Factors 17 (3), 248–256.

Melman, T., De Winter, J., Abbink, D., 2017. Does haptic steering guidance instigate speeding? a driving simulator study into causes and remedies. Accident Analysis & Prevention 98, 372–387.

Milliken, D. L., Kasprzak, E. M., Metz, L. D., Milliken, W. F., 2003. Race car vehicle dynamics problems, answers and experiments. Warrendale, PA: Society of Automotive Engineers, 2003. 294.

MSC Software, 2010. Welcome to Adams / Tire.

Mulder, M., Abbink, D. A., Boer, E. R., 2008. The effect of haptic guidance on curve negotiation behavior of young, experienced drivers. In: Systems, Man and Cybernetics, 2008. SMC 2008. IEEE International Conference on. IEEE, pp. 804–809.

Pfeffer, P. E., Harrer, M., Johnston, D., 2008. Interaction of vehicle and steering system regarding on-centre handling. Vehicle System Dynamics 46 (5), 413–428.

Rajamani, R., 2011. Vehicle dynamics and control. Springer Science & Business Media.

Reimann, G., Brenner, P., Büring, H., 2016. Steering actuator systems. Handbook of driver assistance systems, 745–777.

Reymond, G., Kemeny, A., Droulez, J., Berthoz, A., 2001. Role of lateral acceleration in curve driving: Driver model and experiments on a real vehicle and a driving simulator. Human factors 43 (3), 483–495.

Shyrokau, B., Stroosma, O., Dijksterhuis, C., Loof, J., Van Paassen, M., Happee, R., 2016. The influence of motion and steering-system model complexity on truck steering. In: DSC 2016 Europe: Driving Simulation Conference & Exhibition, Paris, France, 7-9 September 2016.

Theeuwes, J., Alferdinck, J. W., Perel, M., 2002. Relation between glare and driving performance. Human Factors 44 (1), 95–107.

TNO Automotive, 2008. Mf-tyre/mf-swift 6.1. help manual.

Van Doornik, J., 2014. Haptic feedback on the steering wheel near the vehicle's handling limits using wheel load sensing. MSc Thesis, Delft University of Technology.

van Zanten, A., Kost, F., 2014. Brake-based assistance functions. Handbook of Driver Assistance Systems: Basic Information, Components and Systems for Active Safety and Comfort, 1–39.

A

Vehicle Model Validation

In this appendix the vehicle model which is used in the paper is described. First, the equations of motion for the two track model will be given. Followed by the the description of the tyre models. Subsequently, two validation manoeuvres will be presented to show the developed vehicle model does accurately represent a an accurate vehicle model in CarMaker. Finally, the lateral tyre force parameters to create the different vehicle handling characteristics used in the paper are described in section A.9.

A.1. Equations of motion two track model

The lateral vehicle dynamics can be represented by equation A.1. In this equation, M_v represents the vehicle mass, v_y the lateral vehicle velocity, v_x the longitudinal vehicle velocity and r is the yaw-rate of the vehicle. Moreover, Fy_{ij} represents the lateral tyre force of each individual wheel (i = front or rear, j = left or right)

$$M_v(\dot{v_y} + v_x \cdot r) = Fy_{fl} + Fy_{fr} + Fy_{rl} + Fy_{rr} \tag{A.1}$$

The longitudinal vehicle dynamics are represented by equation A.2. Where F_x represents the longitudinal tyre force and F_{RR} the rolling resistance force.

$$M_v(\dot{v_x} - v_y \cdot r) = Fx_{fl} + Fx_{fr} + Fx_{rl} + Fx_{rr} - F_{RR} \tag{A.2}$$

Vehicle yaw dynamics are represented by equation A.3. In this equation t_f represents the front axle track, t_r the rear axle track, I_{zz} the moment of inertia around the vertical axis and M_z the tires self aligning moments. Moreover, l_f represents the distance of the centre of gravity (COG) towards the front axle and l_r the distance from the COG to the rear axle.

$$\begin{aligned} I_{zz}\dot{r} &= (Fy_{fl} + Fy_{fr}) \cdot l_f - (Fy_{rl} + Fy_{rr}) \cdot l_r \\ &+ (-Fx_{fl} + Fx_{fr}) \cdot \frac{1}{2} t_f + (-Fx_{rl} + Fx_{rr}) \cdot \frac{1}{2} t_r \\ &- (Mz_{fl} + Mz_{fr} + Mz_{rl} + Mz_{rr}) \end{aligned} \tag{A.3}$$

A.2. Engine dynamics

Vehicle engine dynamics are copied from the Nissan Cima vehicle model which is used in the HMI-lab.

A.3. Vertical tyre load dynamics

The amount of force a tyre can produce on the road surface depends on the vertical load of the vehicle on the tires. This vertical load consists of a static part (load balance based on the dimensions of the vehicle and the position of the COG in the vehicle) and a dynamic part, which is affected by lateral and longitudinal acceleration and roll dynamics of the vehicle. The vertical tyre load is calculated using equations A.4 to A.7.

$$Fz_{f,l} = \frac{1}{2} M_v \Big(\frac{l_r}{l} g - \frac{h_{COG}}{l} a_x \Big) - M_v \frac{l_r}{l} \frac{h_{roll,f}}{t} a_y \tag{A.4}$$

$$Fz_{f,r} = \frac{1}{2} M_v \Big(\frac{l_r}{l} g - \frac{h_{COG}}{l} a_x \Big) + M_v \frac{l_r}{l} \frac{h_{roll,f}}{t} a_y \tag{A.5}$$

$$Fz_{r,l} = \frac{1}{2} M_v \Big(\frac{l_f}{l} g + \frac{h_{COG}}{l} a_x \Big) - M_v \frac{l_f}{l} \frac{h_{roll,r}}{t} a_y \tag{A.6}$$

$$Fz_{r,r} = \frac{1}{2} M_v \Big(\frac{l_f}{l} g + \frac{h_{COG}}{l} a_x \Big) + M_v \frac{l_f}{l} \frac{h_{roll,r}}{t} a_y \tag{A.7}$$

In the above equations a_x represents the longitudinal acceleration, g the gravitational acceleration (set equal to $9.81 m/s^2$) and l the wheelbase of the vehicle. The roll dynamics are included by identifying the h_{roll} term, such that the vertical load transfer of the tires is in accordance with the IPG vehicle model. The h_{roll} term is identified using the validation manoeuvres described in section A.7, resulting in $h_{roll,f} = 0.05m$ and $h_{roll,r} = 0.35m$. Increasing h_{roll} will increase the effect of roll dynamics on vertical load transfer on the tires. For realistic roll dynamics, suspension kinematics should also be included in the model. However, for simplicity tuning the h_{roll} term is used in this study.

A.4. Lateral tyre force dynamics

The lateral tyre forces are determined using an adapted version of the Pacejka '94 tyre model described by equations A.8 to A.13:

$$Fy = coFy \cdot Fy0 \tag{A.8}$$

$$coFy = cos(A) \text{ where } -0.5\pi \leq A \leq 0.5\pi \tag{A.9}$$

$$A = \frac{am0 \cdot (1.4 - 0.5\mu)}{0.9} \cdot tan^{-1}\Big(\big(am2 \cdot cos(tan^{-1}(am_3 - \alpha_{ij}))\big) \cdot \kappa_{ij}\Big) \tag{A.10}$$

$$Fy0 = B \cdot sin(\boldsymbol{a_0} \cdot tan^{-1}(C \cdot \alpha)) \tag{A.11}$$

$$B = \mu Fz \cdot (\boldsymbol{a_1} F_z + \boldsymbol{a_2}) \tag{A.12}$$

$$C = \begin{cases} \frac{\boldsymbol{a_3} \cdot sin(2 \cdot tan^{-1}(Fz/\boldsymbol{a_4}))}{\boldsymbol{a_0} \cdot B} \text{ if } \boldsymbol{a_0} \cdot B \neq 0 \\ 0 \text{ if } \boldsymbol{a_0} \cdot B = 0 \end{cases} \tag{A.13}$$

In the above described equations F_z represents the tyre vertical load, α the tyre side slip and κ the longitudinal tyre slip. The tyre dynamics are modelled in CarMaker using Delft-tyre 6.1 with a Magic Formula steady-state slip model describing non-linear slip forces and moments. This model represents realistic tyre forces and has been extensively validated (TNO Automotive, 2008). However, Delft-tyre 6.1 is a protected tyre model which cannot be used in the simulator used in this experiment. Therefore, the tyre parameters $\boldsymbol{a_0}$ to $\boldsymbol{a_4}$ of the Pacejka'94 tyre model are identified to represent the characteristic of the Delft-tyre 6.1 model at different vertical tyre loads ($1000N$, $4000N$ and $8000N$). For this identification the longitudinal tyre slip is assumed to be small ($abs(\kappa) < 0.02$) since the longitudinal speed is constant during the experiment. Moreover, the camber angle and turnslip of the Delft-tyre 6.1 model are set to zero. To check if the Pacejka '94 model with identified parameters closely represents the Delft-tyre 6.1 model, these models are compared using the *Variance Accounted For (VAF)* metric. In Table A.1, the corresponding identified parameters $\boldsymbol{a_0}$ to $\boldsymbol{a_4}$ are given.

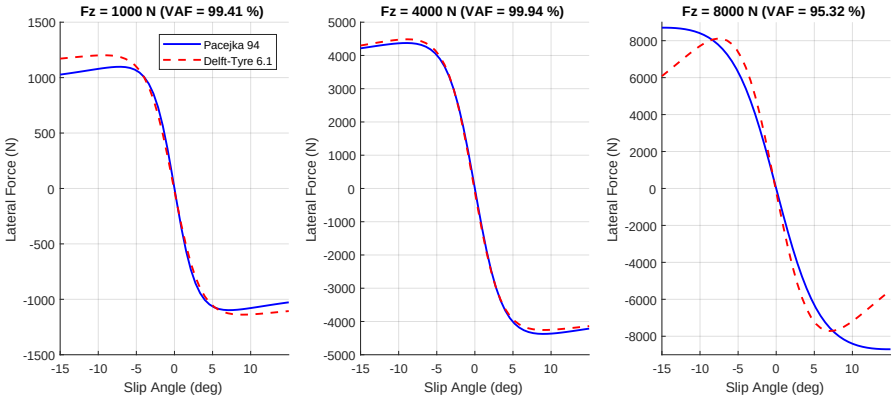

Figure A.1: Validation of the lateral tyre force model

Table A.1: tyre parameters of Pacejka'94 model to represent the Delft-tyre 6.1 model

tyre Parameter	Values
$\boldsymbol{a_0}$	1.47
$\boldsymbol{a_1}$	$-1.51 \cdot 10^{-3}$
$\boldsymbol{a_2}$	1.10
$\boldsymbol{a_3}$	1.58
$\boldsymbol{a_4}$	7.59

A.5. Self-aligning moment

In the HMI-lab vehicle model, there are no accurate steering dynamics i.e. the steering stiffness is constant, independent of vehicle slip. However, in a real vehicle, the steering stiffness decreases once the vehicle starts slipping. This steering stiffness mainly depends on the self-aligning moment of the tires. Consequently, calculation of the self-aligning moment should be added to the vehicle model. The model makes use of an adapted form of Pacejka's Magic formula from 1994. With Pacejka '94, the self aligning moment is calculated using the following empirical equation obtained from the ADAMS manual (MSC Software, 2010), where camber angle dynamics are neglected (equations A.14 to A.22):

$$M_z = M_{z0}(\alpha, F_z) \tag{A.14}$$

$$M_{z0} = \Big(D \cdot sin\big(C \cdot tan^{-1}(B \cdot X1 - E \cdot (B \cdot X1 - tan^{-1}(B \cdot X1)))\big)\Big) + S_v \tag{A.15}$$

The parameters of this equation i.e. D (Peak Factor), C (Shape Factor), B (Stiffness Factor), E (Curvature Factor), S_v (Vertical Shift) and S_h (Horizontal Shift) are determined as follows.

$$C = c_0 \tag{A.16}$$

$$D = c_1 \cdot F_z^2 + c_2 \cdot F_z \tag{A.17}$$

$$B = ((c_3 \cdot F_z^2 + c_4 \cdot F_z) \cdot e^{(} - c_5 * F_z))/(C \cdot D) \tag{A.18}$$

$$S_v = c_{14} \cdot F_z + c_{15} \tag{A.19}$$

$$S_h = c_{11} \cdot F_z + c_{12} \tag{A.20}$$

$$X1 = \alpha + S_h \tag{A.21}$$

$$E = min\Big((c_7 \cdot F_z^2 + c_8 \cdot F_z + c_9) \cdot (1 - (c_{20} \cdot sign(X1))), 1\Big) \tag{A.22}$$

Notice the dependency of this empirical equation of the self aligning moment on the parameters (c_0 to c_{20}). These parameters need to be adapted to the Delft-tyre 6.1 model which is used in CarMaker. The parameters are identified such that the self-aligning moment is represented for three different vertical tyre loads ($1000N$, $4000N$ and $8000N$) and the longitudinal slip is assumed to be small ($abs(\kappa) < 0.02$). In Figure A.2 the self-aligning moment for the three different tyre loads is given. The VAF values range between 83% (at $1000N$) and 97% ($8000N$). Moreover, the maximum self-aligning moment at a vertical load of $1000N$ is approximately $3Nm$, while for the vertical load of $8000N$ this is approximately $150Nm$. Therefore, the lower VAF value on the vertical tyre load of $1000N$ has a lower impact on the total self-aligning moment. Consequently the model with identified parameters is suitable for the experiment. The Corresponding parameters are summarized in Table A.2. A better estimation is possible using vertical load varying parameters (c_0 to c_{20}) of the self-aligning moment. However, for model efficiency and simplicity it is decided to keep these parameters constant.

Table A.2: tyre self-aligning moment parameters

Parameter	**Value**	**Parameter**	**Value**
c_0	2.30	c_8	0
c_1	2.95	c_9	-1.10
c_2	$-7.1339 \cdot 10^{-1}$	c_{11}	0
c_3	53.71	c_{12}	0
c_4	13.41	c_{14}	0
c_5	-0.10	c_{15}	0
c_7	$1.37 \cdot 10^{-2}$	c_{20}	$-2.15 \cdot 10^{-1}$

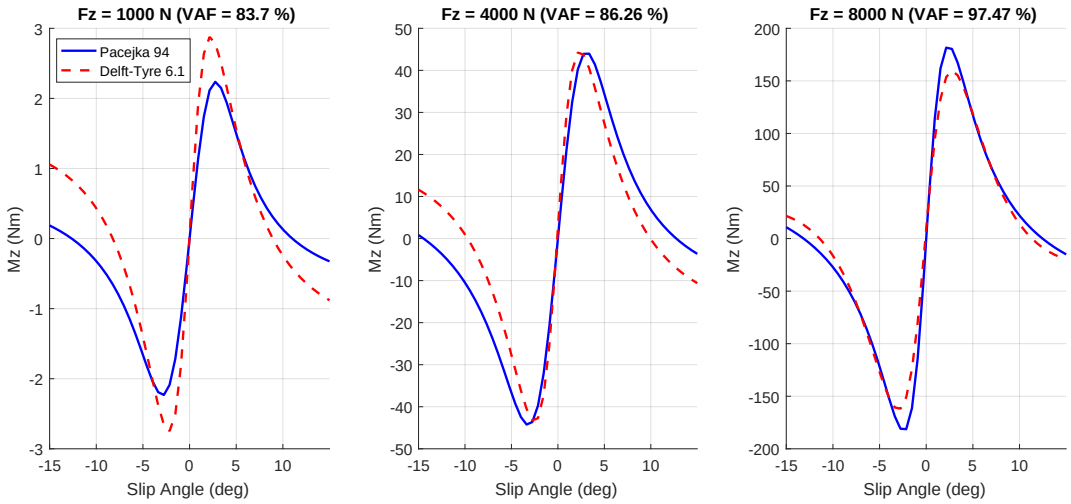

Figure A.2: Validation of the self-aligning moment tyre model

A.6. Steering dynamics

The steering dynamics are simplified to a second order rotational inertia damper system, where the equations of motion are given in equation A.23. M_z represents the self-aligning moment determined by the model described in equation A.14. Moreover, $Fy_f \cdot (r_{wheel} \cdot tan(\nu))$ represents the effect of mechanical trail times the lateral tyre force, which adds an additional torque on the steering rack. The mechanical trail is due to the caster angle ν.

$$I_{sw,col}\ddot{\delta}_{sw} + C_{sw}\dot{\delta}_{sw} = T_{sw} - \frac{M_z + Fy_f \cdot (r_{wheel} \cdot tan(\nu))}{u_{w-r} \cdot u_{r-sw}} + T_{assist} \tag{A.23}$$

The steering dynamics used in the simulation of the CarMaker vehicle is a Pfeffer steering model. The parameters corresponding to this steering model, are given in Table A.3. The sinusoidal steering torque manoeuvre described in section A.7 is used to identify the parameters of the simplified steering dynamics in the vehicle model (represented by equation A.23). In Figure A.3 can be seen that the steering dynamics closely represent the Pfeffer steering model.

Table A.3: Pfeffer steering model parameters

Parameters Steering column	**Value**	**Parameters Steering rack**	**Value**	**Parameters other parts**	**Value**
Inertia upper column $[kgm^2]$	0.03	**Mass including steering rods** $[kg]$	3.0	**Torsion bar stiffness** $[Nm/deg]$	2.0
Inertia lower column $[kgm^2]$	0.001	**Max steering rack travel** $[m]$	0.08	**Amplification factor for sping models**	0.0
Stiffness $[Nm/deg]$	12	**Friction force gradient** $[N/m]$	8e^{6}	**Stiffness of mesh** $[N/m]$	8e^{6}
Friction torque gradient $[Nm/rad]$	7000	**Friction force min/max** $[N]$	-75/75	**Stiffness of hardy disk** $[Nm/deg]$	3.0
Friction torque min/max $[Nm]$	-0.2/0.2	**Friction increase with pressure** $[N/bar]$	13	**IPGDriver steer by torque**	on
Damping coefficient $[Nms/rad]$	0.06	**Damping coefficient** $[Ns/m]$	550	**Rack travel to steering pinion angle** $[rad/m]$	100
Damping torque min/max $[Nm]$	0.1/0.1	**Damping force min/max** $[N]$	25	**Power assistance (EPS to Column)**	off

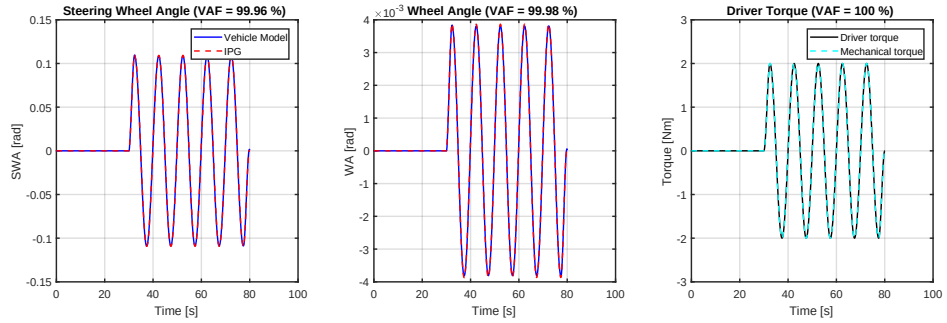

Figure A.3: Validation of the steering dynamics of the vehicle model

A.7. Vehicle validation manoeuvres

To validate the developed vehicle model the lateral dynamics represented by the lateral acceleration (a_y), -velocity (v_y) and yaw-rate (r) are compared with the CarMaker model for two different types of manoeuvres:

- *Sinusoidal* steering torque input with an amplitude of $2Nm$ and a frequency of $0.2Hz$. The vehicle is accelerating from 0 to $100km/h$ with an average acceleration of $2.23m/s^2$.
- *Skid-pad* test on a track with a radius of $100m$. On this track vehicle accelerates with an average acceleration of $0.25m/s^2$ from $30km/h$ until it the moment the vehicle departs from the road. The IPGDriver model (an adaptive driver mode with artificial intelligence) is used to control the steering and gas pedal input of the vehicle.

For the validation of the vehicle model only the lateral dynamics are validated, since these are important for the experiment. Therefore, the longitudinal acceleration from the IPG model is used as an input for the validation manoeuvres.

In Figure A.5, the validation of the Sinusoidal steering manoeuvre is shown. The VAF values indicate that the lateral dynamics of the vehicle model developed for this study closely represents the CarMaker model.

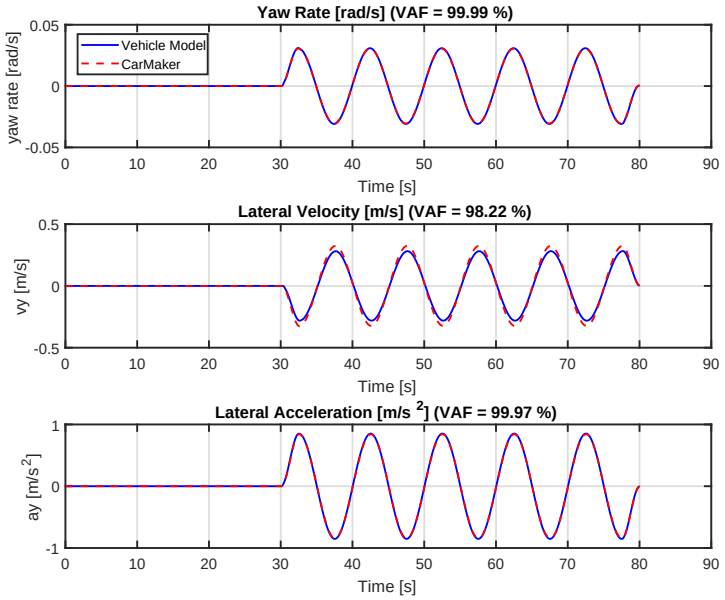

Figure A.4: Validation of the lateral vehicle dynamics with the sinusoidal steering manoeuvre

The dynamics of the vehicle near the VHL are validated using the skid-pad test manoeuvre. The VAF values show that the developed vehicle model closely represents the IPG vehicle model. Therefore, the vehicle model is well suited for the experiment.

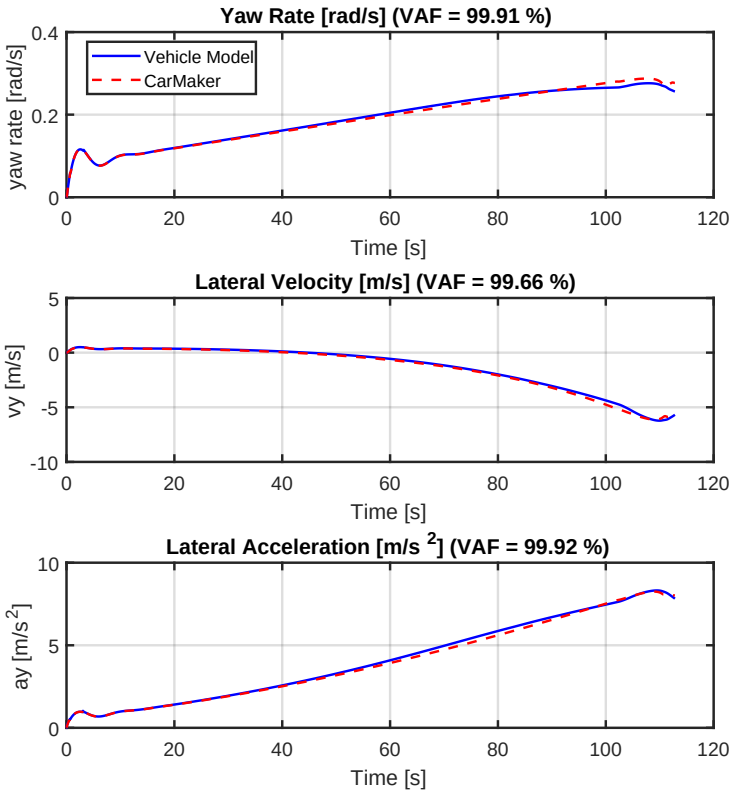

Figure A.5: Validation of the lateral vehicle dynamics with the skid-pad test

A.8. Vehicle parameters

The parameters corresponding to the CarMaker model and the developed vehicle model are given in Table A.4.

Table A.4: Vehicle paramters used for validation

Vehicle Mass (M_v)	$1856.2kg$	Steering Gear Ratio($u_{w-r} \cdot u_{r-sw}$)	20
Yaw moment of inertia (I_{zz})	$2806.023kg \cdot m^2$	Wheel Base (l)	$2.55m$
Front axel to COG (l_f)	$0.968m$	Rear axel to COG (l_r)	$1.582m$
Hight COG	$0.592m$	$h_{roll,f}$	$0.05m$
$h_{roll,r}$	$0.35m$	Tread front (t_f)	$0.756m$
Tread rear (t_r)	$0.756m$	Gravitational Acceleration (g)	$9.81m/s^2$

A.9. Vehicle configuration creation by modification of the tyre parameters

To create the different vehicle configurations which are used during the experiment, the lateral tyre force parameters ($\boldsymbol{a_0}$ to $\boldsymbol{a_4}$) of the Pacejka '94 tyre model are manipulated. The front wheel parameters will be separately identified from the rear wheel parameters, to enhance freedom in the design of the characteristics. In Figure A.6, the effect of manipulating the tyre parameters given in Table A.1 on the VHC at a vehicle speed of $100km/s$ and a steering velocity of $3deg/s$ is given. Indicating the effectiveness of manipulating the lateral tyre force parameters to create the different vehicle handling characteristics.

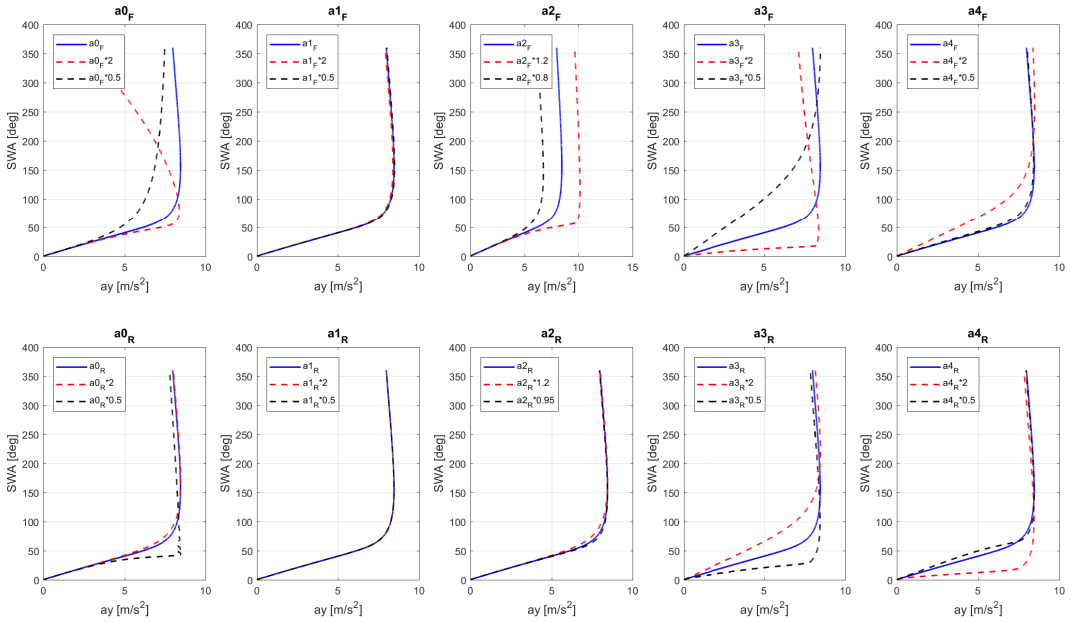

Figure A.6: Vehicle handling characteristic manipulation by modifying lateral tyre force parameters ($\boldsymbol{a_0}$ to $\boldsymbol{a_4}$) of the Pacejka '94 tyre model. For the top row, the front wheel lateral tyre force parameters are modified. For the bottom row the lateral tyre force parameters of the rear wheels are modified.

Figure A.6 is used as a reference to create the *Passive*, *Active* and *Active Sport* vehicle configurations. The tyre parameters corresponding to these characteristics are given in tables A.5 to A.7.

To check if the *Active* and *Active Sport* configurations have a more abrupt transfer into the VHL the jerk of the vehicle in lateral direction is used. In Figure A.7, the jerk of the three configurations at a vehicle speed of $100km/h$ and the steering wheel turned from 0 to $360deg$ with a steering velocity of $3deg/s$ is given. The jerk in lateral direction indicates that *Active* and *Active Sport* have a more abrupt change in lateral acceleration compared to the *Passive* configuration. Where the *Active Sport* one has the most abrupt change.

Table A.5: Pacejka '94 lateral tyre force parameters for *Passive* configuration

Passive Configuration			
Front Wheels		Rear Wheels	
a_0	1.9997	a_0	1.4720
a_1	$-1.5091 \cdot 10^{-3}$	a_1	$-1.5091 \cdot 10^{-3}$
a_2	1.0860	a_2	1.6504
a_3	1.5007	a_3	1.5797
a_4	7.5862	a_4	7.5862

Table A.6: Pacejka '94 lateral tyre force parameters for *Active* configuration

Active Configuration			
Front Wheels		Rear Wheels	
a_0	2.3073	a_0	1.0304
a_1	$-1.5091 \cdot 10^{-3}$	a_1	$-1.5091 \cdot 10^{-3}$
a_2	1.0893	a_2	1.003
a_3	1.5797	a_3	1.5797
a_4	7.5862	a_4	7.5862

Table A.7: Pacejka '94 lateral tyre force parameters for *Active Sport* configuration

Active Sport Configuration			
Front Wheels		Rear Wheels	
a_0	2.6150	a_0	1.1776
a_1	$-1.5091 \cdot 10^{-3}$	a_1	$-1.5091 \cdot 10^{-3}$
a_2	1.0849	a_2	1.003
a_3	1.8956	a_3	1.4217
a_4	7.5862	a_4	7.5862

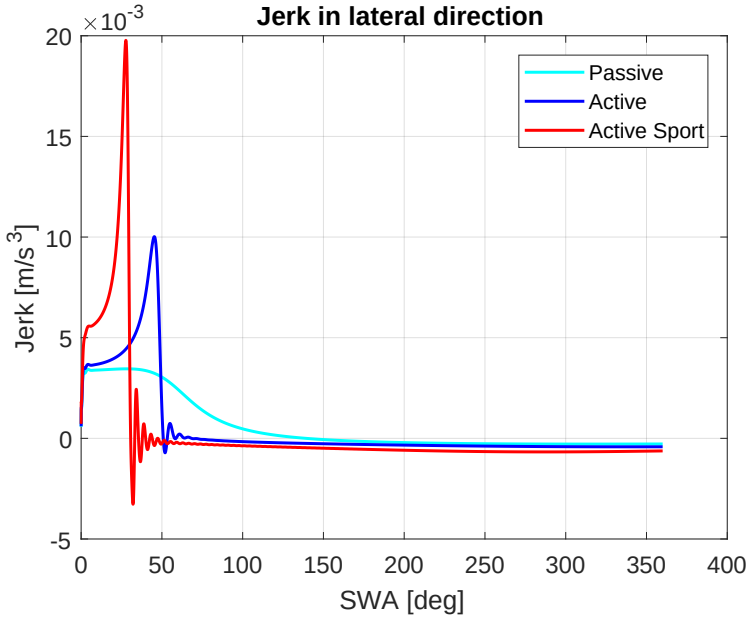

Figure A.7: Jerk in lateral direction of the vehicle. The vehicle is driving at a constant speed of $100 km/h$ and the steering wheel is turned from 0 to 360 degrees with a steering velocity of $3 deg/s$

B

VHL Inflection Points

B.1. VHL entry based on ESC activation which depends on vehicle yaw-rate

In this study it is very important to determine the point when a vehicle enters the VHL. For a conventional vehicle, the VHL is started when ESC is activated. In Lu et al., (2009) is mentioned ESC activates when absolute difference between the reference yaw-rate (equation B.1, which is based on linear dynamics of the vehicle) and the actual yaw-rate is greater than an activation limit (normally around 0.05).

$$r_{ref} = \frac{v_x}{L + (1 + K_{us} v_x^2)} \cdot \delta \tag{B.1}$$

v_x is the longitudinal vehicle speed, L the wheel base of the vehicle, δ the wheel angle and K_{us} the vehicle understeer gradient. The vehicle understeer gradient depends on the tire characteristics and is calculated using equation B.2.

$$K_{us} = \frac{Fz_f}{C_f} - \frac{Fz_r}{C_r} \tag{B.2}$$

The understeering gradients corresponding the the three vehicle configurations are given in Table B.1.

Table B.1: Understeering gradients for the different vehicle configurations

	Passive	*Active*	*Active Sport*
K_{us}	0.016	0.016	0.0

Using this strategy, the ESC system will be active too early. In Figure B.1, one can see that ESC is sometimes activated for the *Active Sport* and *Active* configurations due to "oversteering" behaviour (reference yaw-rate is lower than actual yaw-rate). However, the vehicle is configured such that it will understeer and the "oversteering" behaviour is caused by the extension of the linear handling region, changing the shape of a conventional vehicle handling characteristic. As a consequence, it will not be required for ESC to activate. This makes the *definition of ESC activation based on the yaw-rate as a VHL entry point invalid.*

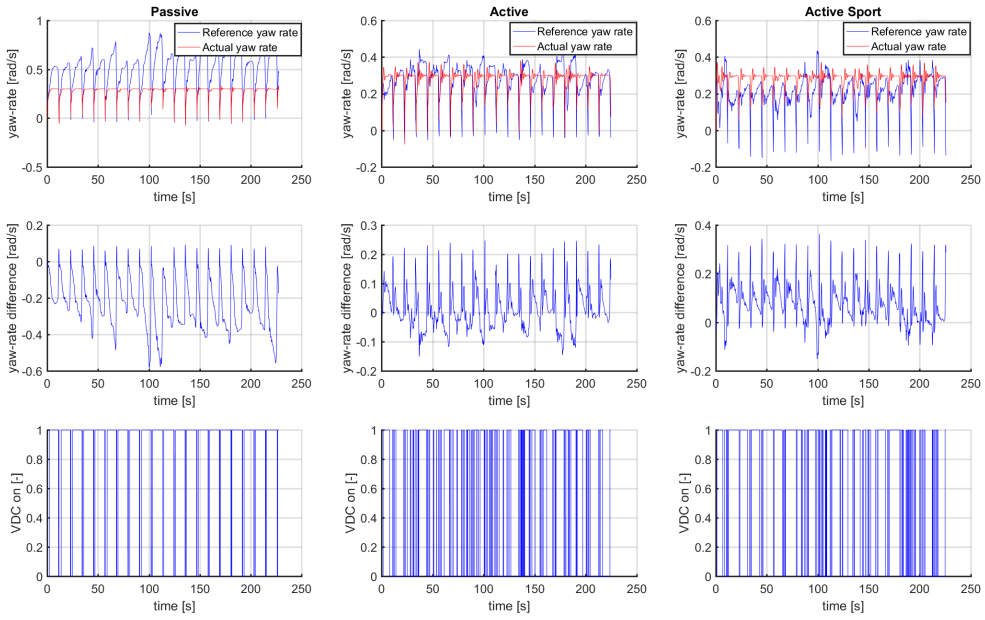

Figure B.1: Activation of ESC for the three vehicle configurations

B.2. VHL entry based on body slip angle of the vehicle

In the study of He et al. (2006) systems which can extend the linear handling region, such as ARS and AFS, are used in conjunction with ESC. ARS and AFS are used to extend the linear handling region by trying to follow the reference yaw-rate based on a linear vehicle model (as in equation B.1). ESC is used to guarantee stability, because if the vehicle enters the VHL the behaviour is unstable and it is difficult to control by the driver as shown in this thesis. ESC activation in the study of He et al. (2006) is based on the body slip angle, since it is directly related to the vehicle stability. The body slip angle should be bounded in the phase plane of the body slip angle gradient vs body slip angle. Vehicle body slip angle is calculated in the vehicle model by equation B.3. So, the usage of the vehicle body slip as entry point in the VHL looks promising to be used for this thesis. However, for the experiment, the vehicle dynamics are modified to ensure a constant longitudinal vehicle velocity (removed the effect of lateral vehicle velocity and yaw-rate on the longitudinal velocity). *Consequently, the body slip angle will not be a valid measure to represent entry into the VHL.*

$$\beta = \arctan \frac{v_y}{v_x} \tag{B.3}$$

B.3. VHL entry based on the inflection point of the vehicle handling characteristic

The inflection point depends on the vehicle velocity (which is constant in this study) and the steering velocity. The steering velocity will influence the roll of the vehicle and thereby the vertical load distribution. In Figure B.2, the effect of the steering velocity on the location of the inflection point can be observed. For an average steering velocity of $3deg/s$ the inflection point for the *Active Sport* configuration is at a steering angle of $30.7deg$. When the steering velocity is $10deg/s$ the inflection point shifts to a steering angle of $41.3deg$. This is a significant difference and therefore the *steering velocity should be included in the determination of the inflection point as entry point of the VHL.* Hence, the average steering velocity over the participants is calculated when the driver is entering the turn with the vehicle. Steering is assumed to be initiated when the drivers steer the steering wheel more than $3deg$ and have a steering velocity above $3deg/s$ (Theeuwes et al., 2002). The average steering velocity is taken from this point onwards until the steering velocity $< 3deg/s$ or reaches a steady state (in the *Passive* configuration since significantly more steering angle is required to go through the corner). The resulting average steering velocities are given in Table B.2.

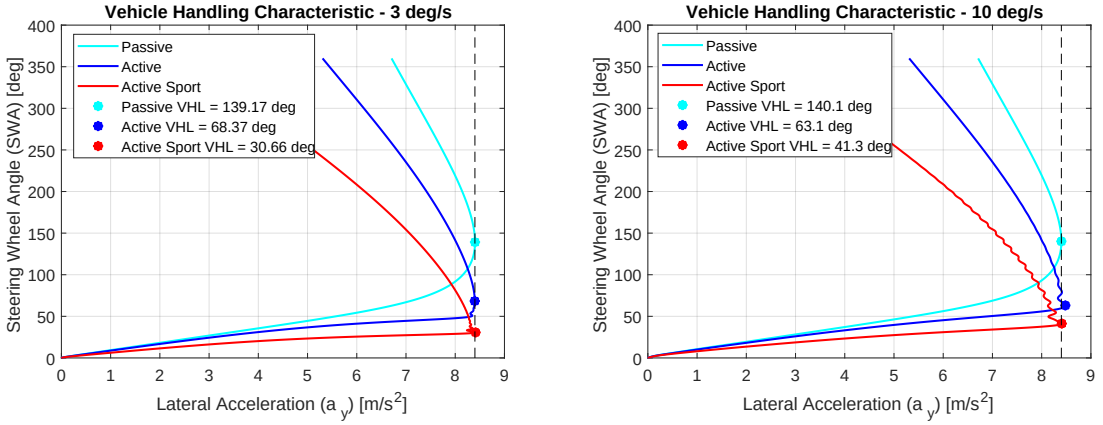

(a) $\dot{\delta} = 3deg/s$ (b) $\dot{\delta} = 10deg/s$

Figure B.2: The VHL entry point of the vehicle configurations depend on the steering velocity. For the *Active Sport* configuration the inflection point increases by $11deg$ when the steering velocity is increased from 3 to $10deg/s$. The inflection point of the other configurations also changes with steering velocity.

In Figure B.3 one can see the average steering velocity over all the participants during the main phase in the experiment. The average steering velocity used for the calculation of the inflection point is the average over the steering velocity in the blue area. These average steering velocities result in the inflection points given in Table B.2. When a driver is steering more than the steering angle corresponding to the inflection point, he is entering the VHL.

Table B.2: Average steering speed and corresponding VHL entry points

	Passive	*Active*	*Active Sport*
Steering speed (deg/s)	30.11	21.26	13.95
VHL Inflection point (deg)	**140.91**	**75.03**	**45.61**

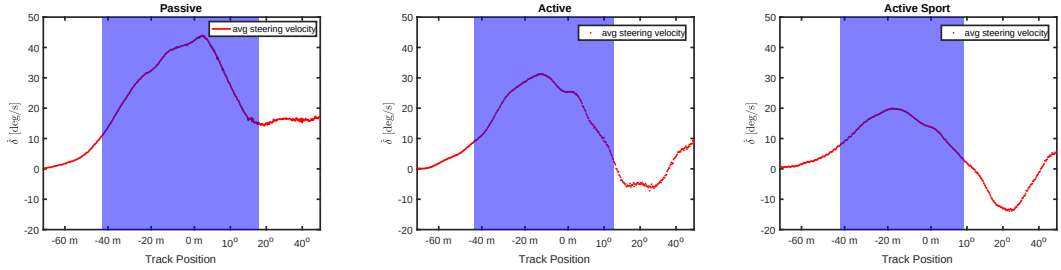

(a) *Passive* (b) *Active* (c) *Active Sport*

Figure B.3: The avarage steering velocity over all the participants for the three vehicle configurations. The blue area is the region over which the avarage entry steering velocity is calculated.

Figures B.4 to B.21 show the vehicle handling characteristics for all the participants obtained during the main phase of the experiment. The red lines represent a vehicle in the VHL according to the calculated inflection points. All these vehicle handling characteristics show, that the a_y will decrease when increasing the steering wheel angle in the red region, indicating that the inflection for each configuration correctly represent an entry in the VHL.

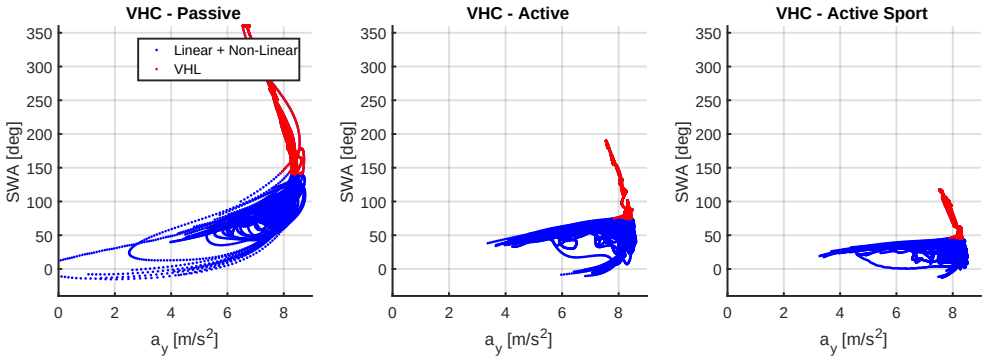

Figure B.4: VHC Participant 1. Blue line represents vehicle not in VHL and red line reprents vehicle in VHL

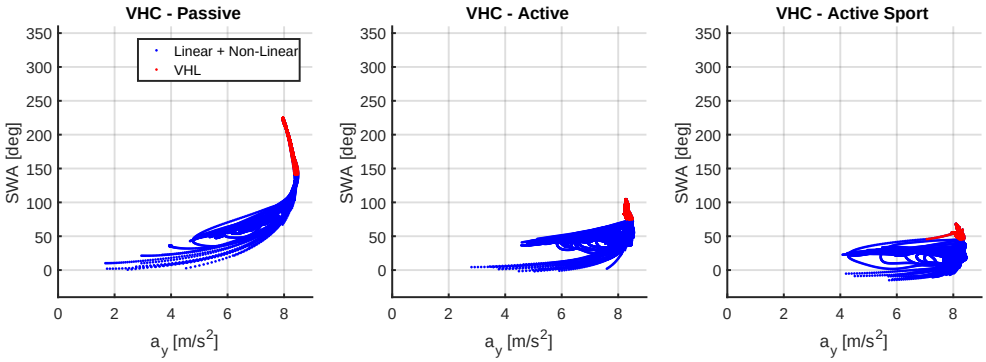

Figure B.5: VHC Participant 2. Blue line represents vehicle not in VHL and red line reprents vehicle in VHL

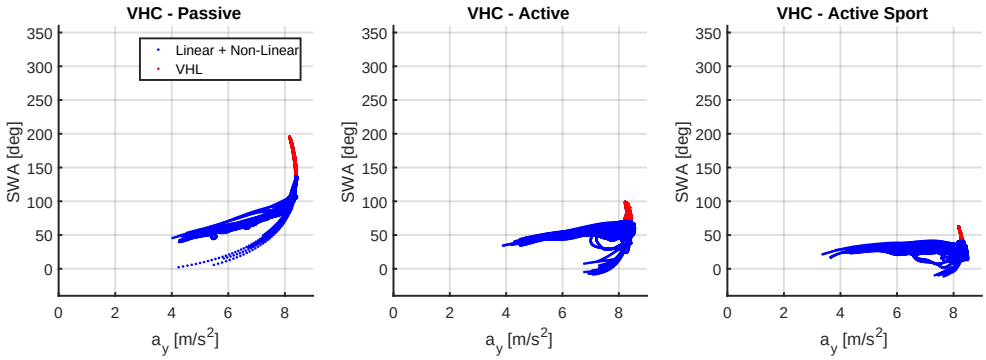

Figure B.6: VHC Participant 3. Blue line represents vehicle not in VHL and red line reprents vehicle in VHL

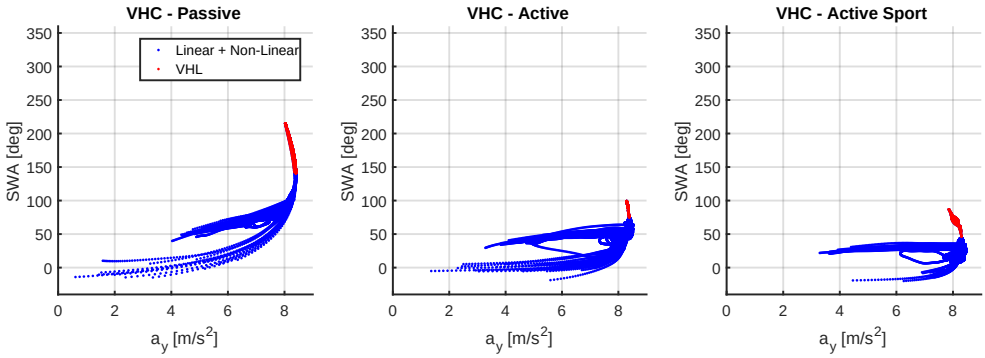

Figure B.7: VHC Participant 4. Blue line represents vehicle not in VHL and red line reprents vehicle in VHL

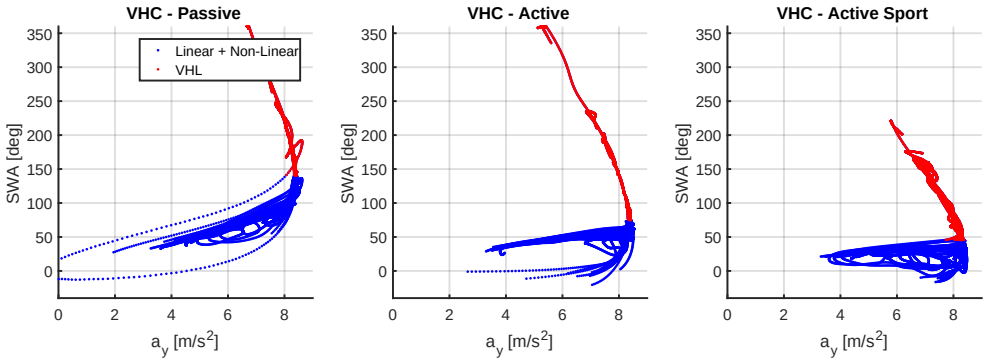

Figure B.8: VHC Participant 5. Blue line represents vehicle not in VHL and red line reprents vehicle in VHL

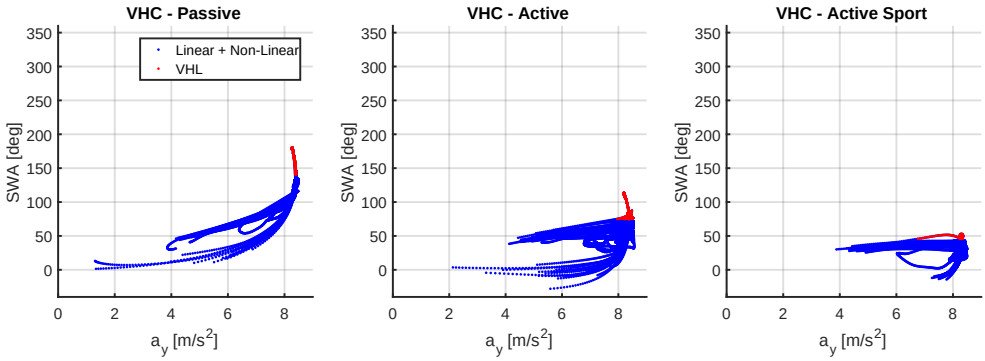

Figure B.9: VHC Participant 6. Blue line represents vehicle not in VHL and red line reprents vehicle in VHL

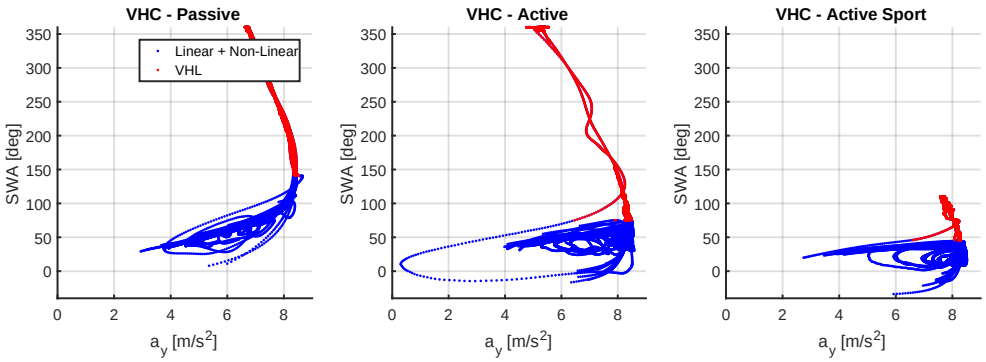

Figure B.10: VHC Participant 7. Blue line represents vehicle not in VHL and red line reprents vehicle in VHL

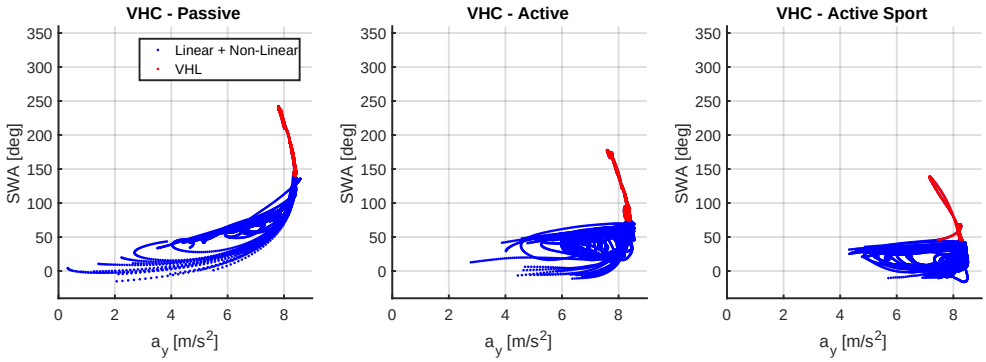

Figure B.11: VHC Participant 8. Blue line represents vehicle not in VHL and red line reprents vehicle in VHL

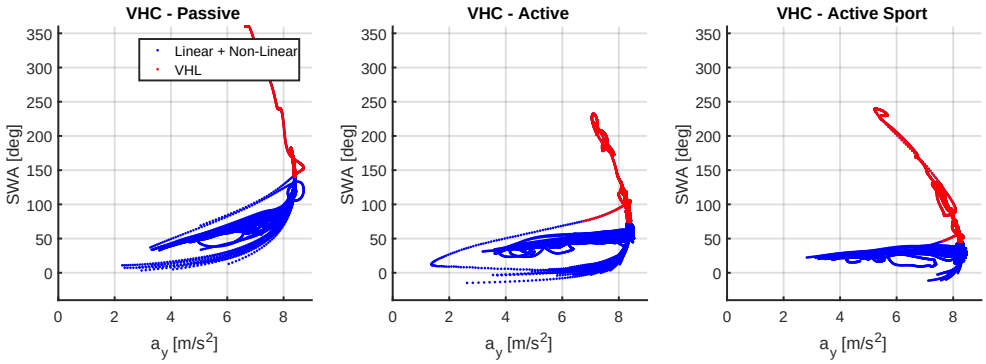

Figure B.12: VHC Participant 9. Blue line represents vehicle not in VHL and red line reprents vehicle in VHL

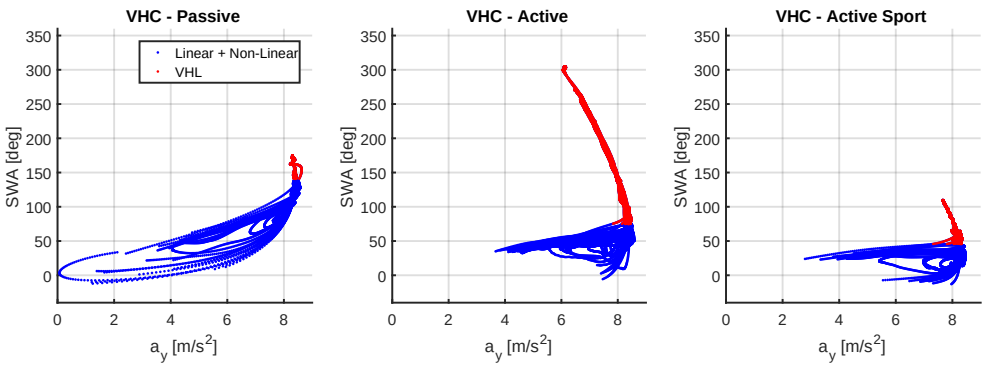

Figure B.13: VHC Participant 10. Blue line represents vehicle not in VHL and red line reprents vehicle in VHL

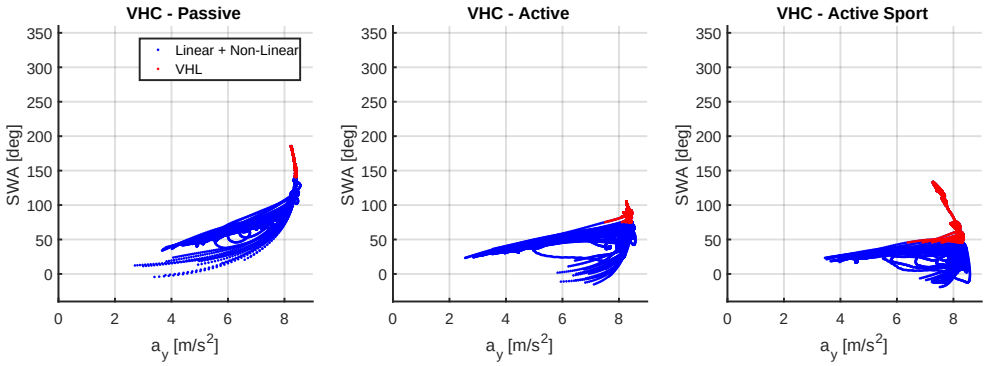

Figure B.14: VHC Participant 11. Blue line represents vehicle not in VHL and red line reprents vehicle in VHL

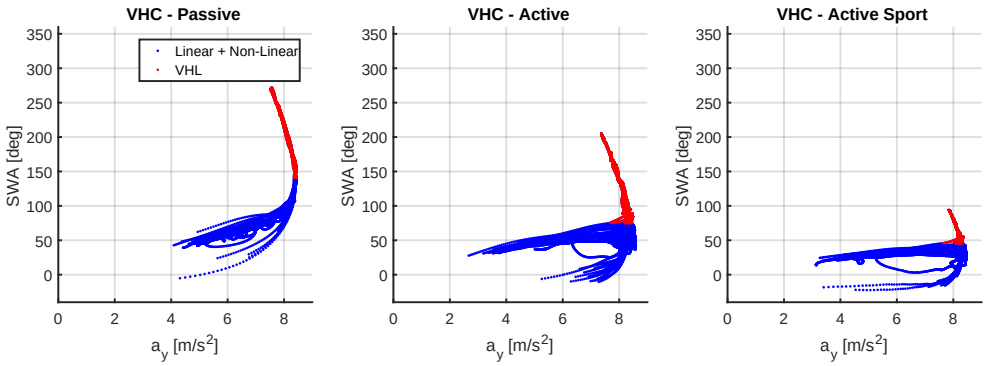

Figure B.15: VHC Participant 12. Blue line represents vehicle not in VHL and red line reprents vehicle in VHL

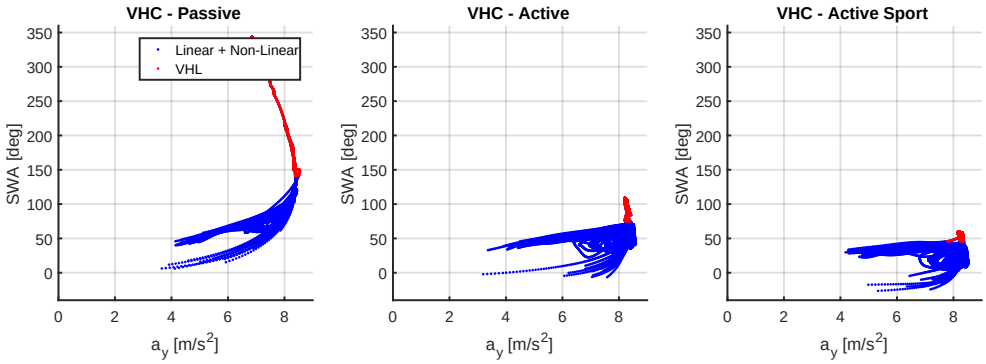

Figure B.16: VHC Participant 13. Blue line represents vehicle not in VHL and red line reprents vehicle in VHL

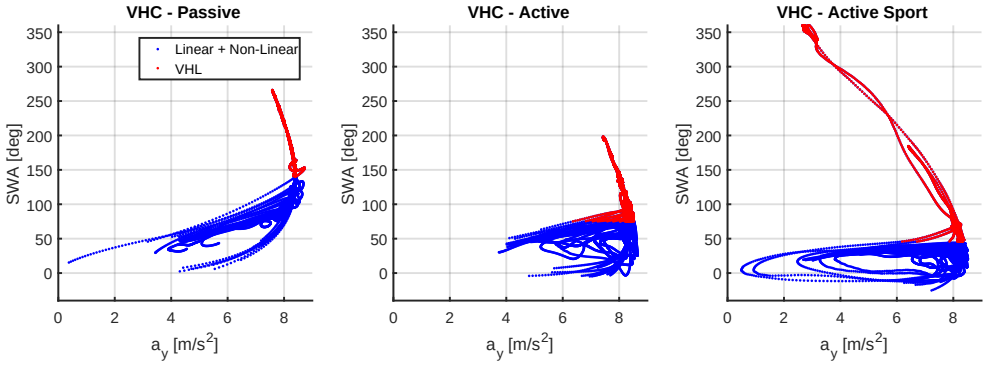

Figure B.17: VHC Participant 14. Blue line represents vehicle not in VHL and red line reprents vehicle in VHL

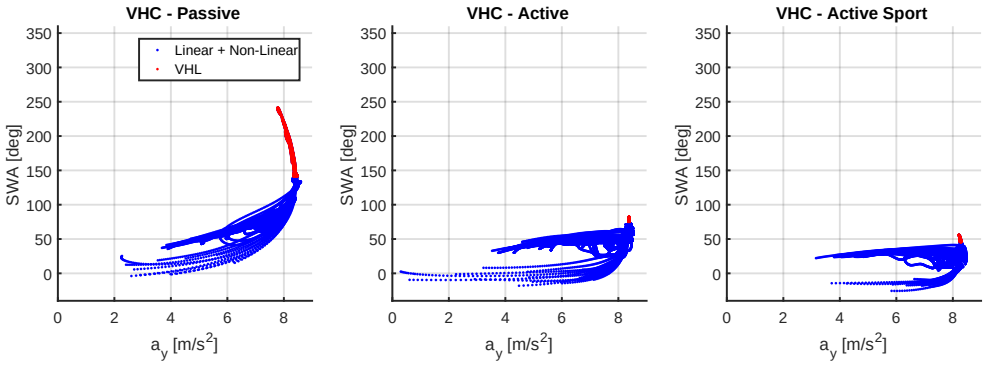

Figure B.18: VHC Participant 15. Blue line represents vehicle not in VHL and red line reprents vehicle in VHL

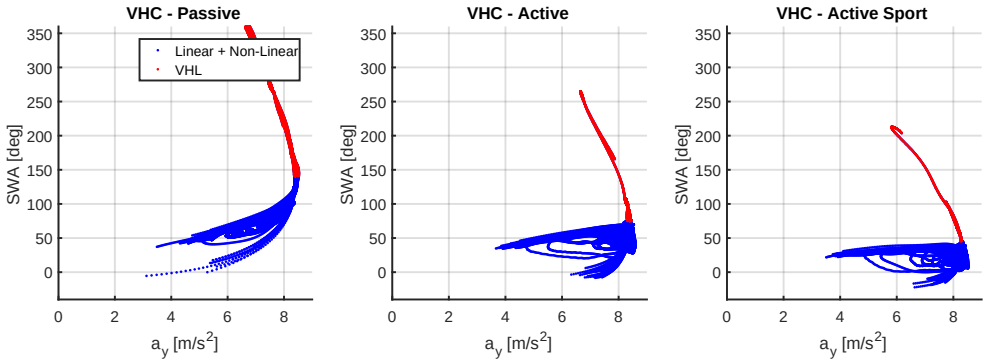

Figure B.19: VHC Participant 16. Blue line represents vehicle not in VHL and red line reprents vehicle in VHL

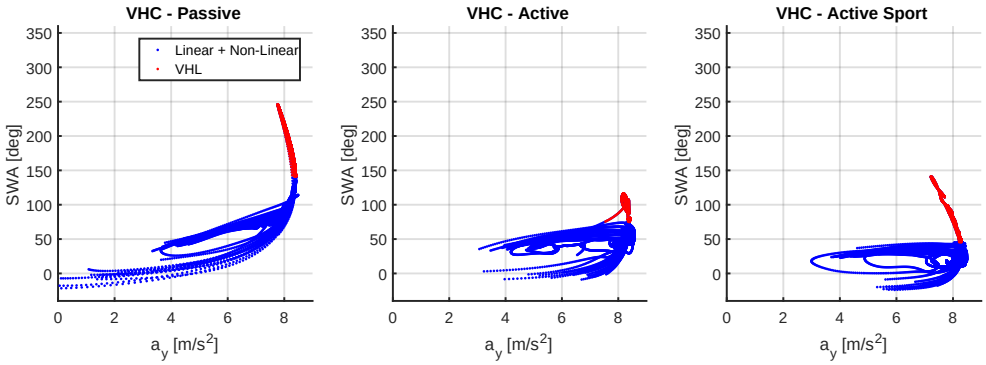

Figure B.20: VHC Participant 17. Blue line represents vehicle not in VHL and red line reprents vehicle in VHL

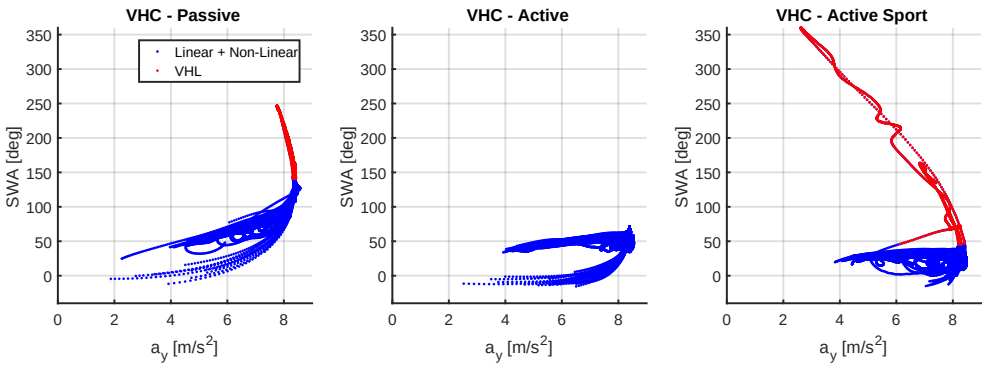

Figure B.21: VHC Participant 18. Blue line represents vehicle not in VHL and red line reprents vehicle in VHL

C

Steering Feel

As explained in the paper, it is not possible to use the empirical equations of the self-aligning moment for the steering feel. The reason for this is that, instead of applying ARS or TV, the *Active* and *Active Sport* configurations are created by modification of the lateral tire force parameters of the Pacejka '94 tire model. Therefore, the steering feels are created manually. In this Appendix, the rotational stiffness vs steering wheel angle and measured steering toque vs steering wheel angle for the *Active*, *Active Sport* and *Passive* configurations are presented.

C.1. Steering stiffness versus steering wheel angle

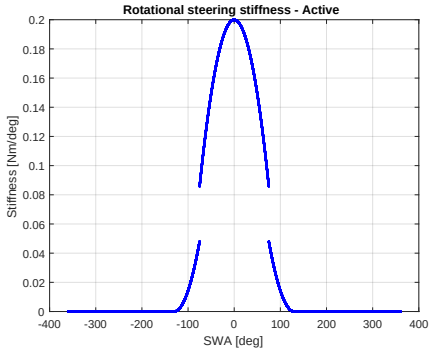

Figure C.1: Steering stiffness vs steering wheel angle for the *Active* configuration. The jump is stiffness is used to create the abrupt change in stiffness when entering the VHL at $75deg$ steering angle.

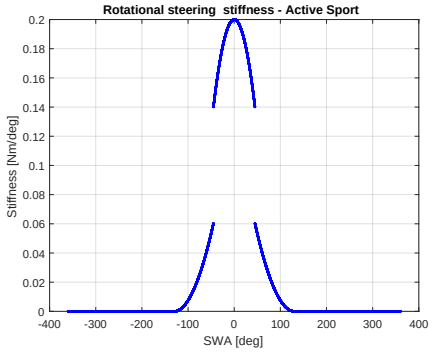

Figure C.2: Steering stiffness vs steering wheel angle for the *Active Sport* configuration. The jump is stiffness is used to create the abrupt change in stiffness when entering the VHL at $45deg$ steering angle.

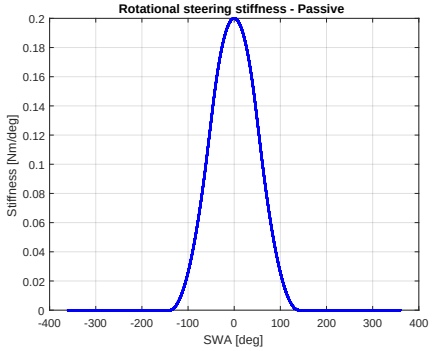

Figure C.3: Steering stiffness vs steering wheel angle for the *Passive* configuration. The steering stiffness gradually goes to zero which is reached at 140 degrees steering angle

C.2. Measured steering torque versus steering wheel angle

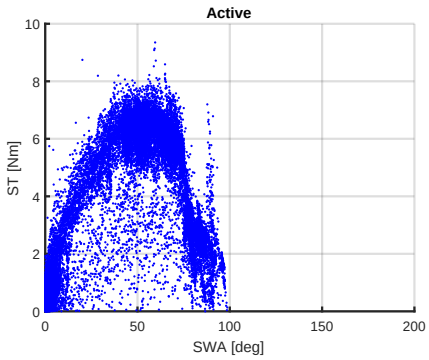

Figure C.4: Steering torque vs steering wheel angle for the *Active* configuration for one participant. Once VHL is entered ($75deg$) the measured data shows a drop in applied steering torque

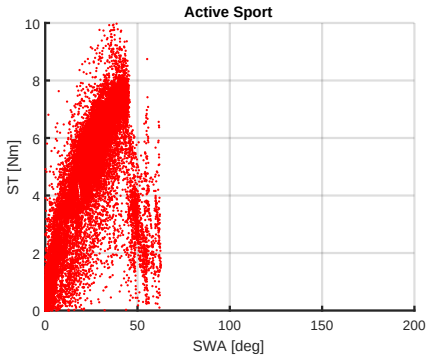

Figure C.5: Steering torque vs steering wheel angle for the *Active Sport* configuration for one participant. Once VHL is entered ($45deg$) the measured data shows a drop in applied steering torque

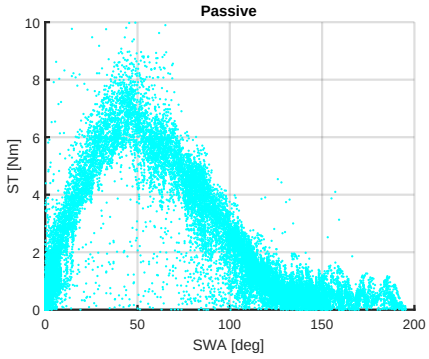

Figure C.6: Steering torque vs steering wheel angle for the *Passive* configuration for one participant. The steering torque gradually drops to the VHL at approximately $140deg$

D

Tracks during the experiment

D.1. Familiarization phase track

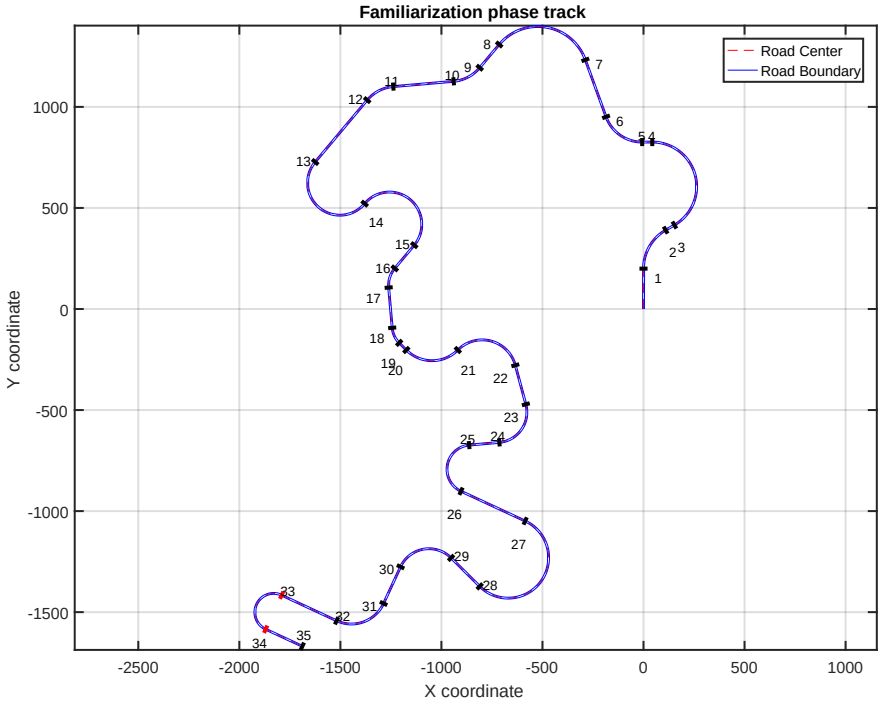

Figure D.1: Track used during the familiarization phase of the experiment, last turn between the red lines is the catch trial turn 1. The dimensions for all the 35 segments of this track are given in table D.1.

Table D.1: Track dimensions - Familiarization phase

Section	Type	Length/ Angular Span	Radius (m)	Section	Type	Length/ Angular Span	Radius (m)
1	Straight	200 m	N.A.	19	Corner	40 deg	-120
2	Corner	60 deg	220	20	Straight	50 m	N.A.
3	Straight	50 m	N.A.	21	Corner	90 deg	-180
4	Corner	150 deg	-220	22	Corner	120 deg	170
5	Straight	50 m	N.A.	23	Straight	200 m	N.A.
6	Corner	70 deg	190	24	Corner	100 deg	150
7	Straight	300 m	N.A.	25	Straight	150 m	N.A.
8	Corner	120 deg	-250	26	Corner	150 deg	-120
9	Straight	150 m	N.A.	27	Straight	350 m	N.A.
10	Corner	45 deg	190	28	Corner	200 deg	200
11	Straight	300 m	N.A.	29	Straight	200 m	N.A.
12	Corner	45 deg	-190	30	Corner	110 deg	-155
13	Straight	400 m	N.A.	31	Straight	200 m	N.A.
14	Corner	180 deg	-160	32	Corner	90 deg	175
15	Corner	180 deg	160	33	Straight	300 m	N.A.
16	Straight	150 m	N.A.	34	Corner	180 deg	-93
17	Corner	45 deg	-130	35	Straight	200 n	N.A.
18	Straight	200 m	N.A.				

D.2. Oval track training and main phase

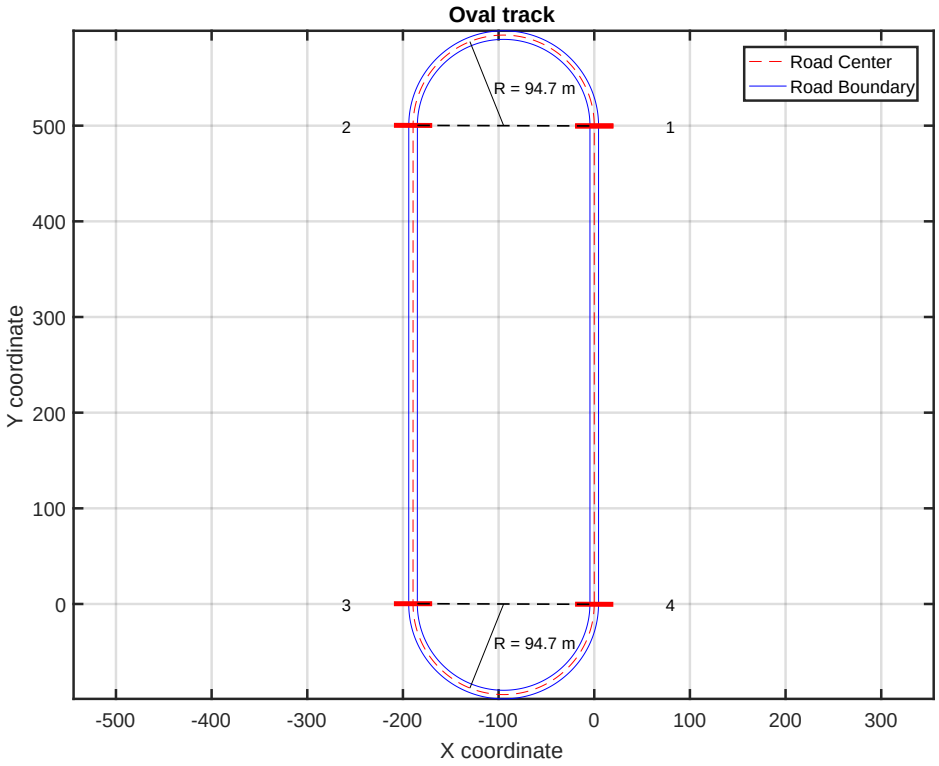

Figure D.2: Oval track, the dimensions for all the segments of this track are given in table D.2.

Table D.2: Track dimensions - Oval track

Section	Type	Length/ Angular Span	Radius (m)
1	Straight	500 m	N.A.
2	Corner	180 deg	-94.7
3	Straight	500 m	N.A.
4	Corner	180 deg	-94.7

D.3. Post experiment run track

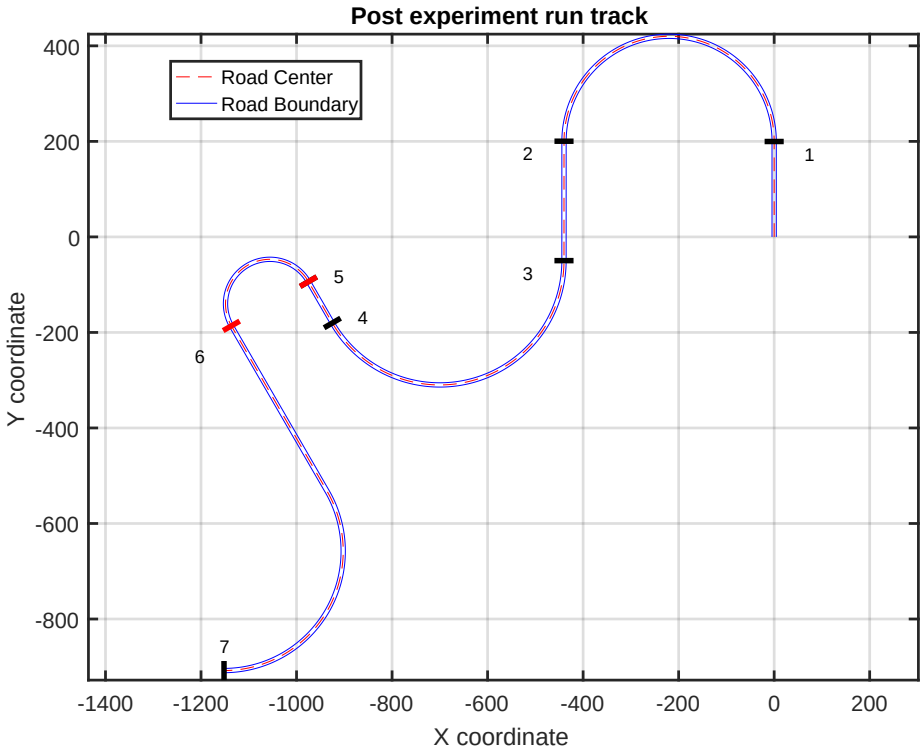

Figure D.3: Track during the post experimental run of the experiment. The turn between the red lines is the catch trial turn 2. The dimensions for all the 8 segments of this track are given in table D.3.

Table D.3: Track dimensions Post experiment run

Section	Type	Length/ Angular Span	Radius (m)	Section	Type	Length/ Angular Span	Radius (m)
1	Straight	200 m	N.A.	5	Straight	100 m	N.A.
2	Corner	180 deg	-220	6	Corner	180 deg	-93
3	Straight	250 m	N.A.	7	Straight	400 m	N.A.
4	Corner	150 deg	260	8	Corner	120 deg	250

E

Informed Consent + Participant Instructions

CONSENT FOR HUMAN SUBJECT RESEARCH

Vehicle control performance study

This is an invitation to participate in the research of master student R.M.A. Bekkers. The experiment takes place in the HMI lab driving simulator at the aerospace faculty of Delft university of technology. It is a study about the vehicle control performance of a human, where we want to investigate the difference in vehicle control of a conventional vehicle and a vehicle which can steer with four wheels. You are invited to participate in this research because you have a driving licence for at least one year.

Description of the experiment: It is a fixed base driving simulator experiment. Your task will be to control three different vehicle configurations on an oval track. Before starting a condition you can practice on a training track to get used to the simulator. Subsequently, you will train with a configuration on the oval track, where you need to successfully complete 4 consecutive turns to continue to the main part of the experiment. In the main part of the experiment you will drive again on the same oval track for 10 laps (20 turns) followed by a simple winding road which you will drive for 2 minutes. Each condition is approximately 25 minutes, making the total length of your participation around 75 minutes. During the experiment, the vehicle speed is held constant by a cruise control system. Therefore, you will be only able to change the vehicle trajectory via the steering wheel. Your goal during the experiment will be to score the highest number of points displayed by a counter on the vehicle dashboard. You will receive points when you are driving on the track, the more you are in the left lane, the higher the number of points you score. However, if you cross the inner or outer road boundary, you will lose all your points and you have to start collecting points again. The experimental results will be treated anonymously.

Research goals: The goal of this research is to get a better understanding of the the vehicle control performance of a human with different type of vehicles. The recorded data in this experiment is the steering wheel input and the simulated vehicle motion. The data obtained via this research will be used for publication in a paper.

Risks and benefits: There is a minor risk of simulator sickness, when you are not feeling comfortable you are free to abort the experiment. We cannot guarantee or promise that you as a participant will receive any benefits from this research, but there are expected benefits for the society.

Participants rights: Participating in this experiment is entirely voluntary, you are free to abort participation at any time and refusal of participation will involve no penalty. You are requested to read and understand the information in this consent, prior to deciding whether or not to participate. You can ask questions about anything related to this experiment anytime.

Payment: Participating in this experiment will be entirely voluntary.

Contact details: For more information or concerns about this experiment please feel free to contact:

R.M.A. Bekkers
Faculty of Mechanical Engineering, Delft University of Technology
Mekelweg 2, 2628 CD Delft, Phone: +31-657225547 , Email: R.M.A.Bekkers@student.tudelft.nl

I acknowledge that I completely understand this consent and I agree to participate in this study.

Signature of participant _____ Date _____

Participant Instructions

for the research by R.M.A. Bekkers

This research is conducted in order to get a better understanding of the the vehicle control performance of a human with different type of vehicles.

Location: HMI lab driving simulator, Faculty of Aerospace Engineering, Delft University of Technology

- Please sit down behind the steering wheel in the driving simulator
- Please use the provided headphones, to prevent any disturbance during the experiment
- During the experiment you will have to drive three different vehicle configurations
- The coordinator will start the simulator and initialize one out of the thee different vehicle configurations
- Before each the experiment starts there will be a training track where you can get used to the simulator and the vehicle dynamics
- Subsequently the vehicle will be placed on an oval track where you will have to try to keep the vehicle on the track
- When the simulation has started you will see two counters below the speedometer in the dashboard. The left counter shows you the number of points you score in the last turn while the right counter shows the cumulative score. When you are driving on the track you receive points and when you cross the road boundary all your points will be lost. The more you are driving in the left lane, the higher the number of points you receive. Be aware that you can score points only in the turns and the first couple of meters before a turn starts. On the straight lines, except for the final 30 meters before the turn, no points can be gained or lost.
- Please be aware that steering maximally does not lead to the optimal performance. This will lead to a point that your vehicle is slipping a lot and you are unable to hold the turn.
- Once you have successfully completed 4 consecutive turns with a minimum number of 50 points per turn you are allowed to continue to the main part of the experiment
- In the main part of the experiment you will drive again on the same oval track for 10 laps (20 turns) followed by a simple winding road which you will drive for 2 minutes.
- When completing a condition you will have a two minute break. However, if you prefer a longer break you are free to take your time. Subsequently, a new condition will start.

Participant Questionnaire

Participant Number	
Gender	Male/Female
Age	
Driving Licence	
How long do you hace a licence (years)	
How often do you drive per month	
Did you ever do a skid training (yes/no)	
Do you play racing games once a week (yes/no)	

F

Spearman Correlation Matrices

This appendix will show the spearman correlations between all dependent measures and participant characteristics for each configuration in a matrix. To obtain these Spearman correlations the data is first converted to ranks. A correlation between 0.1 and 0.15 is considered as a small effect. A correlation around 0.25 is a medium effect and correlations greater than 0.4 is a large effect (Cohen, 1988).

F.1. Passive vehicle

Table F.1: Spearman Correlation Matrix for the **Passive** vehicle configuration, RD is road departure

Passive	RD in VHL(%)	Turns in VHL (%)	Turns RD out (%)	Turns RD (%)	Turns RD in (%)	Turns training phase (-)	mean SRR (rev/s)	mean ABS ST (Nm)	Cumulative score (-)	Summed lap scores (-)	Driver age	Years Licence	Monthly Driving	Skid Training	Racing Games
RD in VHL (%)	1.00	0	0	0	0	0	0	0	0	0	0	0	0	0	0
Turns in VHL (%)	0.24	1.00	0	0	0	0	0	0	0	0	0	0	0	0	0
Turns RD out (%)	0.89	0.23	1.00	0	0	0	0	0	0	0	0	0	0	0	0
Turns RD (%)	0.86	0.18	0.98	1.00	0	0	0	0	0	0	0	0	0	0	0
Turns RD in (%)	0.04	0.05	0.08	0.21	1.00	0	0	0	0	0	0	0	0	0	0
Turns training phase (-)	-0.13	-0.11	-0.19	-0.18	0.07	1.00	0	0	0	0	0	0	0	0	0
mean SRR (rev/s)	-0.11	0.06	0.01	0.09	0.20	0.24	1.00	0	0	0	0	0	0	0	0
mean ABS ST (Nm)	0.22	0.23	0.34	0.34	0.39	-0.14	0.12	1.00	0	0	0	0	0	0	0
Cumulative score (-)	-0.70	-0.19	-0.63	-0.65	-0.38	0.03	-0.10	-0.43	1.00	0	0	0	0	0	0
Summed lap scores (-)	-0.56	-0.24	-0.57	-0.55	-0.02	0	0.04	-0.22	0.66	1.00	0	0	0	0	0
Driver age	-0.13	0.29	-0.18	-0.16	0.40	0.11	0.15	0.48	-0.18	-0.11	1.00	0	0	0	0
Years Licence	-0.07	0.31	-0.13	-0.11	0.35	0	0.20	0.52	-0.20	-0.14	0.93	1.00	0	0	0
Monthly Driving	0.23	0.04	0.14	0.05	-0.26	-0.38	-0.35	-0.14	-0.17	-0.16	0.14	0.20	1.00	0	0
Skid Training	0.54	-0.12	0.41	0.38	0.07	-0.43	-0.43	0.27	-0.49	-0.18	0.04	0.14	0.37	1.00	0
Racing Games	0.04	0.03	0.01	-0.01	-0.24	-0.35	-0.43	-0.06	-0.01	-0.13	-0.35	-0.23	-0.01	0.48	1.00

F.2. Active vehicle

Table F.2: Spearman Correlation Matrix for the **Active** vehicle configuration, RD is road departure

Active	RD in VHL(%)	Turns in VHL (%)	Turns RD out (%)	Turns RD (%)	Turns RD in (%)	Turns training phase (-)	mean SRR (rev/s)	mean ABS ST (Nm)	Cumulative score (-)	Summed lap scores (-)	Driver age	Years Licence	Monthly Driving	Skid Training	Racing Games
RD in VHL (%)	1.00	0	0	0	0	0	0	0	0	0	0	0	0	0	0
Turns in VHL (%)	0.04	1.00	0	0	0	0	0	0	0	0	0	0	0	0	0
Turns RD out (%)	0.64	0.22	1.00	0	0	0	0	0	0	0	0	0	0	0	0
Turns RD (%)	0.49	0.36	0.75	1.00	0	0	0	0	0	0	0	0	0	0	0
Turns RD in (%)	0.09	0.38	0.20	0.76	1.00	0	0	0	0	0	0	0	0	0	0
Turns training phase (-)	0.35	0.31	0.36	0.27	0.09	1.00	0	0	0	0	0	0	0	0	0
mean SRR (rev/s)	0.15	0.46	0.13	0.03	-0.06	0.21	1.00	0	0	0	0	0	0	0	0
mean ABS ST (Nm)	-0.37	-0.70	-0.52	-0.73	-0.61	-0.47	-0.50	1.00	0	0	0	0	0	0	0
Cumulative score (-)	-0.38	-0.24	-0.76	-0.79	-0.47	-0.01	-0.16	0.55	1.00	0	0	0	0	0	0
Summed lap scores (-)	-0.54	0.13	-0.72	-0.54	-0.16	-0.17	-0.30	0.32	0.67	1.00	0	0	0	0	0
Driver age	-0.32	0.16	0.02	-0.18	-0.28	-0.12	0.29	0.07	-0.18	0.03	1.00	0	0	0	0
Years Licence	-0.34	0.15	-0.12	-0.32	-0.39	-0.21	0.30	0.16	0	0.20	0.93	1.00	0	0	0
Monthly Driving	-0.20	-0.08	-0.09	-0.12	0.01	-0.23	0.14	0.13	0.02	0.14	0.14	0.20	1.00	0	0
Skid Training	0.05	-0.17	0.04	-0.19	-0.22	0.25	-0.17	0.09	0.23	0.31	0.04	0.14	0.37	1.00	0
Racing Games	0.07	-0.36	-0.09	-0.31	-0.34	-0.13	-0.29	0.32	0.42	0.16	-0.35	-0.23	-0.01	0.48	1.00

F.3. Active Sport vehicle

Table F.3: Spearman Correlation Matrix for the **Active Sport** vehicle configuration, RD is road departure

Active Sport	RD in VHL(%)	Turns in VHL (%)	Turns RD out (%)	Turns RD (%)	Turns RD in (%)	Turns training phase (-)	mean SRR (rev/s)	mean ABS ST (Nm)	Cumulative score (-)	Summed lap scores (-)	Driver age	Years Licence	Monthly Driving	Skid Training	Racing Games
RD in VHL (%)	1.00	0	0	0	0	0	0	0	0	0	0	0	0	0	0
Turns in VHL (%)	0.05	1.00	0	0	0	0	0	0	0	0	0	0	0	0	0
Turns RD out (%)	0.82	0.11	1.00	0	0	0	0	0	0	0	0	0	0	0	0
Turns RD (%)	0.79	0.09	0.86	1.00	0	0	0	0	0	0	0	0	0	0	0
Turns RD in (%)	0.20	0.14	0.06	0.50	1.00	0	0	0	0	0	0	0	0	0	0
Turns training phase (-)	0.07	-0.44	-0.13	-0.11	-0.05	1.00	0	0	0	0	0	0	0	0	0
mean SRR (rev/s)	-0.05	0.40	0.23	0.26	0.06	-0.25	1.00	0	0	0	0	0	0	0	0
mean ABS ST (Nm)	-0.48	-0.03	-0.50	-0.45	-0.07	0.26	0.22	1.00	0	0	0	0	0	0	0
Cumulative score (-)	-0.22	-0.17	-0.56	-0.61	-0.44	0.13	-0.24	0.22	1.00	0	0	0	0	0	0
Summed lap scores (-)	-0.64	0.23	-0.81	-0.77	-0.09	0.04	-0.22	0.46	0.55	1.00	0	0	0	0	0
Driver age	-0.06	-0.06	0.17	-0.06	-0.35	0.52	0.35	0.40	-0.16	-0.09	1.00	0	0	0	0
Years Licence	-0.15	-0.06	0.05	-0.17	-0.41	0.52	0.40	0.57	-0.04	0	0.93	1.00	0	0	0
Monthly Driving	-0.16	-0.30	-0.14	-0.14	0.07	-0.02	0.12	0.23	-0.04	-0.14	0.14	0.20	1.00	0	0
Skid Training	-0.06	0.18	-0.17	-0.36	-0.31	-0.05	0.04	-0.06	0.32	0.26	0.04	0.14	0.37	1.00	0
Racing Games	0.01	-0.03	-0.07	-0.27	-0.42	-0.19	-0.14	-0.20	0.31	0.16	-0.35	-0.23	-0.01	0.48	1.00

G

Extensive Results

This Appendix will start with the raw data and statistical analysis of the metrics and other results shown in Table 5 of the paper (sections G.1 to G.13). Subsequently, if the VHL entry point would be based on the steering stiffness drop inflection points (*Passive* = 140deg, *Active* = 75deg and *Active Sport* = 45deg) the statistical analysis show the same statistical differences as in the paper (section G.15). The same analysis is done for the VHL entry point based on the average steering velocity of each participant (section G.16). All three methods will show the same statistical significant differences.

After this analysis, the vehicle trajectories per participant for the different vehicle configurations is shown in section G.17 with corresponding average trajectories in section G.18. Finally, the effect of training is given in section G.19.

G.1. Percentage of turns where the vehicle enter the VHL

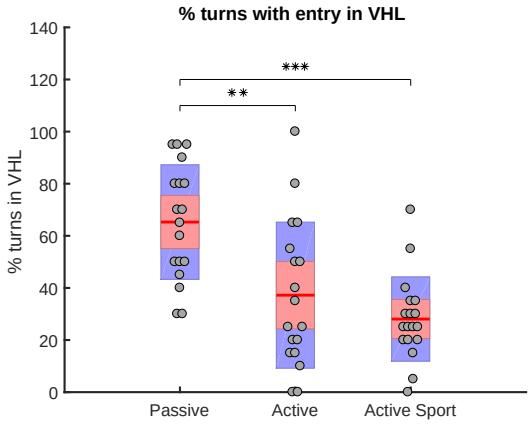

Figure G.1: Percentage of turns where the vehicle enters the VHL within the road boundaries in the main phase of the experiment. The grey points represent the raw data, the 95% confidence interval on the mean is given in red and the standard deviation in blue. * mean $p \leq 0.05$, ** mean $p \leq 0.01$, *** $p \leq 0.001$. So, in the *Passive* configuration there is a significant higher percentage of VHL entry compared to the vehicles with an extended linear handling region.

Table G.1: Statistical Analysis for the metric: Percentage of turns where the vehicle enters the VHL within the road boundaries in the main phase of the experiment.

Turns in VHL (%)	Passive (1)	Active (2)	Active Sport (3)
Mean	65.28	37.22	28.06
SD	21.99	28.04	16.19
RM ANOVA	$F(2,34) = 18.73$, $p = 3.29 \cdot 10^{-6}$		
Pairwise Comparison	(1) - (2)	(1) - (3)	(2) - (3)
	$p = 2.11 \cdot 10^{-3}$	$p = 1.40 \cdot 10^{-5}$	$p = 0.69$

G.2. Percentage of turns where vehicle departs from road after entering the VHL

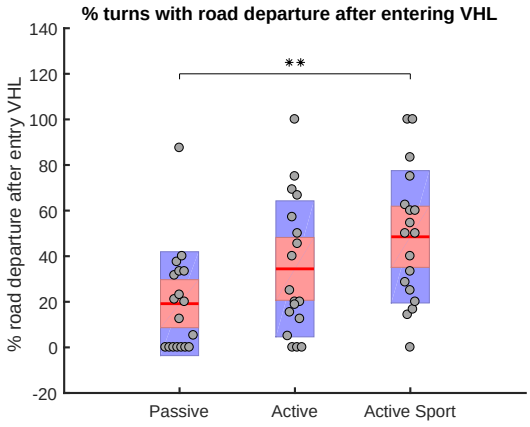

Figure G.2: Percentage of turns where vehicle departs from road after entering the VHL in the main phase of the experiment. The grey points represent the raw data, the 95% confidence interval on the mean is given in red and the standard deviation in blue. * mean $p \leq 0.05$, ** mean $p \leq 0.01$, *** $p \leq 0.001$. So, there is a higher percentage of road departures in the VHL with the *Active Sport* configuration compared to the *Passive* one.

Table G.2: Statistical Analysis for the metric: Percentage of turns where vehicle departs from road after entering the VHL in the main phase of the experiment.

road departure in VHL (%)	Passive (1)	Active (2)	Active Sport (3)
Mean	19.17	34.45	48.51
SD	22.78	29.83	29.03
RM ANOVA	$F(2,34) = 7.91$, $p = 1.52 \cdot 10^{-3}$		
Pairwise Comparison	(1) - (2)	(1) - (3)	(2) - (3)
	$p = 0.23$	$p = 1.48 \cdot 10^{-3}$	$p = 0.20$

G.3. Mean steering reversal rate (SRR)

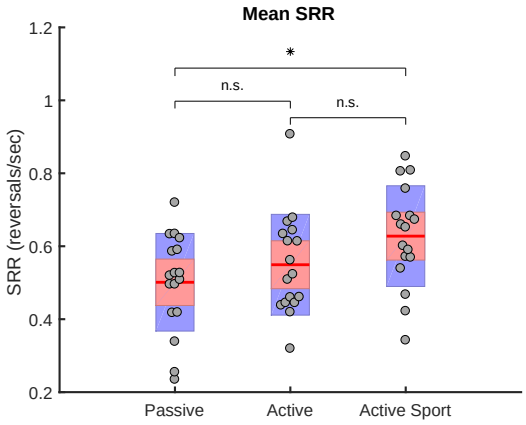

Figure G.3: Mean of the SRR in the main phase of the experiment. The grey points represent the raw data, the 95% confidence interval on the mean is given in red and the standard deviation in blue. * mean $p \leq 0.05$, ** mean $p \leq 0.01$, *** $p \leq 0.001$ and n.s. $p > 0.05$ (Not Significant). The *Active Sport* configuration has a significantly higher SRR compared to the *Passive* and *Active* one. Consequently, the *Active Sport* condition has a higher task difficulty according to the SRR. This is also indicated by the cumulative score obtained during the main phase, see Figure G.9.

Table G.3: Statistical Analysis for the metric: Mean of the SRR in the main phase

mean SRR	Passive (1)	Active (2)	Active Sport (3)
Mean	0.57	0.65	0.70
SD	0.30	0.43	0.33
RM ANOVA	$F(2,34) = 5.52,\ p = 8.36 \cdot 10^{-3}$		
Pairwise Comparison	(1) - (2)	(1) - (3)	(2) - (3)
	$p = 1$	$p = 1.88 \cdot 10^{-2}$	$p = 9.88 \cdot 10^{-2}$

G.4. Mean absolute driver torque

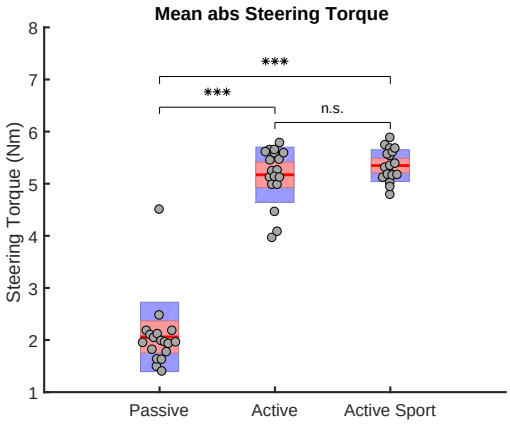

Figure G.4: Mean of the absolute steering torque applied by the driver in the main phase of the experiment. The grey points represent the raw data, the 95% confidence interval on the mean is given in red and the standard deviation in blue. * mean $p \leq 0.05$, ** mean $p \leq 0.01$, *** $p \leq 0.001$ and n.s. $p > 0.05$ (Not Significant). The result shows that more physical effort is required by the drivers when driving a vehicle with an extended linear handling region near the VHL. This is a result of steering stiffness for such type of vehicles. Before the VHL is entered the stiffness is increasing. While for the *Passive* configuration the stiffness drops gradually before entering the VHL.

Table G.4: Statistical Analysis for the metric: Mean of the steering torque applied by the driver in the main phase

Steering Torque (Nm)	Passive (1)	Active (2)	Active Sport (3)
Mean	2.06	5.17	5.35
SD	0.67	0.53	0.30
RM ANOVA	$F(2,34) = 55.60$, $p = 1.91 \cdot 10^{-11}$		
Pairwise Comparison	(1) - (2)	(1) - (3)	(2) - (3)
	$p = 7.02 \cdot 10^{-7}$	$p = 8.35 \cdot 10^{-9}$	$p = 1$

G.5. Percentage of turns where the vehicle departs from the road on the outside

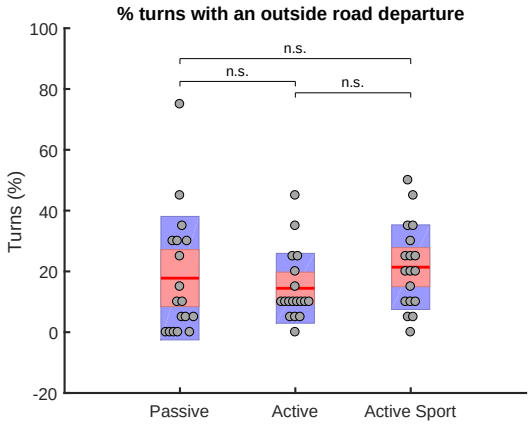

Figure G.5: Percentage of turns where the vehicle departs from the road on the outside in the main phase of the experiment. The grey points represent the raw data, the 95% confidence interval on the mean is given in red and the standard deviation in blue. * mean $p \leq 0.05$, ** mean $p \leq 0.01$, *** $p \leq 0.001$ and n.s. $p > 0.05$ (Not Significant). There are no significant differences.

Table G.5: Statistical Analysis for the metric: Percentage of turns where the vehicle departs from the road on the outside in the main phase.

Turns road departure Outside (%)	Passive (1)	Active (2)	Active Sport (3)
Mean	17.78	14.44	21.40
SD	20.31	11.49	13.91
RM ANOVA	$F(2,34) = 1.62$, $p = 0.21$		
Pairwise Comparison	(1) - (2)	(1) - (3)	(2) - (3)
	$p = 1$	$p = 0.47$	$p = 0.24$

G.6. Percentage of turns where the vehicle departs from the road

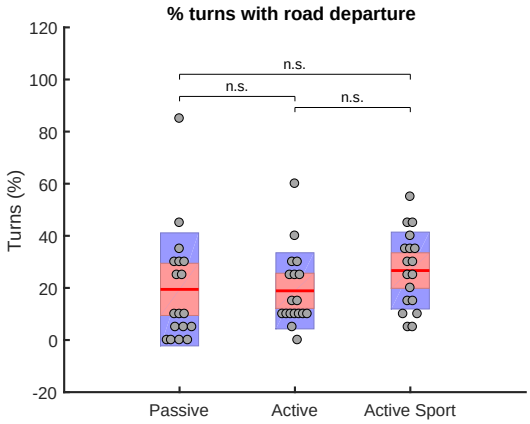

Figure G.6: Percentage of turns where the vehicle departs from the road in the main phase of the experiment. The grey points represent the raw data, the 95% confidence interval on the mean is given in red and the standard deviation in blue. * mean $p \leq 0.05$, ** mean $p \leq 0.01$, *** $p \leq 0.001$ and n.s. $p > 0.05$ (Not Significant). There are no significant differences.

Table G.6: Statistical Analysis for the metric: Percentage of turns where the vehicle departs from the road.

Turns road departure (%)	Passive (1)	Active (2)	Active Sport (3)
Mean	19.44	18.89	26.67
SD	21.69	14.61	14.75
RM ANOVA	$F(2,34) = 3.28$, $p = 4.98 \cdot 10^{-2}$		
Pairwise Comparison	(1) - (2)	(1) - (3)	(2) - (3)
	$p = 1$	$p = 8.47 \cdot 10^{-2}$	$p = 0.13$

G.7. Percentage of turns where the vehicle departs from the road on the inside

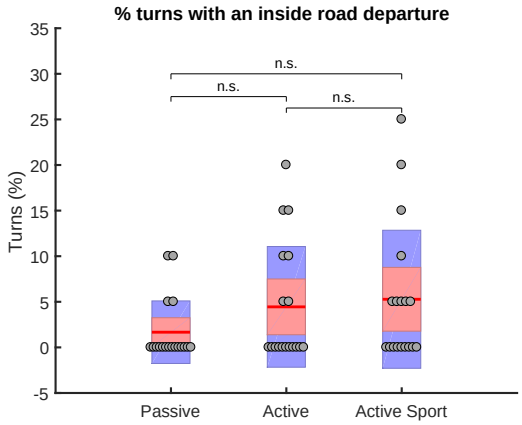

Figure G.7: Percentage of turns where the vehicle departs from the road on the inside in the main phase of the experiment. The grey points represent the raw data, the 95% confidence interval on the mean is given in red and the standard deviation in blue. * mean $p \leq 0.05$, ** mean $p \leq 0.01$, *** $p \leq 0.001$ and n.s. $p > 0.05$ (Not Significant). There are no significant differences.

Table G.7: Statistical Analysis for the metric: Percentage of turns where the vehicle departs from the road on the inside in the main phase.

Turns road departure Inside (%)	Passive (1)	Active (2)	Active Sport (3)
Mean	1.67	4.44	5.28
SD	3.43	6.62	7.57
RM ANOVA	$F(2,34) = 2.21$, $p = 0.13$		
Pairwise Comparison	(1) - (2)	(1) - (3)	(2) - (3)
	$p = 0.50$	$p = 0.27$	$p = 1$

G.8. Turns in the training phase

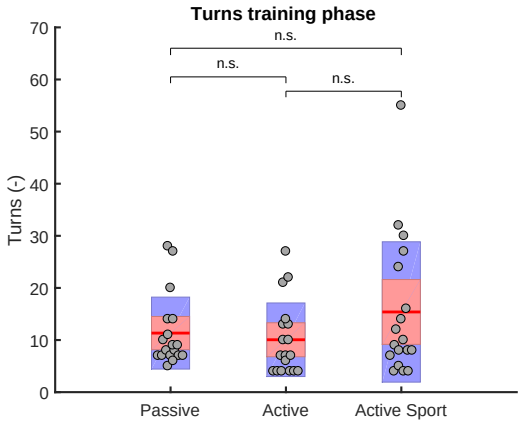

Figure G.8: Number of turns in the training phase of the experiment. The grey points represent the raw data, the 95% confidence interval on the mean is given in red and the standard deviation in blue. * mean $p \leq 0.05$, ** mean $p \leq 0.01$, *** $p \leq 0.001$ and n.s. $p > 0.05$ (Not Significant). There are no significant differences.

Table G.8: Statistical Analysis for the metric: Turns in the training phase

Turns training phase	Passive (1)	Active (2)	Active Sport (3)
Mean	11.33	10.06	15.39
SD	6.90	7.06	13.47
RM ANOVA	$F(2,34) = 1.37$, $p = 0.27$		
Pairwise Comparison	(1) - (2)	(1) - (3)	(2) - (3)
	$p = 0.65$	$p = 1$	$p = 0.58$

G.9. Cumulative Score main phase

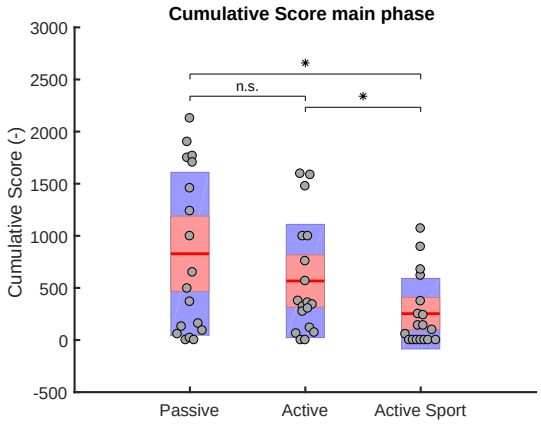

Figure G.9: Cumulative score obtained during the main phase of the experiment. The grey points represent the raw data, the 95% confidence interval on the mean is given in red and the standard deviation in blue. * mean $p \leq 0.05$, ** mean $p \leq 0.01$, *** $p \leq 0.001$ and n.s. $p > 0.05$ (Not Significant). There are significant differences between the *Active Sport* and the *Passive* and *Active* vehicle configurations. Indicating the task difficulty for the *Active Sport* condition is highest.

Table G.9: Statistical Analysis for the metric: Cumulative score in the main phase

Cumulative Score	Passive (1)	Active (2)	Active Sport (3)
Mean	828.03	567.54	253.14
SD	781.39	543.24	338.10
RM ANOVA	$F(2,34) = 4.40,\ p = 2.00 \cdot 10^{-2}$		
Pairwise Comparison	(1) - (2)	(1) - (3)	(2) - (3)
	$p = 1$	$p = 2.87 \cdot 10^{-2}$	$p = 4.77 \cdot 10^{-2}$

G.10. Total obtained turn scores during the main phase

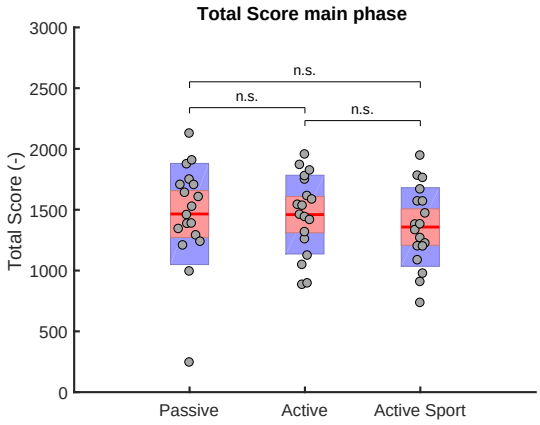

Figure G.10: Total of the obtained turn scores in the main phase of the experiment. The grey points represent the raw data, the 95% confidence interval on the mean is given in red and the standard deviation in blue. * mean $p \leq 0.05$, ** mean $p \leq 0.01$, *** $p \leq 0.001$ and n.s. $p > 0.05$ (Not Significant). There are no significant differences.

Table G.10: Statistical Analysis for the metric: Total of the obtained turn scores in the main phase

Total Score	Passive (1)	Active (2)	Active Sport (3)
Mean	1465.30	1460.10	1358.00
SD	415.92	323.55	323.36
RM ANOVA	$F(2,34) = 1.80$, $p = 0.18$		
Pairwise Comparison	(1) - (2)	(1) - (3)	(2) - (3)
	$p = 1$	$p = 0.16$	$p = 0.38$

G.11. Mean score per turn (No Road Departure)

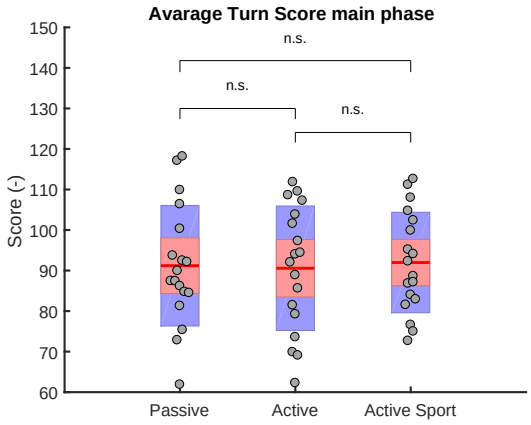

Figure G.11: Mean of the scores obtained during the turns where the vehicle did not depart from the road in the main phase of the experiment. The grey points represent the raw data, the 95% confidence interval on the mean is given in red and the standard deviation in blue. * mean $p \leq 0.05$, ** mean $p \leq 0.01$, *** $p \leq 0.001$ and n.s. $p > 0.05$ (Not Significant). There are no significant differences.

Table G.11: Statistical Analysis for the metric: Mean of the scores obtained during the turns where the vehicle did not depart from the road in the main phase

avg Turn Score	Passive (1)	Active (2)	Active Sport (3)
Mean	91.20	90.57	91.98
SD	14.87	15.35	12.40
RM ANOVA	$F(2,34) = 0.05$, $p = 0.95$		
Pairwise Comparison	(1) - (2)	(1) - (3)	(2) - (3)
	$p = 1$	$p = 1$	$p = 1$

G.12. Mean of the maximum scores obtained by a participant during a turn

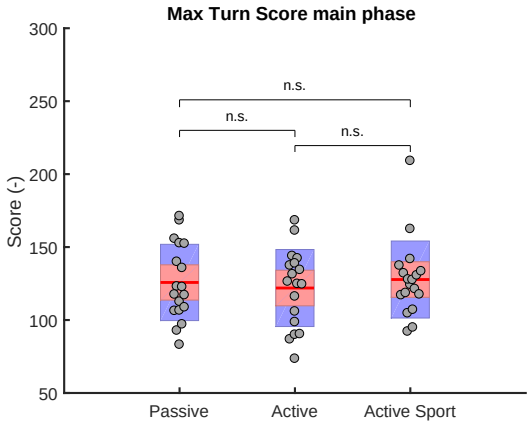

Figure G.12: Mean of the maximum scores obtained by a participant in the main phase of the experiment. The grey points represent the raw data, the 95% confidence interval on the mean is given in red and the standard deviation in blue. * mean $p \leq 0.05$, ** mean $p \leq 0.01$, *** $p \leq 0.001$ and n.s. $p > 0.05$ (Not Significant). There are no significant differences.

Table G.12: Statistical Analysis for the metric: Mean of the maximum scores obtained by a participant in the main phase of the experiment

mean(Max Score)	Passive (1)	Active (2)	Active Sport (3)
Mean	125.76	121.94	127.76
SD	26.14	26.40	26.39
RM ANOVA	$F(2,34) = 0.10$, $p = 0.91$		
Pairwise Comparison	(1) - (2)	(1) - (3)	(2) - (3)
	$p = 1$	$p = 1$	$p = 1$

G.13. Mean lateral distance per turn (No Road Departure)

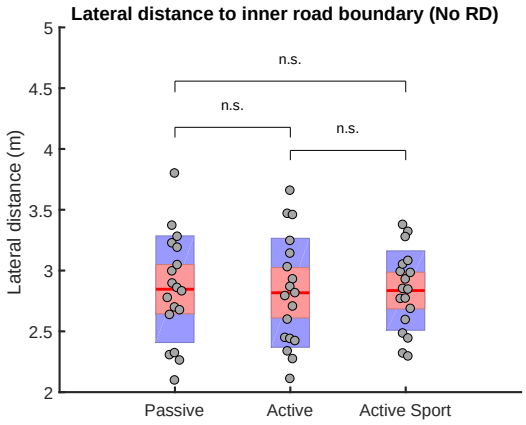

Figure G.13: Mean of the lateral distance per turn when the vehicle does not depart from the road in the main phase of the experiment. The grey points represent the raw data, the 95% confidence interval on the mean is given in red and the standard deviation in blue. * mean $p \leq 0.05$, ** mean $p \leq 0.01$, *** $p \leq 0.001$ and n.s. $p > 0.05$ (Not Significant). There are no significant differences.

Table G.13: Statistical Analysis for the metric: Mean of the lateral distance per turn when the vehicle does not depart from the road in the main phase

Lateral Distance (m)	Passive (1)	Active (2)	Active Sport (3)
Mean	2.85	2.82	2.84
SD	0.44	0.45	0.33
RM ANOVA	$F(2,34) = 4.10 \cdot 10^{-2}$, $p = 0.96$		
Pairwise Comparison	(1) - (2)	(1) - (3)	(2) - (3)
	$p = 1$	$p = 1$	$p = 1$

G.14. Mean SRR in VHL

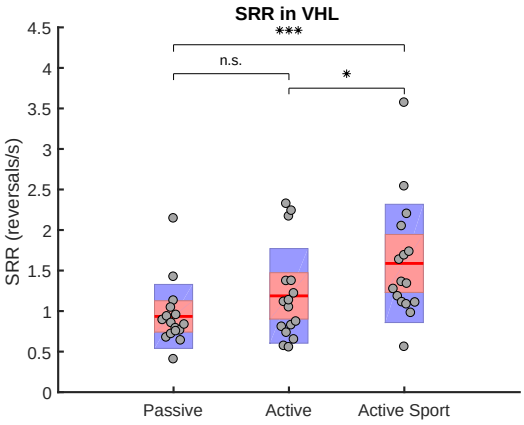

Figure G.14: mean SRR when vehicles are in VHL. The grey points represent the raw data, the 95% confidence interval on the mean is given in red and the standard deviation in blue. * mean $p \leq 0.05$, ** mean $p \leq 0.01$, *** $p \leq 0.001$ and n.s. $p > 0.05$ (Not Significant). The *Active Sport* configuration shows the highest mean SRR in VHL. This is as expected since the result of the percentage of road departures after entering the VHL indicates it is more difficult to keep this vehicle under control in the VHL, see table G.2.

Table G.14: Statistical Analysis for the metric: Mean SRR in VHL during the main phase of the experiment

Lateral Distance (m)	Passive (1)	Active (2)	Active Sport (3)
Mean	0.93	1.19	1.59
SD	0.40	0.58	0.73
RM ANOVA	$F(2,34) = 15.26$, $p = 2.68 \cdot 10^{-5}$		
Pairwise Comparison	(1) - (2)	(1) - (3)	(2) - (3)
	$p = 7.46 \cdot 10^{-2}$	$p = 3.27 \cdot 10^{-4}$	$p = 2.07 \cdot 10^{-2}$

G.15. Statistical analysis with inflection point based on steering stiffness drop

During the Pilot study the following inflection points where determined as entry of the VHL:

- *Passive* - 140 degrees
- *Active* - 75 degrees
- *Active Sport* - 45 degrees

With these inflection points the same statistical differences are found as with the inflection points used in the paper, see figures G.15a and G.15b.

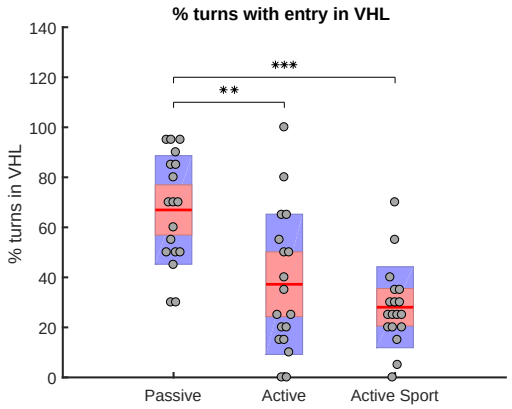

(a) Percentage of turns with an entry in the VHL within the road boundaries in the main phase of the experiment. The *Passive* configuration has a significant higher percentage of VHL entry compared to the vehicles with an extended linear handling region. This is the same result as in Figure G.1.

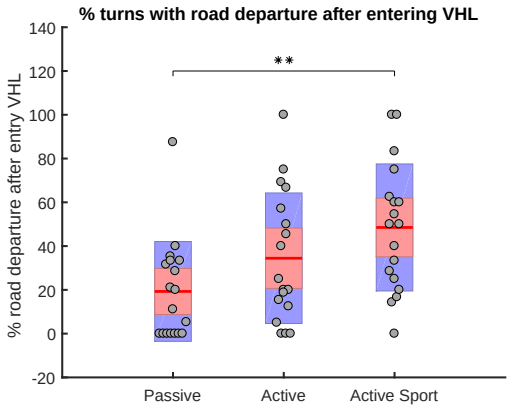

(b) Percentage of turns where the vehicle departs from the road after entering the VHL during the main phase. There are more road departures when the *Active Sport* configuration is in the VHL compared to the *Passive* one. This is the same result as in Figure G.2.

Figure G.15: The grey points represent the raw data, the 95% confidence interval on the mean is given in red and the standard deviation in blue. * mean $p \leq 0.05$, ** mean $p \leq 0.01$ and *** $p \leq 0.001$. The inflection points are set equal to the steering stiffness drop determined in during the pilot study.

Table G.15: Statistical Analysis for the metric: Turns where vehicle enters the VHL (%) within the road boundaries in the main phase of the experiment. For this Table the inflection points are set equal to the steering stiffness drop determined in during the pilot study.

Turns in VHL (%)	Passive (1)	Active (2)	Active Sport (3)
Mean	66.94	37.22	28.06
SD	21.70	28.04	16.19
RM ANOVA	$F(2,34) = 20.72$, $p = 1.30 \cdot 10^{-6}$		
Pairwise Comparison	(1) - (2)	(1) - (3)	(2) - (3)
	$p = 1.17 \cdot 10^{-3}$	$p = 8.01 \cdot 10^{-6}$	$p = 0.72$

Table G.16: Statistical Analysis for the metric: Turns where vehicle departs from road after entering the VHL (%) in the main phase of the experiment. For this Table the inflection points are set equal to the steering stiffness drop determined in during the pilot study.

RD in VHL (%)	Passive (1)	Active (2)	Active Sport (3)
Mean	19.28	34.45	48.51
SD	22.81	29.83	29.03
RM ANOVA	$F(2,34) = 7.70$, $p = 1.75 \cdot 10^{-3}$		
Pairwise Comparison	(1) - (2)	(1) - (3)	(2) - (3)
	$p = 0.25$	$p = 1.65 \cdot 10^{-3}$	$p = 0.20$

G.16. Statistical analysis with participant specific inflection point

In this section the statistical results are shown in case individual inflection point would be determined for each participant. These inflection points are based on the average steering velocity of each participant. In figures G.16a and G.16b the results of this method are shown. With these inflection points the same statistical significant differences are found as with the inflection points applied in the paper.

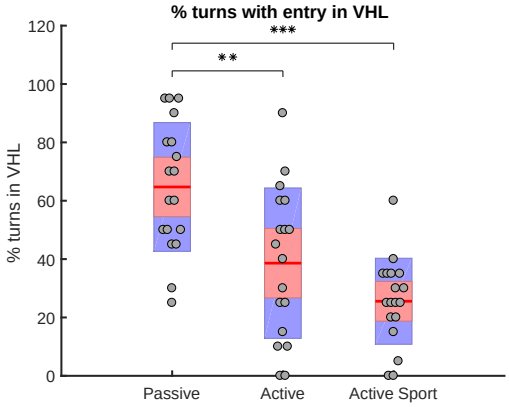

(a) Percentage of turns with an entry in the VHL within the road boundaries in the main phase of the experiment. The *Passive* configuration has a significant higher frequency of VHL entry compared to the vehicles with an extended linear handling region. This is the same result as in Figure G.1.

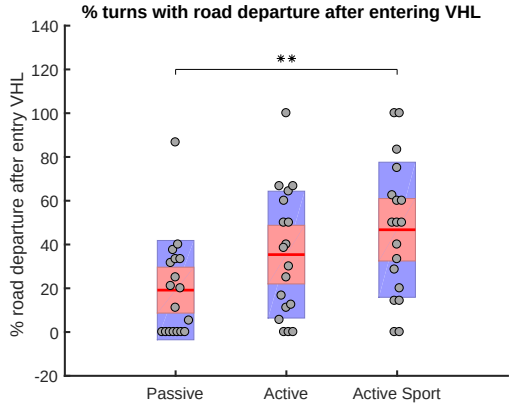

(b) Percentage of turns where the vehicle departs from the road after entering the VHL during the main phase. There are more road departures when the *Active Sport* configuration is in the VHL compared to the *Passive* one. This is the same result as in Figure G.2.

Figure G.16: The grey points represent the raw data, the 95% confidence interval on the mean is given in red and the standard deviation in blue. * mean $p \leq 0.05$, ** mean $p \leq 0.01$ and *** $p \leq 0.001$. The inflection point are determined for each participant individually.

Table G.17: Statistical Analysis for the metric: Turns where vehicle enters the VHL (%) within the road boundaries in the main phase of the experiment. For this table the inflection point are determined for each participant individually.

Turns in VHL (%)	Passive (1)	Active (2)	Active Sport (3)
Mean	64.72	38.61	25.56
SD	22.06	25.77	14.74
RM ANOVA	$F(2,34) = 20.91,\ p = 1.20 \cdot 10^{-6}$		
Pairwise Comparison	(1) - (2)	(1) - (3)	(2) - (3)
	$p = 8.53 \cdot 10^{-3}$	$p = 5.52 \cdot 10^{-6}$	$p = 6.17 \cdot 10^{-2}$

Table G.18: Statistical Analysis for the metric: Turns where vehicle departs from road after entering the VHL (%) in the main phase of the experiment. For this table the inflection point are determined for each participant individually.

RD in VHL (%)	Passive (1)	Active (2)	Active Sport (3)
Mean	19.16	35.38	46.74
SD	22.69	28.98	30.86
RM ANOVA	$F(2,34) = 6.34,\ p = 4.56 \cdot 10^{-3}$		
Pairwise Comparison	(1) - (2)	(1) - (3)	(2) - (3)
	$p = 0.13$	$p = 2.40 \cdot 10^{-3}$	$p = 0.79$

G.17. Trajectories per participant during the main phase of the experiment

The trajectories taken by each participant in the three different vehicle configurations are given Figures G.17 to G.34. In those figures the red lines represent a vehicle in the VHL. Hence, more lines contain a red part for the *Passive* configuration compared to the *Active* and *Active Sport* configurations. Moreover, one can see that the road departures on the inside of the curve are not a consequence of the entry in the VHL, since almost none of the trajectories enter the VHL before crossing the inner road boundary. Hence, these type of road departures are caused by a misjudgement of the vehicle dynamics in the regions before the VHL.

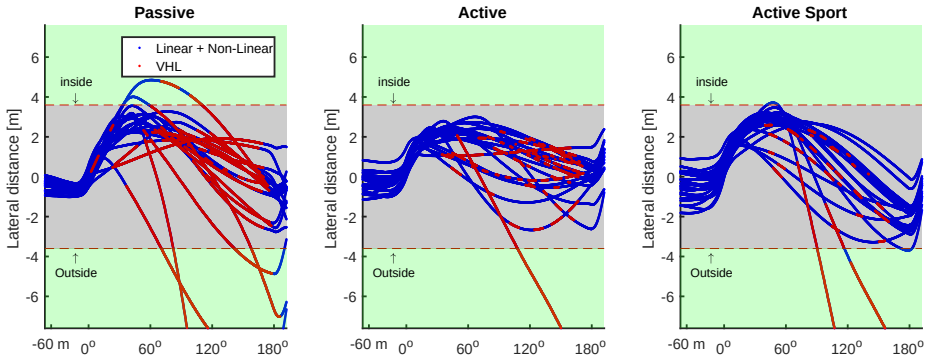

Figure G.17: Trajectories Participant 1. Blue line represents vehicle not in VHL and red line represents vehicle in VHL

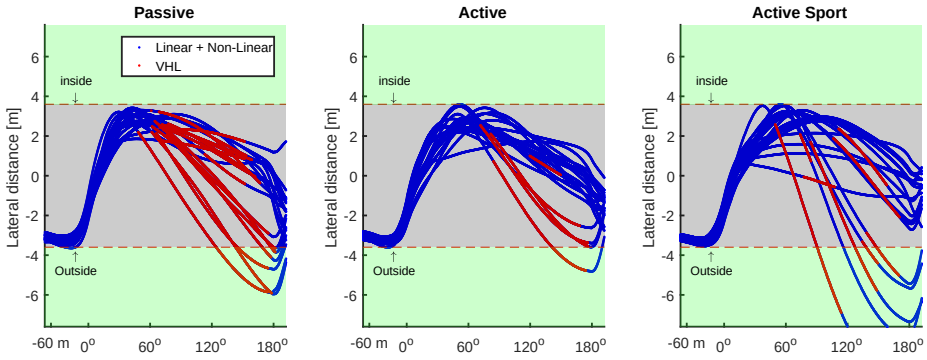

Figure G.18: Trajectories Participant 2. Blue line represents vehicle not in VHL and red line represents vehicle in VHL

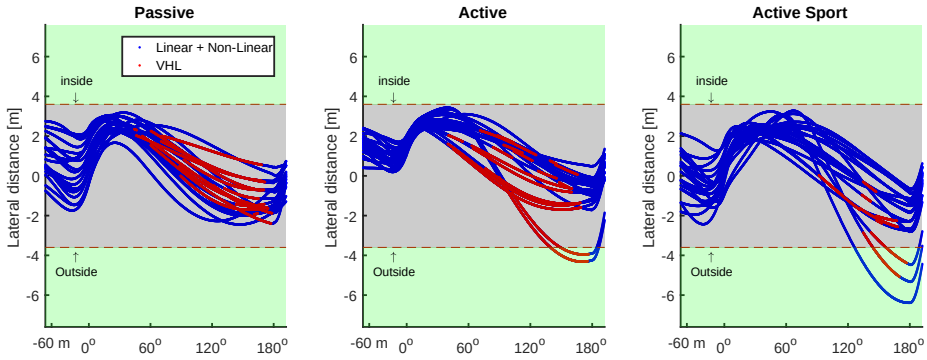

Figure G.19: Trajectories Participant 3. Blue line represents vehicle not in VHL and red line represents vehicle in VHL

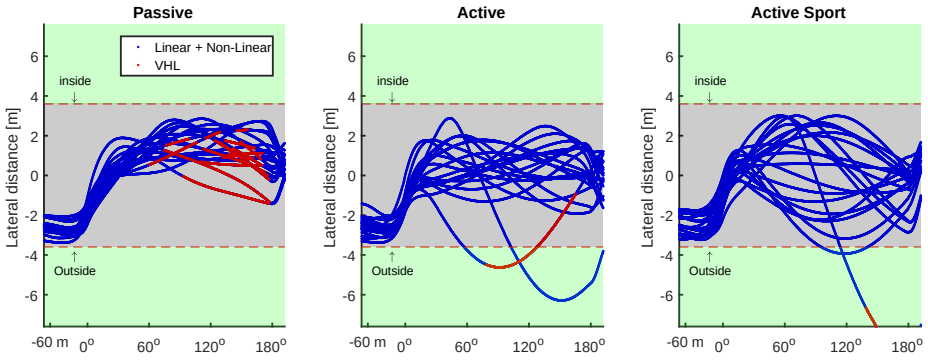

Figure G.20: Trajectories Participant 4. Blue line represents vehicle not in VHL and red line represents vehicle in VHL

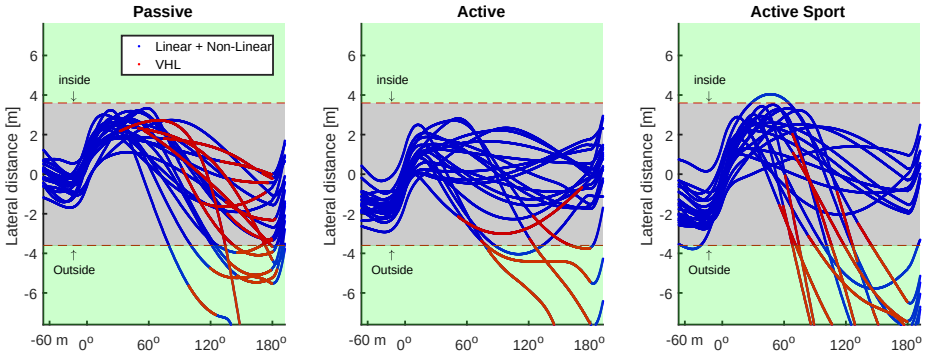

Figure G.21: Trajectories Participant 5. Blue line represents vehicle not in VHL and red line represents vehicle in VHL

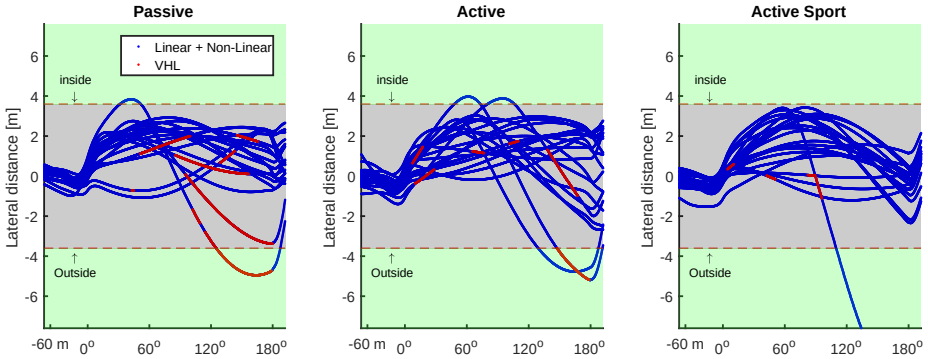

Figure G.22: Trajectories Participant 6. Blue line represents vehicle not in VHL and red line represents vehicle in VHL

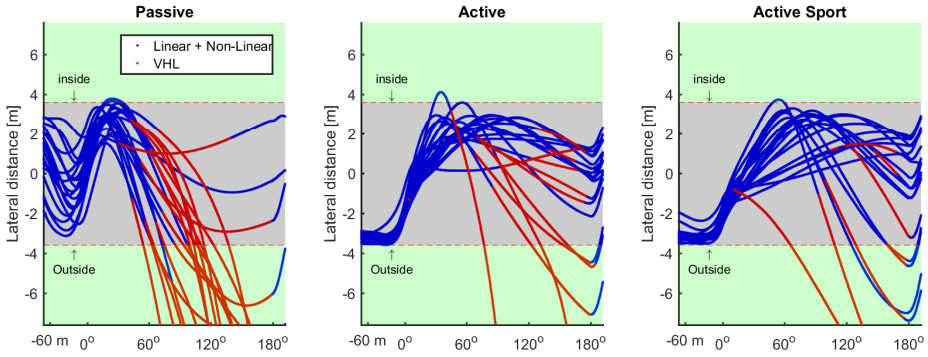

Figure G.23: Trajectories Participant 7. Blue line represents vehicle not in VHL and red line represents vehicle in VHL

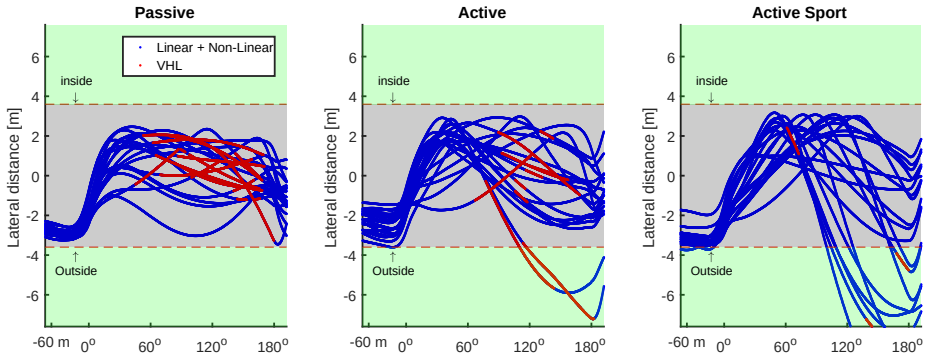

Figure G.24: Trajectories Participant 8. Blue line represents vehicle not in VHL and red line represents vehicle in VHL

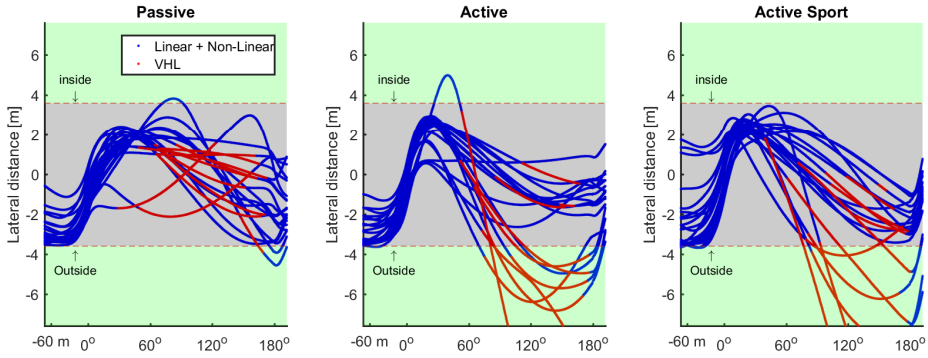

Figure G.25: Trajectories Participant 9. Blue line represents vehicle not in VHL and red line represents vehicle in VHL

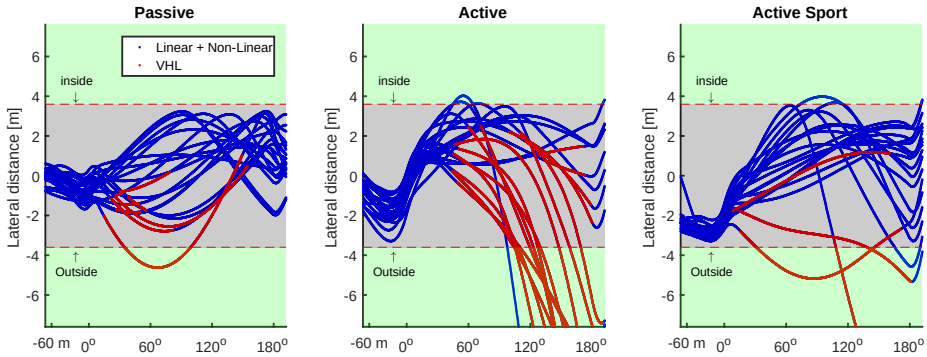

Figure G.26: Trajectories Participant 10. Blue line represents vehicle not in VHL and red line represents vehicle in VHL

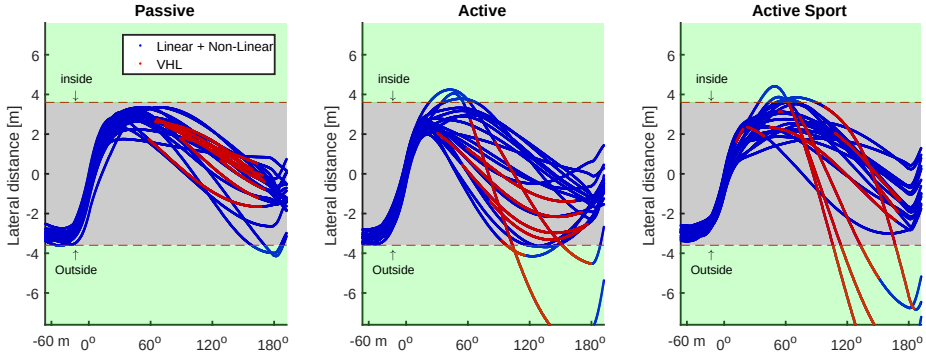

Figure G.27: Trajectories Participant 11. Blue line represents vehicle not in VHL and red line represents vehicle in VHL

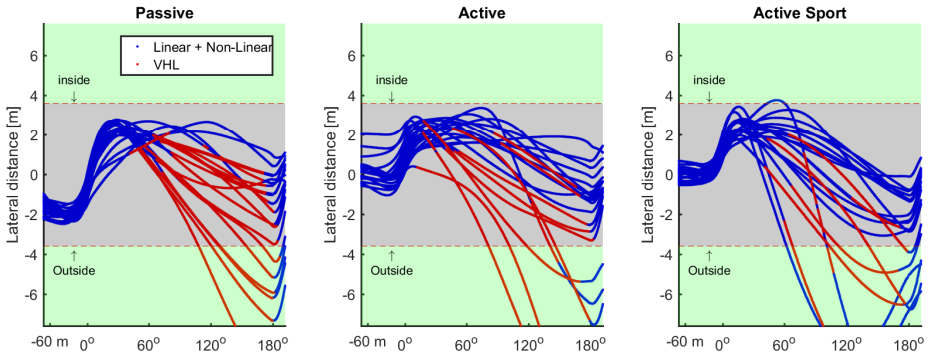

Figure G.28: Trajectories Participant 12. Blue line represents vehicle not in VHL and red line represents vehicle in VHL

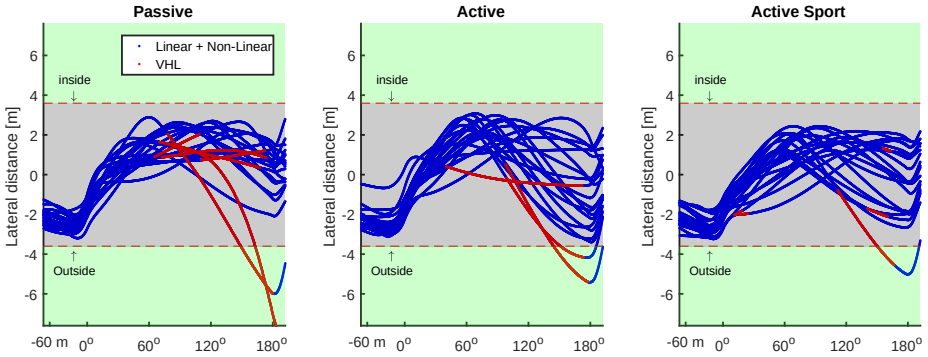

Figure G.29: Trajectories Participant 13. Blue line represents vehicle not in VHL and red line represents vehicle in VHL

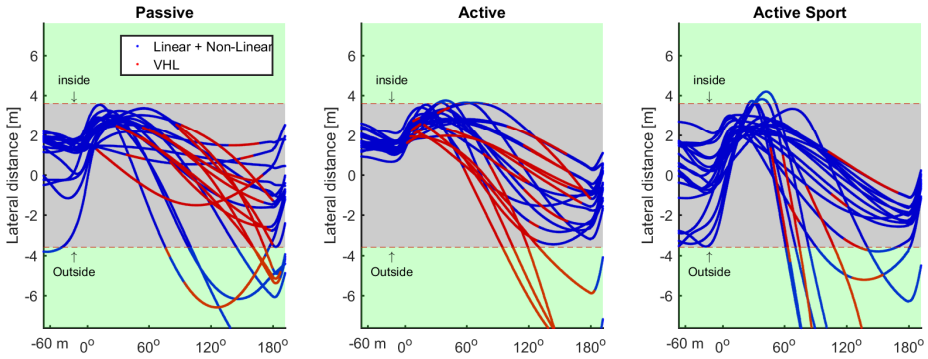

Figure G.30: Trajectories Participant 14. Blue line represents vehicle not in VHL and red line represents vehicle in VHL

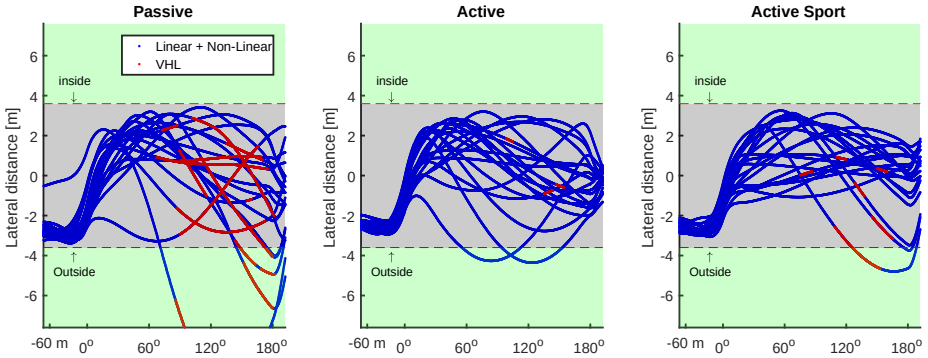

Figure G.31: Trajectories Participant 15. Blue line represents vehicle not in VHL and red line represents vehicle in VHL

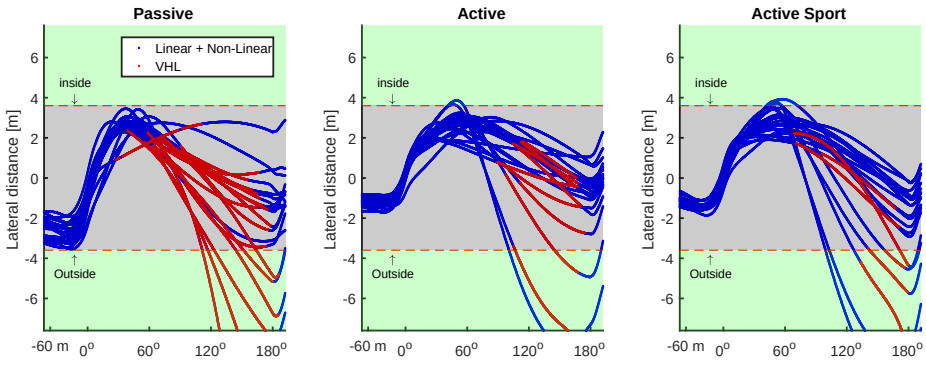

Figure G.32: Trajectories Participant 16. Blue line represents vehicle not in VHL and red line represents vehicle in VHL

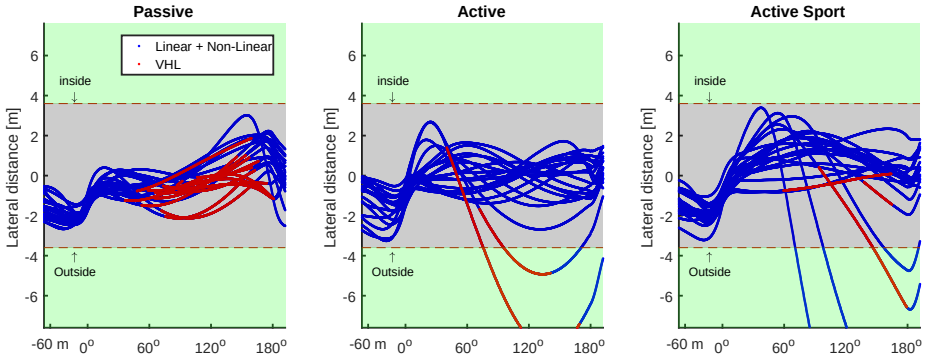

Figure G.33: Trajectories Participant 17. Blue line represents vehicle not in VHL and red line represents vehicle in VHL

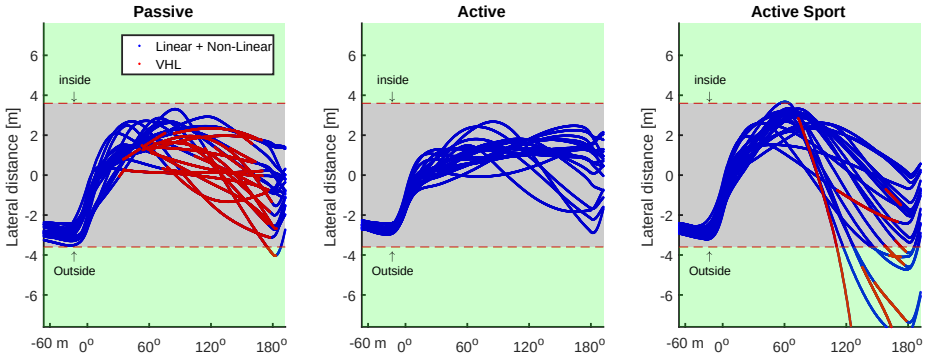

Figure G.34: Trajectories Participant 18. Blue line represents vehicle not in VHL and red line represents vehicle in VHL

G.18. Average trajectories

In this section the following average vehicle trajectories will be presented:

- Average trajectory over all the turns in the training and main phase
- Average trajectory over all turns with no road departure in the training and main phase
- Average trajectory over all the turns with a road departure after entering the VHL while being on the road in the training and main phase
- Average trajectory over all the turns with a road departure in the training and main phase
- Average trajectory over all the turns in catch trial 1 and 2

G.18.1. All the turns

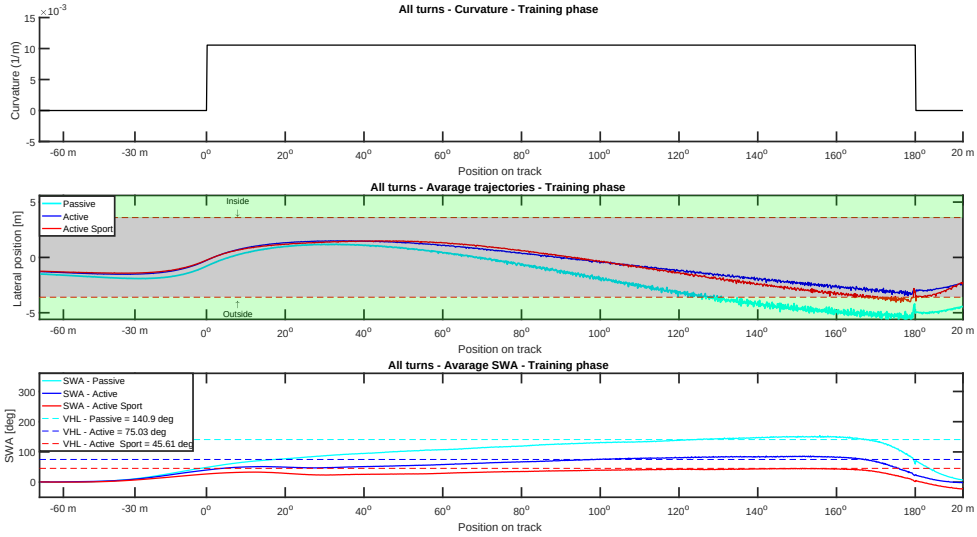

Figure G.35: Average trajectory over all the participants during the training phase. Top: curvature ($1/R_{curve}$) of the road. Middle: average trajectory across all the participants per vehicle configuration. The dashed lines indicate the road boundary and the solid lines represents the trajectory of the COG of the vehicle. Bottom: average SWA input across all the participants, if the SWA of a vehicle configuration is above the corresponding dashed line the vehicle enters the VHL. The position on track is defined by meters and degrees. $-60m$ implies that the vehicle is at the point 60 meters before the turn starts and for example $20deg$ implies the vehicle position is at an angular span of 20 degrees in the turn. In the middle figure the trajectories show that the *Passive* configuration performs worst. This might be due to the fact that this configuration slowly responds to a steering wheel angle change. Moreover, the abrupt drop of steering stiffness is not present, which can cause participants who drove another configuration before to search for this point.

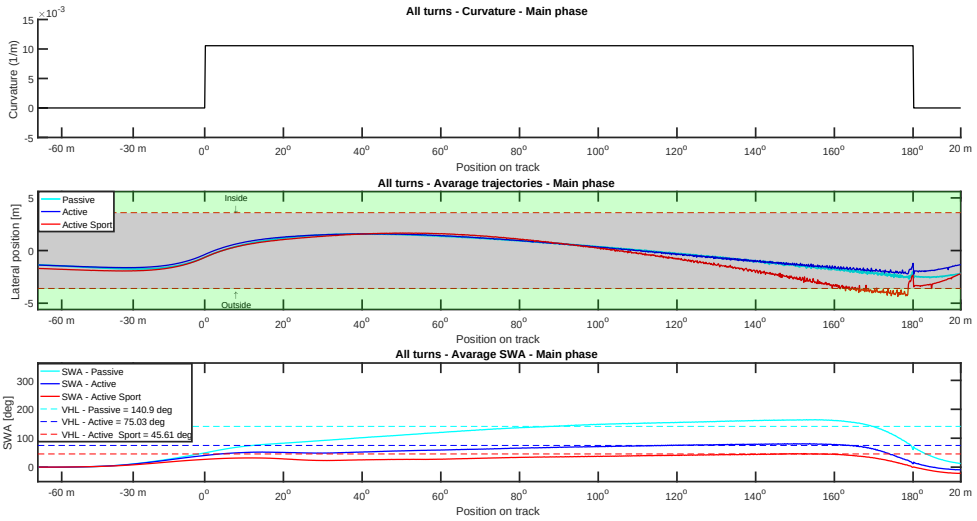

Figure G.36: Average trajectory over all the participants during the main phase. Top: curvature ($1/R_{curve}$) of the road. Middle: average trajectory across all the participants per vehicle configuration. The dashed lines indicate the road boundary and the solid lines represents the trajectory of the COG of the vehicle. Bottom: average SWA input across all the participants, if the SWA of a vehicle configuration is above the corresponding dashed line the vehicle enters the VHL. The position on track is defined by meters and degrees. $-60m$ implies that the vehicle is at the point 60 meters before the turn starts and for example $20deg$ implies the vehicle position is at an angular span of 20 degrees in the turn. In the middle figure can be seen on average all the drivers will approach the turn from the outside of the curve and subsequently steer towards the inside. *The lateral distance to the inner road boundary is approximately equal in the three configurations.* This is also supported by the average lateral distance and average number of points per turn scored during the experiment when the vehicle did not crash (table G.11), where no significant differences between the configurations can be detected. The *Active sport* configuration has an average RD on the outside. In first instance one might think the vehicle departs more often compared to staying on the road. However, this is not the case, with the *Active Sport* configuration this average road departure is caused by some extreme road departures due to abrupt drop in lateral acceleration when entering the VHL.

G.18.2. No road departure

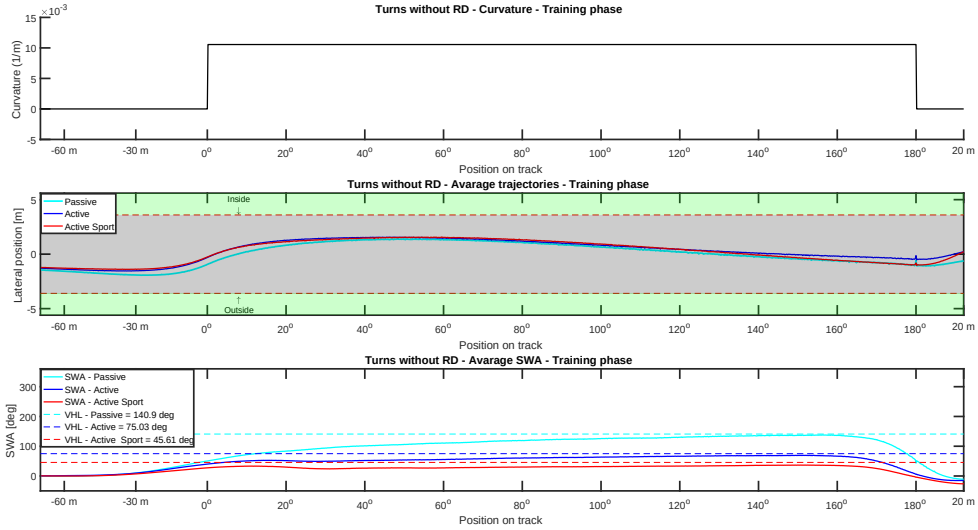

Figure G.37: Average trajectory in the turns where the vehicle did not depart from the road over all the participants during the training phase. Top: curvature $(1/R_{curve})$ of the road. Middle: average trajectory across all the participants per vehicle configuration. The dashed lines indicate the road boundary and the solid lines represents the trajectory of the COG of the vehicle. Bottom: average SWA input across all the participants, if the SWA of a vehicle configuration is above the corresponding dashed line the vehicle enters the VHL. The position on track is defined by meters and degrees. $-60m$ implies that the vehicle is at the point 60 meters before the turn starts and for example $20deg$ implies the vehicle position is at an angular span of 20 degrees in the turn. The steering wheel angles show that the drivers are on average not entering the VHL. Consequently, the vehicles are easier to control and stay on the road. Moreover, as can be seen in figure 3 of the paper, all vehicles are designed to have the same cornering capability. Therefore, all the trajectories are more or less similar when the vehicle does not enter the VHL.

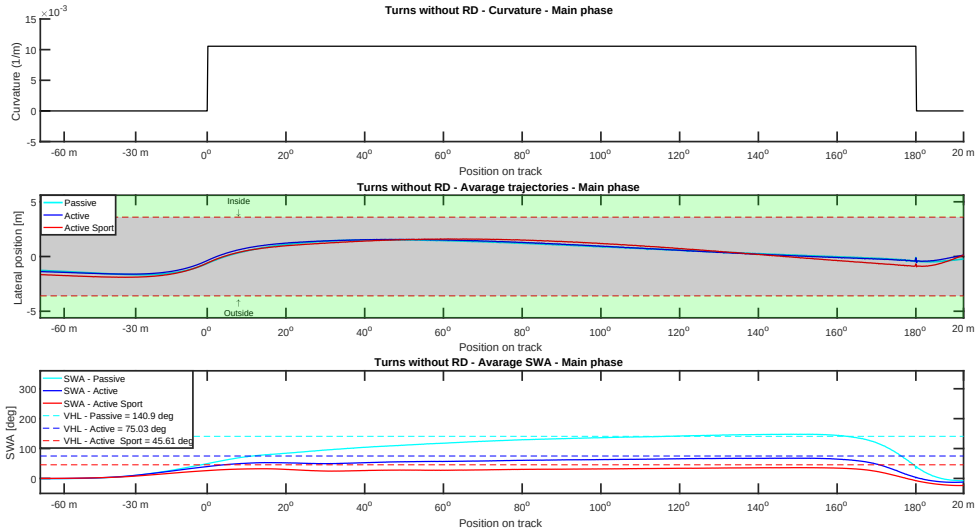

Figure G.38: Average trajectory in the turns where the vehicle did not depart from the road over all the participants during the main phase. Top: curvature $(1/R_{curve})$ of the road. Middle: average trajectory across all the participants per vehicle configuration. The dashed lines indicate the road boundary and the solid lines represents the trajectory of the COG of the vehicle. Bottom: average SWA input across all the participants, if the SWA of a vehicle configuration is above the corresponding dashed line the vehicle enters the VHL. The position on track is defined by meters and degrees. $-60m$ implies that the vehicle is at the point 60 meters before the turn starts and for example $20deg$ implies the vehicle position is at an angular span of 20 degrees in the turn. The steering wheel angles show that the drivers are on average not entering the VHL, except for the *Passive* configuration.

G.18.3. Road departure due to entry in VHL

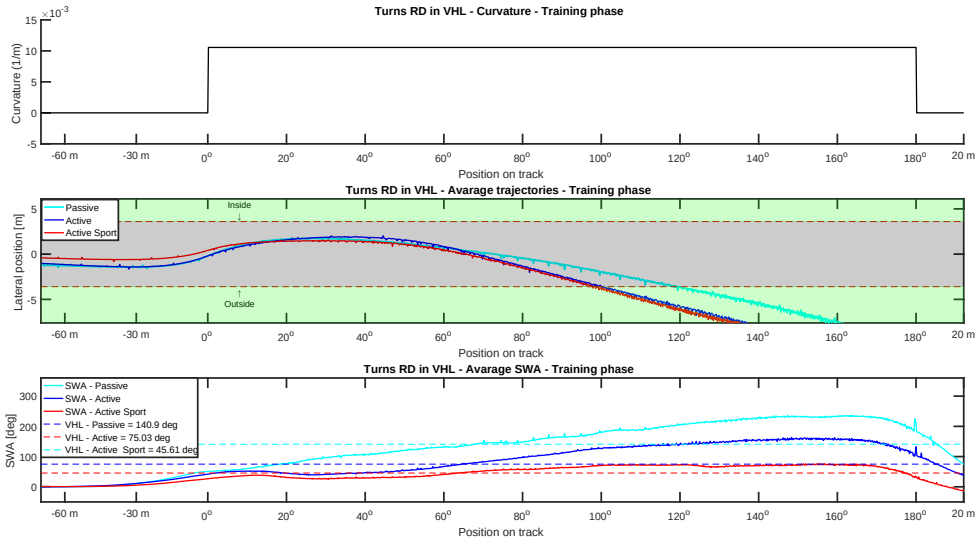

Figure G.39: Average trajectory in the turns where the vehicle departs from the road due to entry in the VHL during the training phase. Top: curvature ($1/R_{curve}$) of the road. Middle: average trajectory across all the participants per vehicle configuration. The dashed lines indicate the road boundary and the solid lines represents the trajectory of the COG of the vehicle. Bottom: average SWA input across all the participants, if the SWA of a vehicle configuration is above the corresponding dashed line the vehicle enters the VHL. The position on track is defined by meters and degrees. $-60m$ implies that the vehicle is at the point 60 meters before the turn starts and for example $20deg$ implies the vehicle position is at an angular span of 20 degrees in the turn. The steering wheel angles show that the drivers enter the VHL. In the VHL, the vehicles with an extended linear handling region are more difficult to control due to the abrupt change in lateral acceleration. Consequently, the trajectories of these configurations go out of the road more significantly

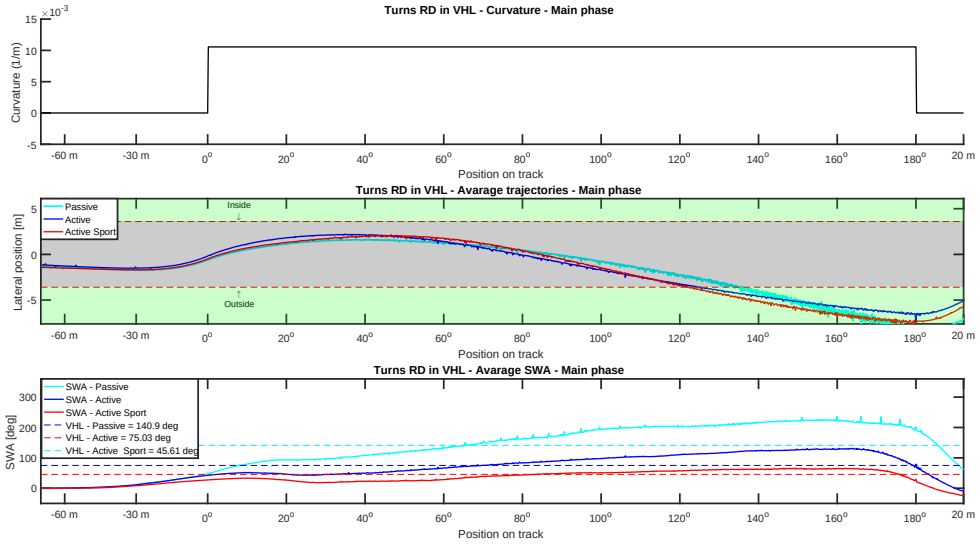

Figure G.40: Average trajectory in the turns where the vehicle departs from the road due to entry in the VHL during the main phase. Top: curvature ($1/R_{curve}$) of the road. Middle: average trajectory across all the participants per vehicle configuration. The dashed lines indicate the road boundary and the solid lines represents the trajectory of the COG of the vehicle. Bottom: average SWA input across all the participants, if the SWA of a vehicle configuration is above the corresponding dashed line the vehicle enters the VHL. The steering wheel angles show that the drivers enter the VHL. In the VHL, the vehicles with an extended linear handling region are more difficult to control due to the abrupt change in lateral acceleration. When comparing these trajectories with the ones in figure G.39, it can be observed that the average steering wheel angle input decreases when driving in the VHL. So, the drivers are better able to correct the vehicle motion.

G.18.4. All the turns with a road departure

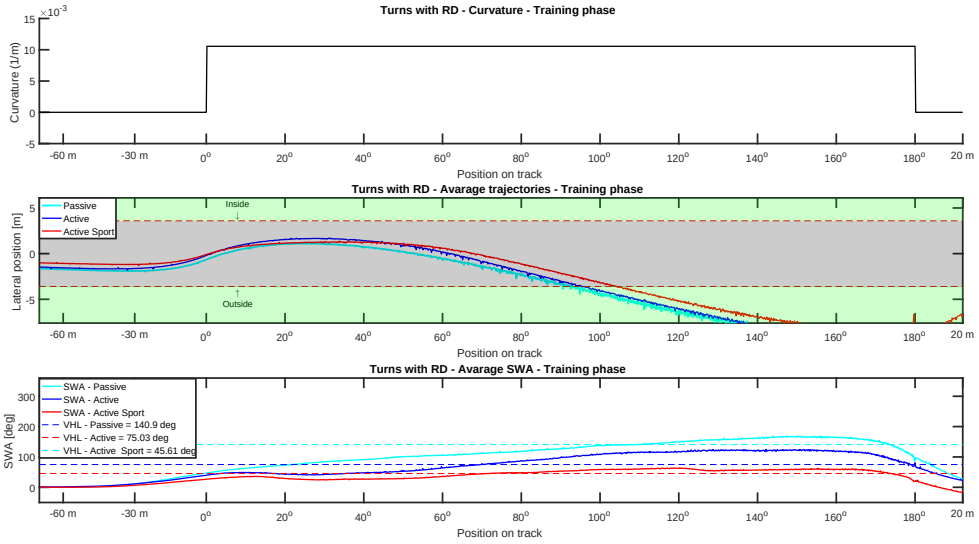

Figure G.41: Average trajectory in the turns where the vehicle departs from the road during the training phase. Top: curvature $(1/R_{curve})$ of the road. Middle: average trajectory across all the participants per vehicle configuration. The dashed lines indicate the road boundary and the solid lines represents the trajectory of the COG of the vehicle. Bottom: average SWA input across all the participants, if the SWA of a vehicle configuration is above the corresponding dashed line the vehicle enters the VHL. The position on track is defined by meters and degrees. $-60m$ implies that the vehicle is at the point 60 meters before the turn starts and for example $20deg$ implies the vehicle position is at an angular span of 20 degrees in the turn. On average the drivers steer into the VHL making it difficult to control the vehicle, resulting in more road departures.

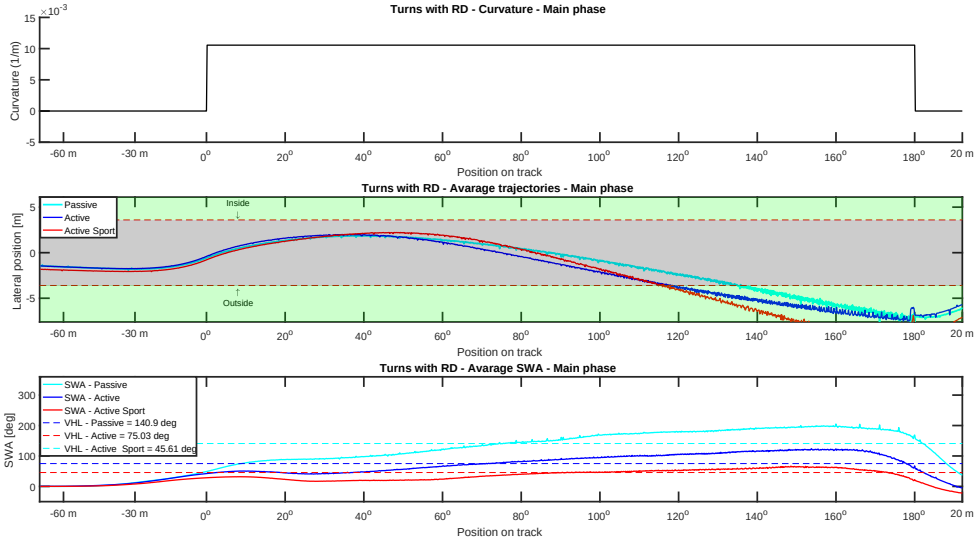

Figure G.42: Average trajectory in the turns where the vehicle departs from the road during the main phase of the experiment. Top: curvature $(1/R_{curve})$ of the road. Middle: average trajectory across all the participants per vehicle configuration. The dashed lines indicate the road boundary and the solid lines represents the trajectory of the COG of the vehicle. Bottom: average SWA input across all the participants, if the SWA of a vehicle configuration is above the corresponding dashed line the vehicle enters the VHL. The position on track is defined by meters and degrees. $-60m$ implies that the vehicle is at the point 60 meters before the turn starts and for example $20deg$ implies the vehicle position is at an angular span of 20 degrees in the turn. The *Active Sport* configuration departs from the road more significantly. Therefore, in figure G.36 the *Active Sport* configuration has a road departure on average.

G.18.5. All participants in catch trial 1 and 2

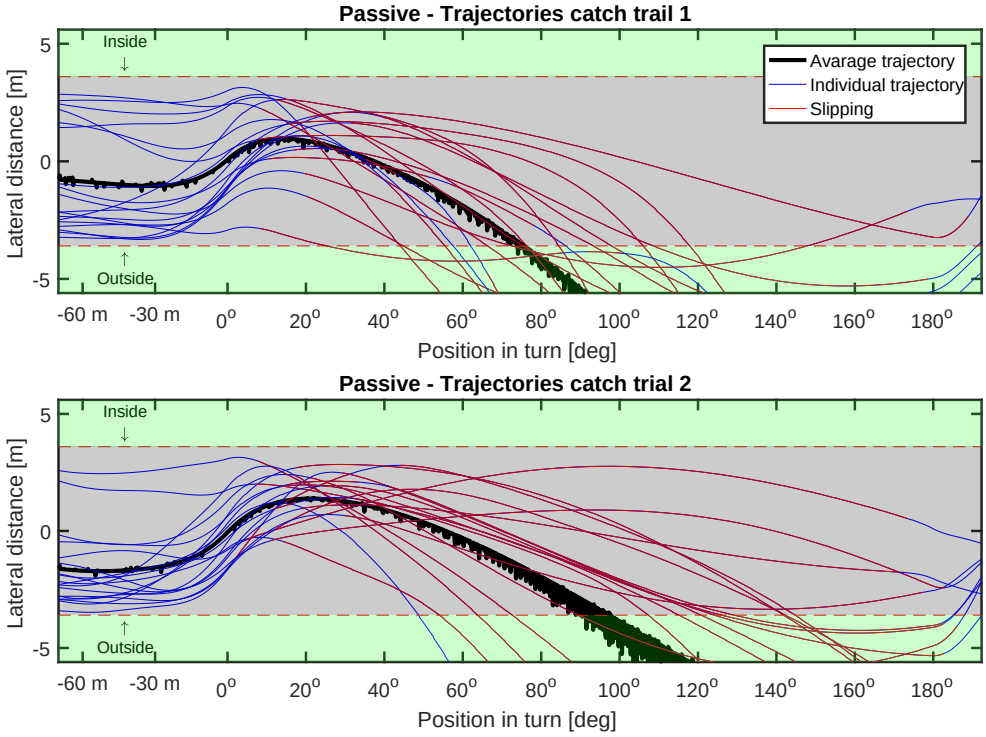

Figure G.43: Trajectory of the participants duringcatch trial 1 and 2 when driving the *Passive* vehicle configuration.

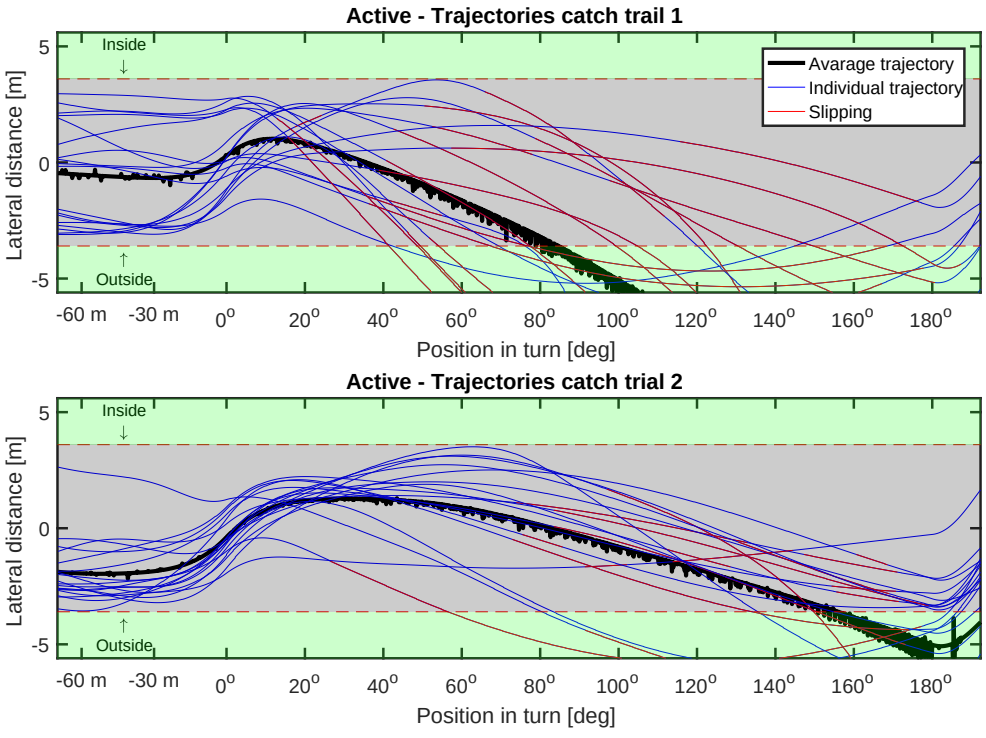

Figure G.44: Trajectory of the participants during catch trial 1 and 2 when driving the *Active* vehicle configuration.

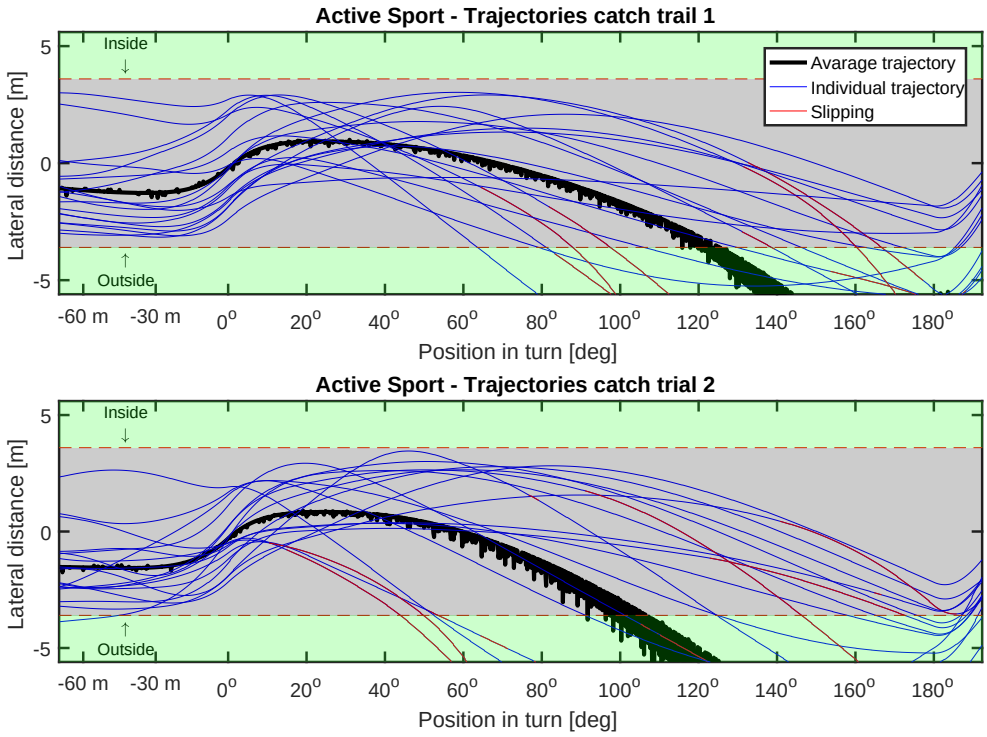

Figure G.45: Trajectory of the participants during catch trial 1 and 2 when driving the *Active Sport* vehicle configuration.

G.19. Learning effect

The effect of learning can be observed in different manners. In this section the development of the lap scores, average lateral distance to inner road boundary and SRR change over the turns is given.

G.19.1. Average lateral distance to inner road boundary

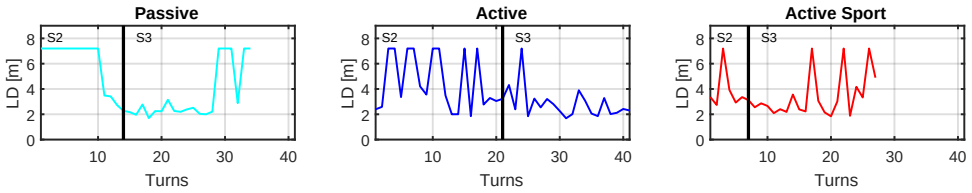

Figure G.46: Participant 1. Black vertical line is separation between training phase (s2) and main phase (s3)

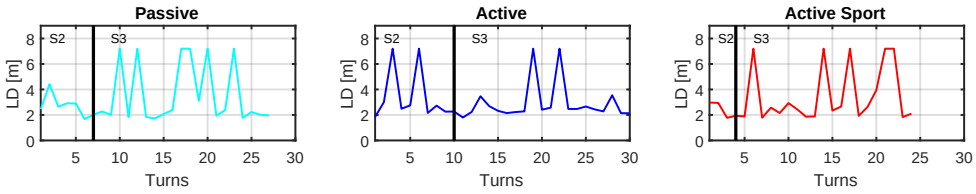

Figure G.47: Participant 2. Black vertical line is separation between training phase (s2) and main phase (s3)

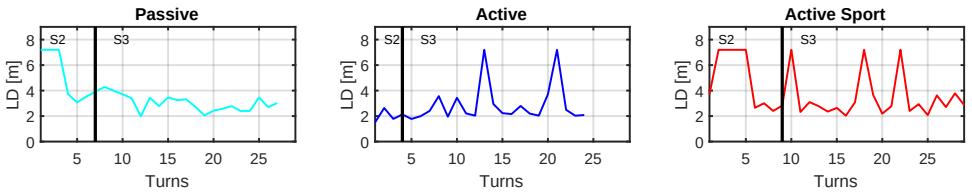

Figure G.48: Participant 3. Black vertical line is separation between training phase (s2) and main phase (s3)

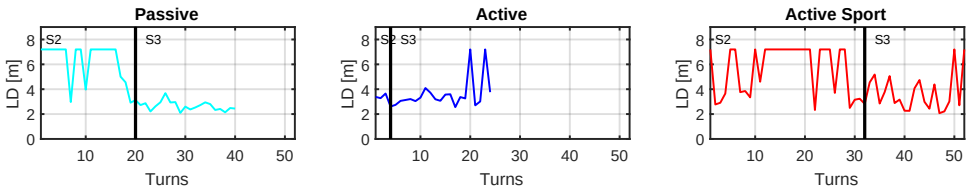

Figure G.49: Participant 4. Black vertical line is separation between training phase (s2) and main phase (s3)

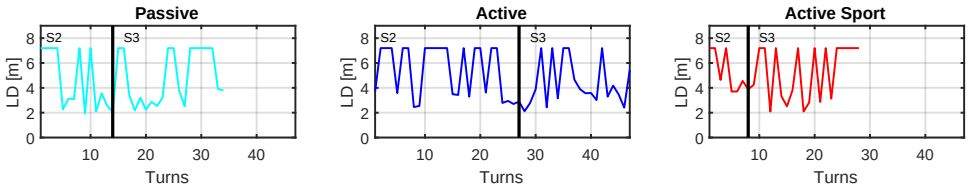

Figure G.50: Participant 5. Black vertical line is separation between training phase (s2) and main phase (s3)

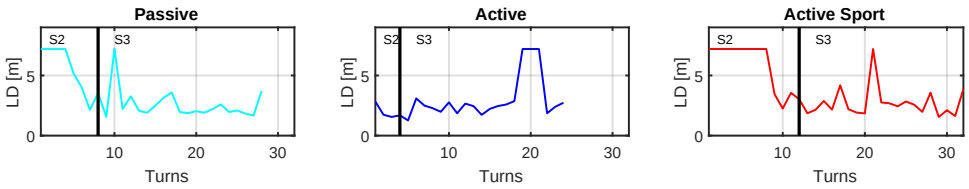

Figure G.51: Participant 6. Black vertical line is separation between training phase (s2) and main phase (s3)

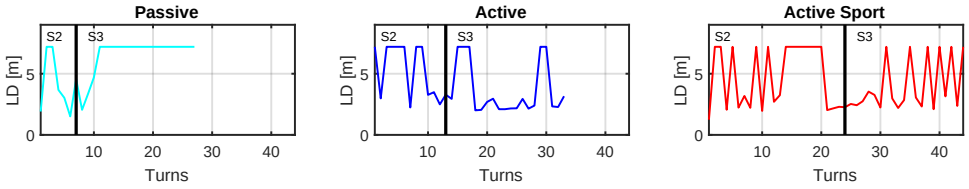

Figure G.52: Participant 7. Black vertical line is separation between training phase (s2) and main phase (s3)

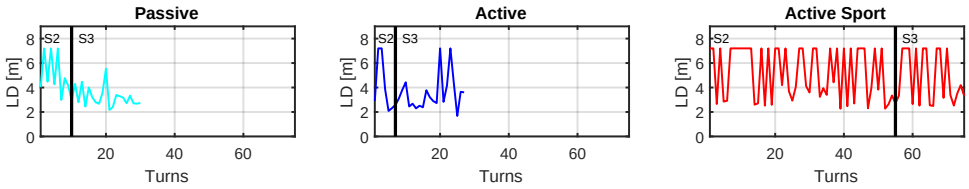

Figure G.53: Participant 8. Black vertical line is separation between training phase (s2) and main phase (s3)

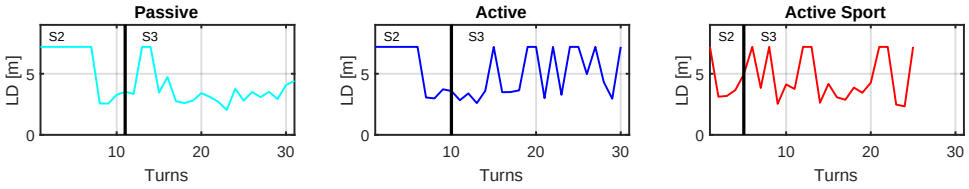

Figure G.54: Participant 9. Black vertical line is separation between training phase (s2) and main phase (s3)

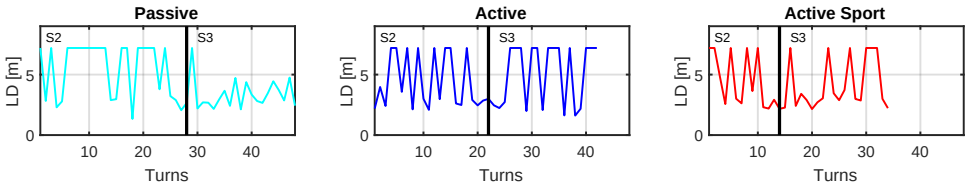

Figure G.55: Participant 10. Black vertical line is separation between training phase (s2) and main phase (s3)

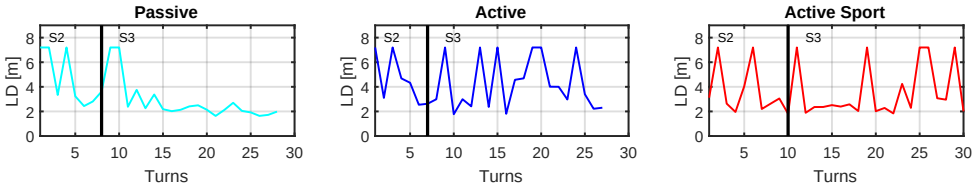

Figure G.56: Participant 11. Black vertical line is separation between training phase (s2) and main phase (s3)

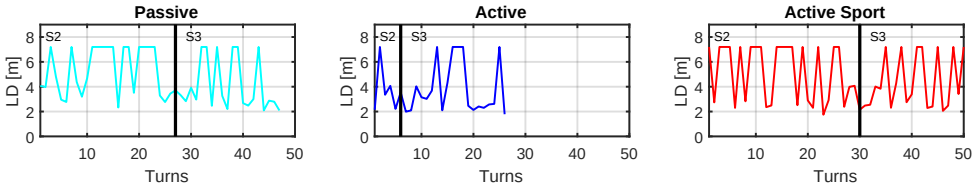

Figure G.57: Participant 12. Black vertical line is separation between training phase (s2) and main phase (s3)

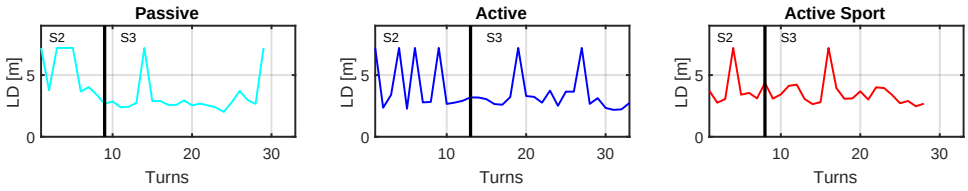

Figure G.58: Participant 13. Black vertical line is separation between training phase (s2) and main phase (s3)

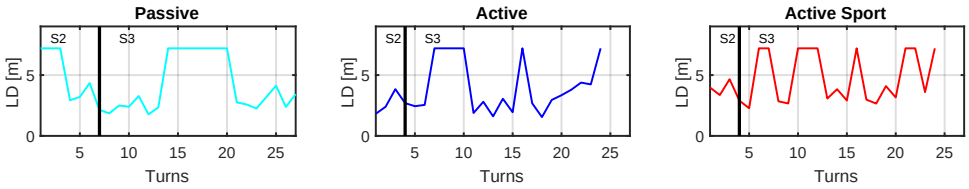

Figure G.59: Participant 14. Black vertical line is separation between training phase (s2) and main phase (s3)

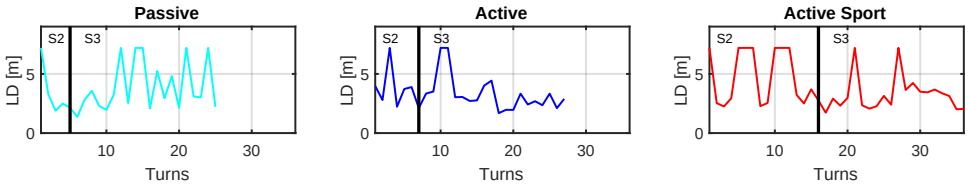

Figure G.60: Participant 15. Black vertical line is separation between training phase (s2) and main phase (s3)

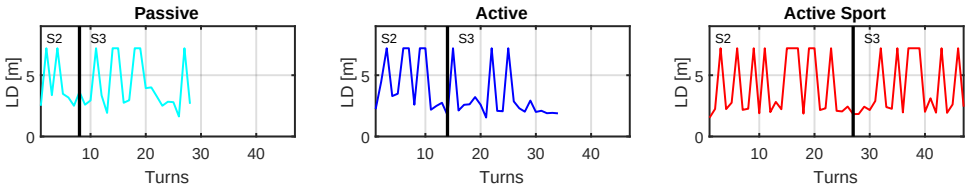

Figure G.61: Participant 16. Black vertical line is separation between training phase (s2) and main phase (s3)

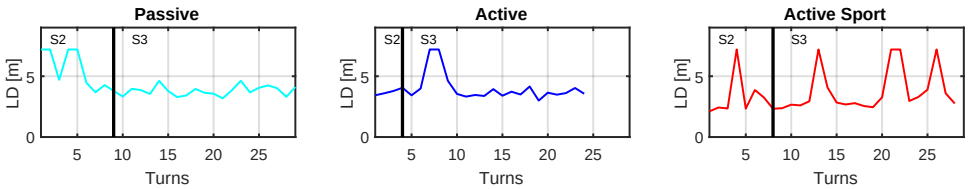

Figure G.62: Participant 17. Black vertical line is separation between training phase (s2) and main phase (s3)

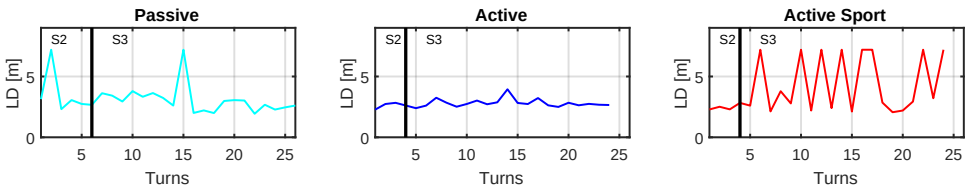

Figure G.63: Participant 18. Black vertical line is separation between training phase (s2) and main phase (s3)

G.19.2. Scores obtained per turn.

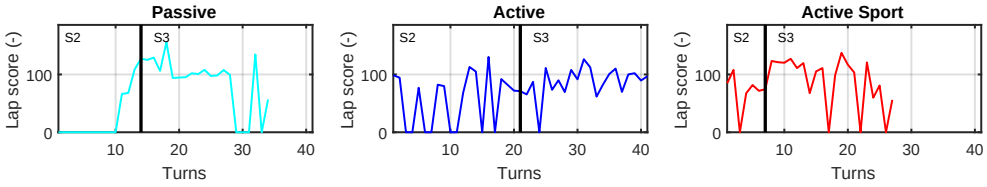

Figure G.64: Participant 1. Black vertical line is separation between training phase (s2) and main phase (s3)

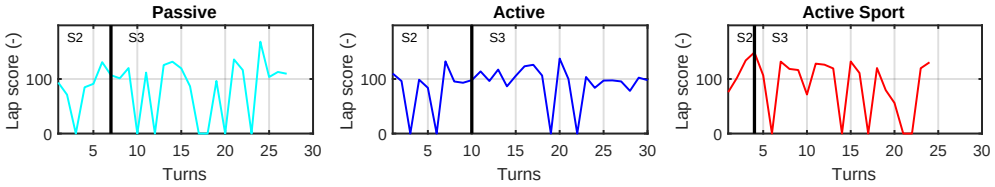

Figure G.65: Participant 2. Black vertical line is separation between training phase (s2) and main phase (s3)

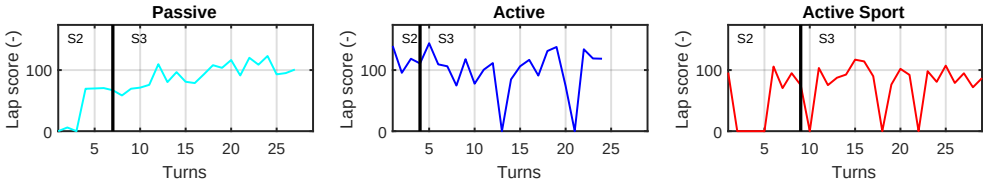

Figure G.66: Participant 3. Black vertical line is separation between training phase (s2) and main phase (s3)

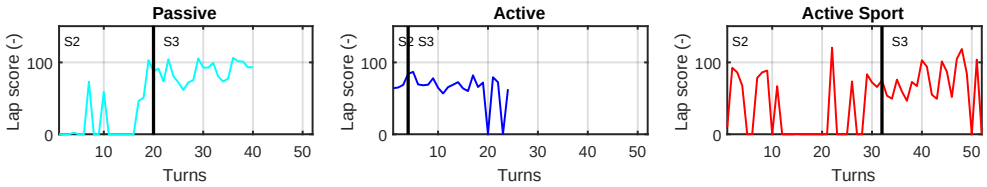

Figure G.67: Participant 4. Black vertical line is separation between training phase (s2) and main phase (s3)

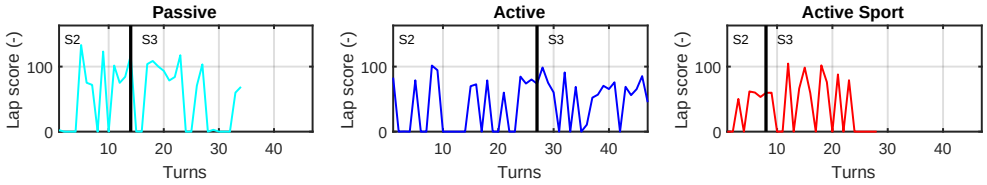

Figure G.68: Participant 5. Black vertical line is separation between training phase (s2) and main phase (s3)

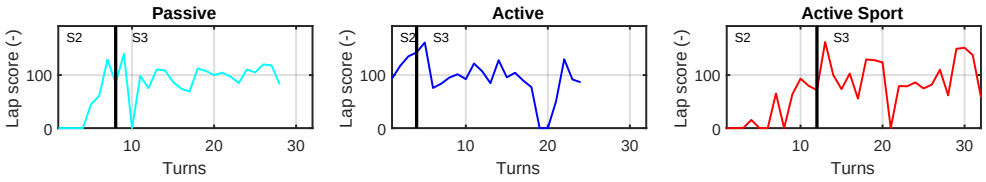

Figure G.69: Participant 6. Black vertical line is separation between training phase (s2) and main phase (s3)

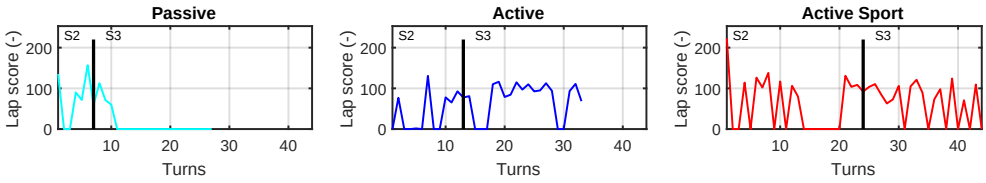

Figure G.70: Participant 7. Black vertical line is separation between training phase (s2) and main phase (s3)

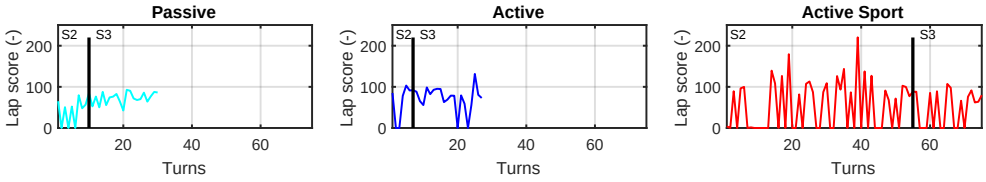

Figure G.71: Participant 8. Black vertical line is separation between training phase (s2) and main phase (s3)

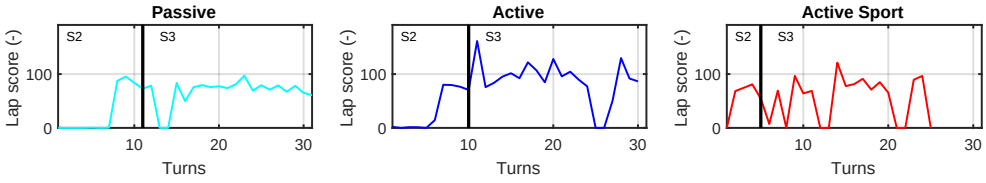

Figure G.72: Participant 9. Black vertical line is separation between training phase (s2) and main phase (s3)

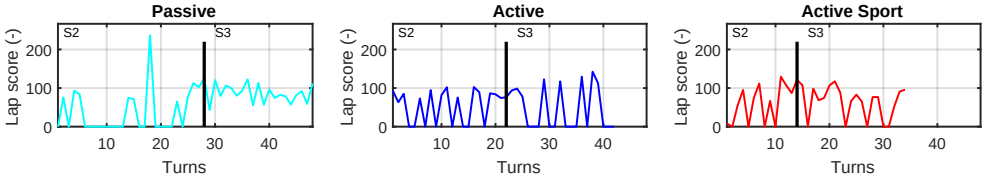

Figure G.73: Participant 10. Black vertical line is separation between training phase (s2) and main phase (s3)

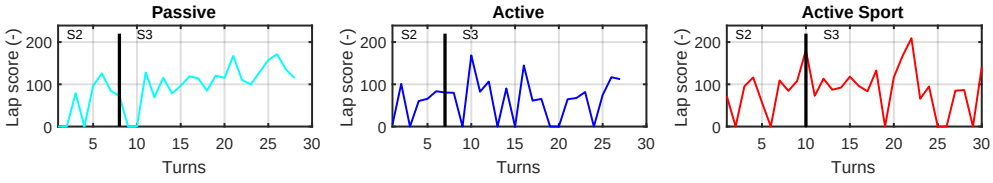

Figure G.74: Participant 11. Black vertical line is separation between training phase (s2) and main phase (s3)

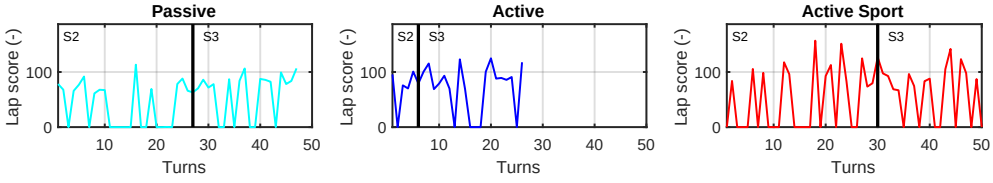

Figure G.75: Participant 12. Black vertical line is separation between training phase (s2) and main phase (s3)

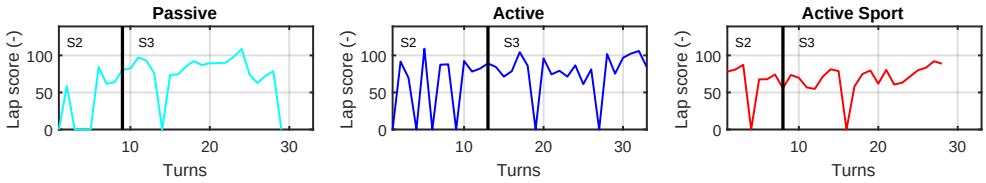

Figure G.76: Participant 13. Black vertical line is separation between training phase (s2) and main phase (s3)

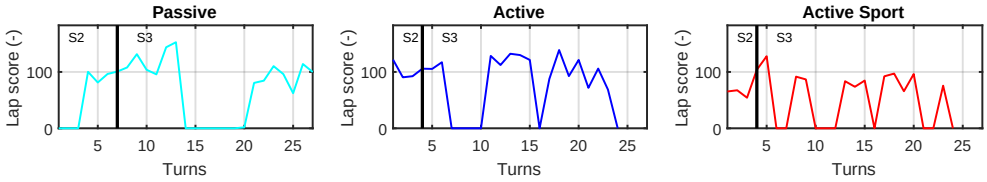

Figure G.77: Participant 14. Black vertical line is separation between training phase (s2) and main phase (s3)

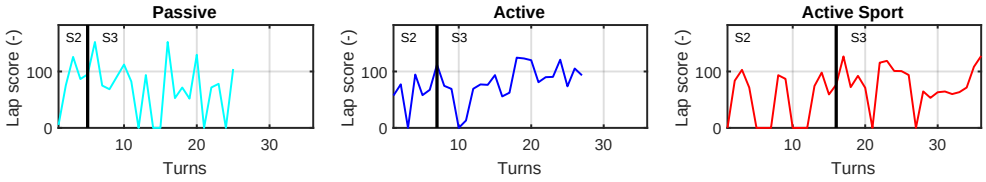

Figure G.78: Participant 15. Black vertical line is separation between training phase (s2) and main phase (s3)

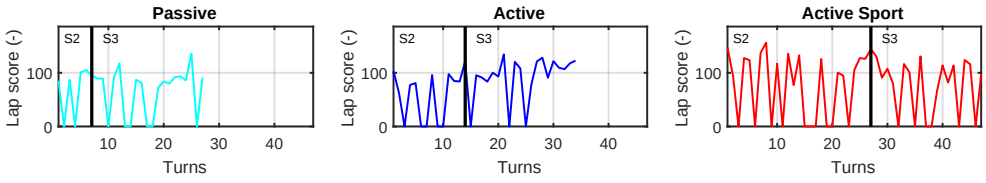

Figure G.79: Participant 16. Black vertical line is separation between training phase (s2) and main phase (s3)

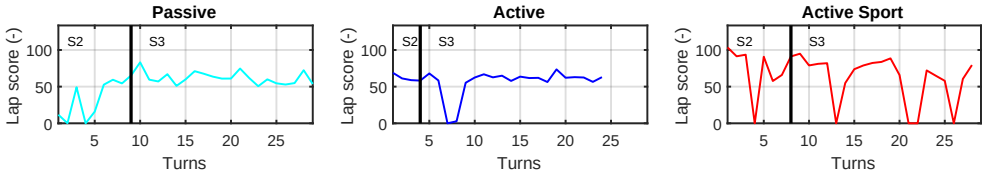

Figure G.80: Participant 17. Black vertical line is separation between training phase (s2) and main phase (s3)

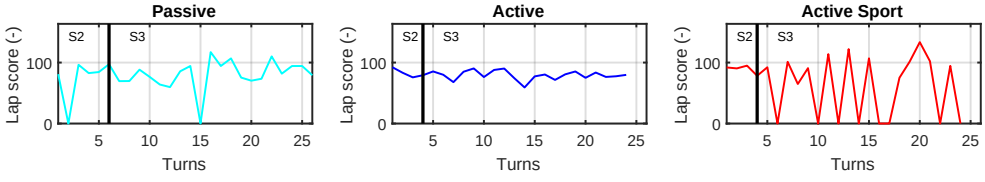

Figure G.81: Participant 18. Black vertical line is separation between training phase (s2) and main phase (s3)

G.19.3. Steering Reversal Rate

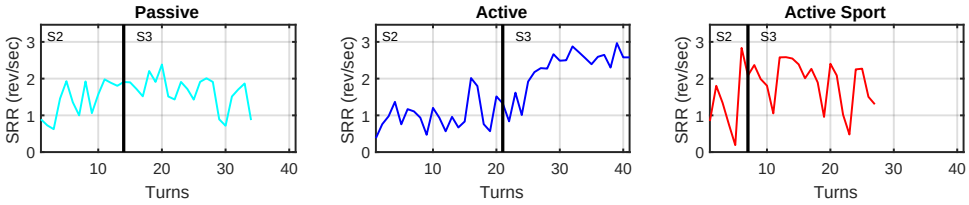

Figure G.82: SRR Participant 1. Black vertical line is separation between training phase (s2) and main phase (s3)

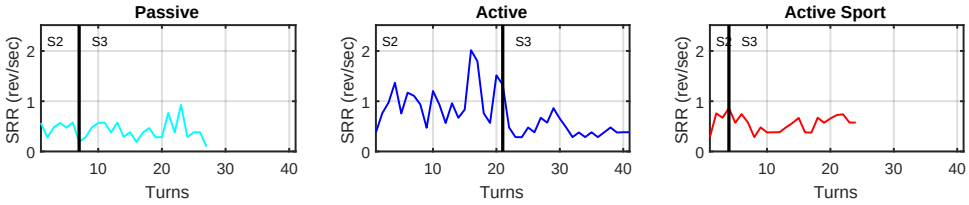

Figure G.83: SRR Participant 2. Black vertical line is separation between training phase (s2) and main phase (s3)

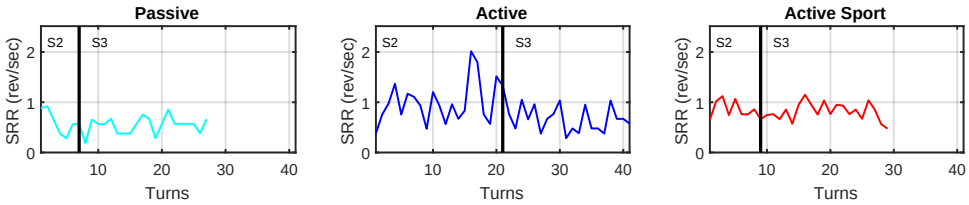

Figure G.84: SRR Participant 3. Black vertical line is separation between training phase (s2) and main phase (s3)

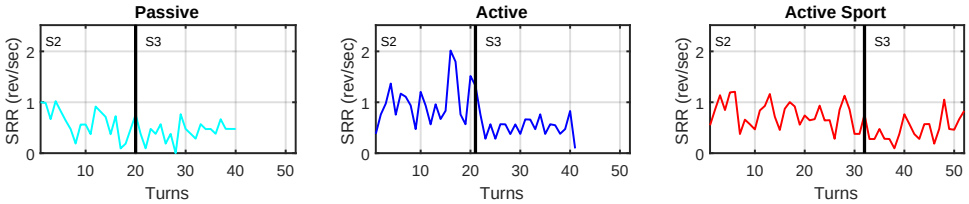

Figure G.85: SRR Participant 4. Black vertical line is separation between training phase (s2) and main phase (s3)

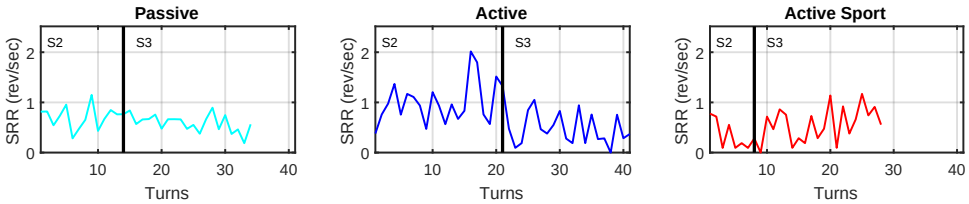

Figure G.86: SRR Participant 5. Black vertical line is separation between training phase (s2) and main phase (s3)

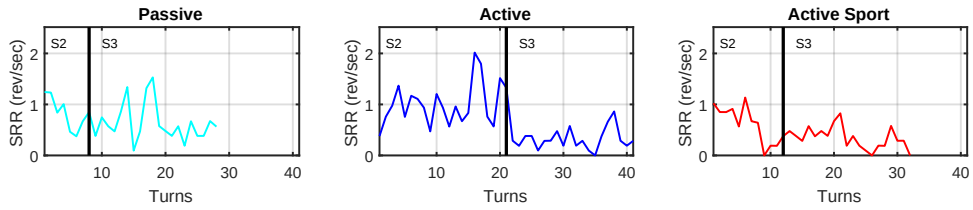

Figure G.87: SRR Participant 6. Black vertical line is separation between training phase (s2) and main phase (s3)

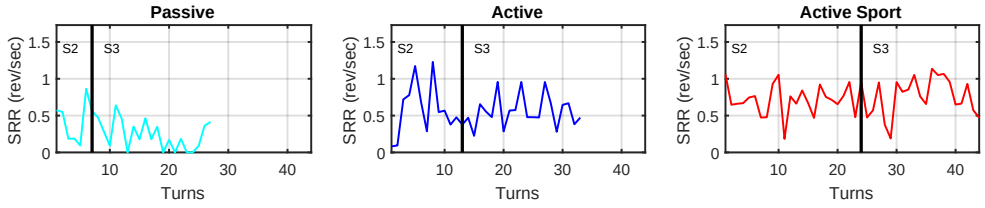

Figure G.88: SRR Participant 7. Black vertical line is separation between training phase (s2) and main phase (s3)

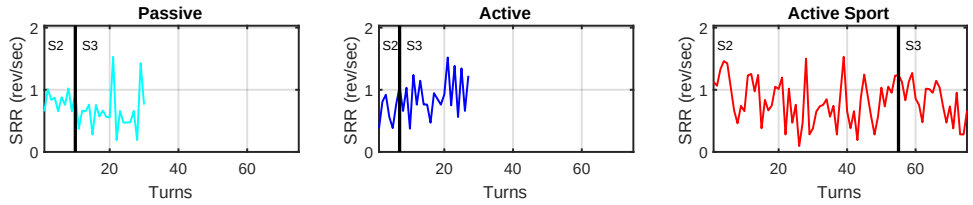

Figure G.89: SRR Participant 8. Black vertical line is separation between training phase (s2) and main phase (s3)

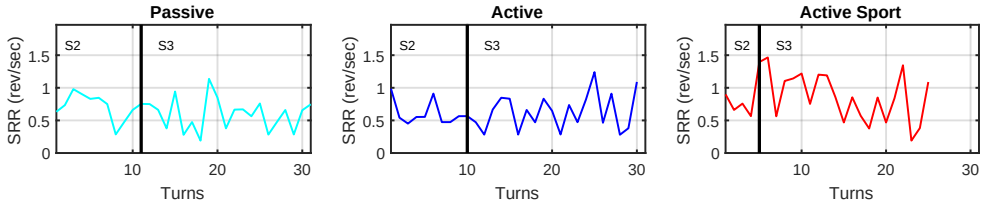

Figure G.90: SRR Participant 9. Black vertical line is separation between training phase (s2) and main phase (s3)

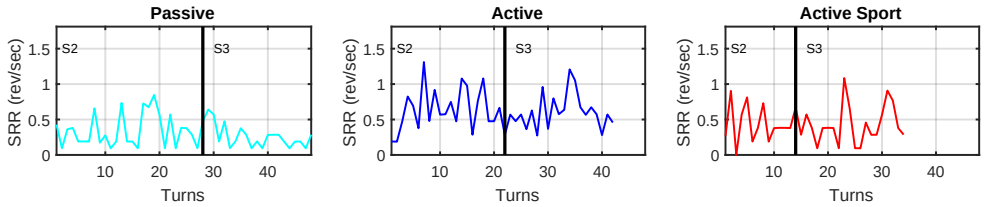

Figure G.91: SRR Participant 10. Black vertical line is separation between training phase (s2) and main phase (s3)

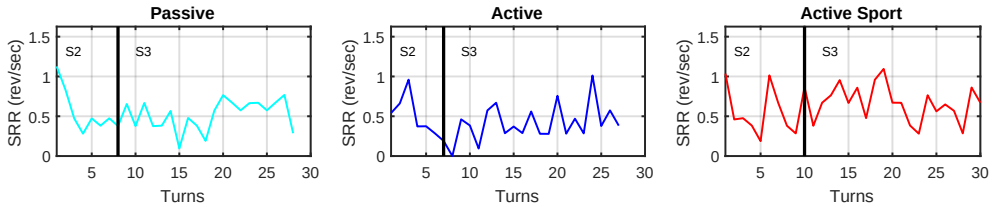

Figure G.92: SRR Participant 11. Black vertical line is separation between training phase (s2) and main phase (s3)

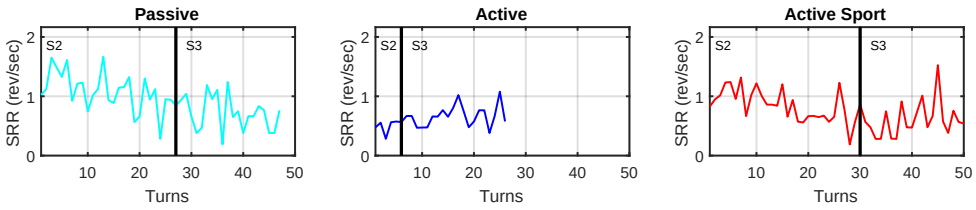

Figure G.93: SRR Participant 12. Black vertical line is separation between training phase (s2) and main phase (s3)

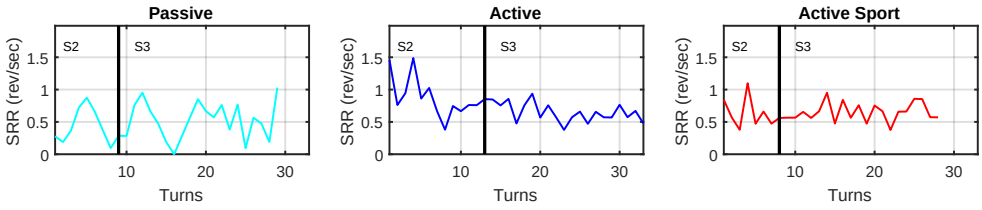

Figure G.94: SRR Participant 13. Black vertical line is separation between training phase (s2) and main phase (s3)

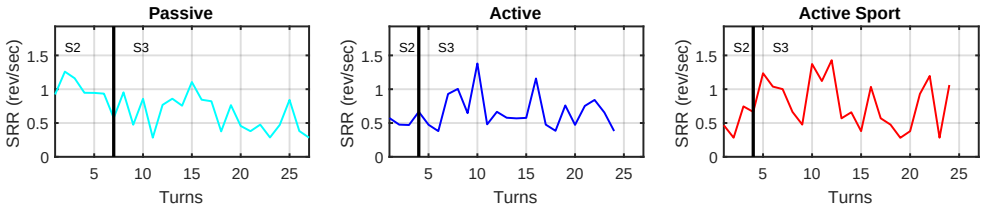

Figure G.95: SRR Participant 14. Black vertical line is separation between training phase (s2) and main phase (s3)

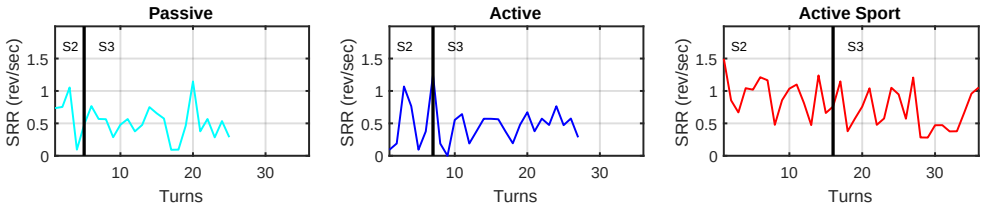

Figure G.96: SRR Participant 15. Black vertical line is separation between training phase (s2) and main phase (s3)

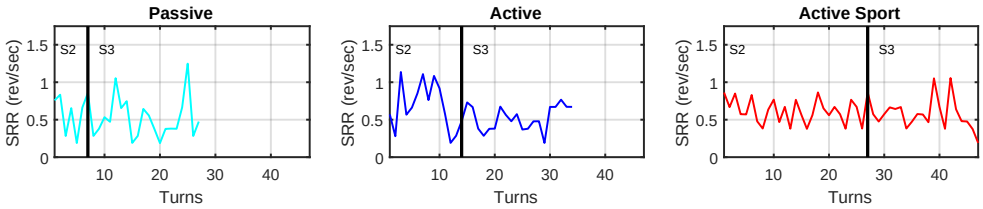

Figure G.97: SRR Participant 16. Black vertical line is separation between training phase (s2) and main phase (s3)

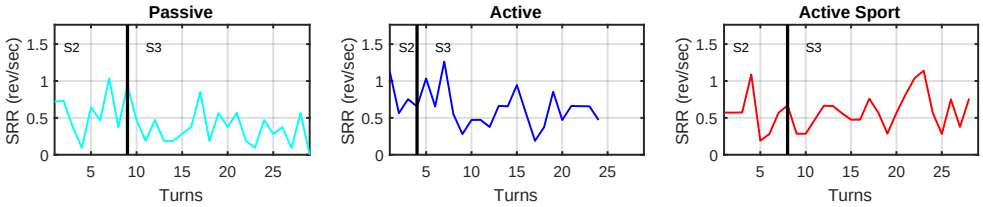

Figure G.98: SRR Participant 17. Black vertical line is separation between training phase (s2) and main phase (s3)

G.20. Participant characteristics

Table G.19: Result of participant questionnaire

Participant Number	**1**	**2**	**3**	**4**	**5**	**6**	**7**	**8**	**9**	**10**	**11**	**12**	**13**	**14**	**15**	**16**	**17**	**18**
Age	24	19	25	27	20	23	36	27	25	21	18	25	22	20	24	22	19	23
Time licence (years)	6	1.5	7	7	2	5	18	9	5	1	1	7	5	3	6	4	2.5	4
How often drive per month (days)	2	2	12	8	2	2	15	2	2	8	2	4	30	24	15	4	4	15
Attended slip course	No	Yes	No	No	No	No	Yes	No	No	No	No	No	Yes	No	Yes	No	No	No
Recing games once a week	No	Yes	No	Yes	No	No	No	No	No	No	No	No	No	No	Yes	No	Yes	No